Supply Shocks and On-shoring: Evidence using an AI-built Production Network

Thiemo Fetzer*
Peter John Lambert†
Bennet Feld‡
Prashant Garg§

July 29, 2024

Click here for the latest version

Abstract

This paper studies supply shocks and their role in industrial transformation via 'on-shoring'. We study a number of exogenous trade-events including blockades, sanctions, trade-wars, and supply shortages. To test for onshoring, we first construct a novel network representation of the production network which links the universe of Harmonized System (HS) products. This AI-built Production Network (AIP-NET) is built entirely with text-data, using a large language model (LLM) trained on production-specific information. We next combine this novel network structure with data from trade-flows and document a number of new facts. We complement our descriptive analysis with a dyadic difference-in-difference (DyDiD) estimation strategy, exploiting various supply-shocks. We find strong evidence that negative supply shocks which hit specific downstream products induce an increase in import demand for vertically linked upstream products, suggestive of 'on-shoring'. This effect is robust to a host of controls and placebo tests, and is strongest for critical upstream capital equipment.

Keywords: Supply-Chain Network Analysis, Large Language Models, On-shoring, industrial policy, Trade wars
JEL Classification: F14, F23, L16, F52, O25, N74, C81,

*Warwick University & University of Bonn, Departments of Economics. Also affiliated or fellowed at Grantham Research Institute, ECONtribute, CEPR, NIESR, CESifo and STICERD.

†London School of Economics and Political Science (LSE), Department of Economics. Also affiliated with: Centre for Economic Performance (CEP), Programme on Innovation and Diffusion (POID). Email: p.j.lambert@lse.ac.uk.

‡London School of Economics and Political Science (LSE), Department of Economics

§Imperial College London, Department of Economics and Public Policy

1 Introduction

This paper studies the connection between negative supply shocks and the recent trend towards 'on-shoring' i.e. the localization of production. To facilitate this work, we build and validate an AI-built Production Network (AIPNET), which maps input-output relationships across 5,648 Harmonized System (HS) product groups.[1] By leveraging recent advances in large language models (LLMs), AIPNET uncovers the latent structure of the global production network, enabling new research on global value chains (GVCs) and the propagation of economic shocks.[2] We next utilize AIPNET to study recent trade-patterns and the rise of 'on-shoring'.

To study onshoring, we combine data on global trade flows with AIPNET. Five key facts emerge from this analysis: First, we find a decrease in global imports of downstream goods relative to upstream raw materials, intermediate goods, and capital inputs. Second, using granular country-level product-dyads based on the AIPNET production network, we show that these aggregate trade patterns reflect micro-level substitution within vertically linked goods, indicative of production process localization. Third, we document how supply shocks, including trade disputes, shortages, and geopolitical events, can explain a substantial fraction of this micro-level on-shoring response. Fourth, we find that this substitution is strongest for capital goods imports, highlighting country-specific build-up of domestic manufacturing capacity. Fifth, we leverage a large exogenous trade shock to a small open economy to causally identify the strength of on-shoring. We find that a 5pp increase in the price of a downstream product caused a 3pp increase in the importation of upstream goods linked to the affected focal product, relative to other upstream goods.

These facts all rely on our ability to use AIPNET to link all six-digit HS products according to production-process relationships. This allows us to directly observe

[1] The 'Harmonized System' is a nomenclature of tradable product codes maintained by the World Customs Organization (WCO) and used universally by national trade authorities. AIPNET is built using the 2017 vintage of HS Codes at the 6-digit level of granularity.

[2] We invite researchers to explore the vast potential of AIPNET, freely available at aipnet.io.

how trends in global trade patterns interact with this network structure. Are countries increasingly importing upstream products? Does this reduce demand for associated downstream products? Such questions are difficult to answer without the ability to empirically recover the latent relationships between goods. Drawing on a comprehensive bilateral trade database, the analysis presents evidence suggestive of an increasing "onshoring" tendency over this period, particularly among certain advanced economies. Using a non-parametric approach to estimate the changes in trade patterns, we observe that since 2016, there has been a notable increase in imports of goods that are linked in an input/output relationship, as identified by AIPNET. This suggests a shift towards localization of production processes.

Our empirical analysis identifies persistent supply shocks, particularly after 2016, as a driving force behind these changes. By constructing unit price indices for each country and good, and identifying periods with persistent positive price shocks, we find that these supply shocks have significantly influenced the import patterns of upstream goods. Notably, there has been an increase in imports of capital and intermediary goods, indicative of investment in localization of machinery and equipment to support domestic production.

To cleanly identify the causal effects of trade shocks on product-level substitution and on-shoring, we leverage the case of the blockade of Qatar in 2017. By leveraging the exogenous timing of this shock as well as substantial variation in the product-specific exposure to this shock, we are able to run a dyadic-difference-in-difference (DyDiD) specification to capture patterns of substitution towards upstream products and away from downstream goods. Overall, we find that a 5pp increase in shock exposure of a focal good leads to a 3pp increase in imports for upstream products. We also find that shock-exposure of downstream goods increases the probability of associated upstream goods having non-zero imports. Overall, the blockade of Qatar dramatically altered it's "make-or-buy" calculus, leading to a shift up the import-value-chain and greater on-shoring of manufacturing capacity.

By combining an analysis of global trade patterns, an empirical analysis of trade shocks, micro-evidence of product-level substitution along production networks, and a quasi-experimental case study where trade shocks are both sizable and plausibly exogenous, the findings in this paper all point to a common shift away from globalization. As countries worldwide grapple with the challenges posed by the COVID-19 pandemic, geopolitical tensions, rising nativist ideologies, and other structural forces, many nations are pursuing on-shoring and industrial policies to bolster economic resilience. AIPNET offers a valuable tool for mapping production linkages and studying the effects of such policies.

The remainder of this paper is organized as follows: Section 2 reviews the literature on trade shocks, industrial transformation, and on-shoring. We also review methodological work related to building network structures with AI tools. Section 3 overviews the various data sources and AI model used in the paper. Section 4 introduces our AI-built Production Network (AIPNET). We discuss the methodology we adopted to fine-tune, test, and validate the network structure, and some key lessons for those wishing to build networks using AI tools. This section also compares the insights from AIPNET to other empirical sources of product-level production characteristics. Section 5 outlines both the empirical design and results testing the micro-foundations of onshoring at the product-dyad level. Section 6 further tests the findings from our micro-econometric setup using a case study with plausibly exogenous and sizable supply shocks. For this, we study the blockade of Qatar in 2017, using the network structure along with high-frequency trade data in a dyadic difference-in-difference (DyDiD) design. Section 7 concludes.

2 Literature

This papers positive analysis connects to work across international trade, industrial organization, economic production, political economy and geoeconomics. It also makes methodological contributions building on work in network econometrics as well as eco-

nomic measurement using AI/LLMs. This section highlights these connections and identifies the many papers under-girding our analysis.

In recent years, the global economic system has faced escalating uncertainties and economic challenges stemming from multiple directions. Structurally, climate change presents a significant uncertainty shock (Tol, 2009; Bauer & Rudebusch, 2021), involving substantial risks and transition costs (Hong, Karolyi, & Scheinkman, 2020). Aging societies pose macro-financial challenges (Auclert, Malmberg, Martenet, & Rognlie, 2021), and structural transformations are slow to deliver large productivity gains (Kehoe, Ruhl, & Steinberg, 2018; Juhász, Squicciarini, & Voigtländer, 2023). Additionally, growing spatial inequalities undermine social cohesion and economic stability (Gaubert, Kline, Vergara, & Yagan, 2021; Becker, Fetzer, & Novy, 2017).

At the same time, the perceptions of poor public sector handling of various crises feed simplistic populist narratives. Once in power, these populist movements often produce economic policies that exacerbate distributional conflicts (Funke, Schularick, & Trebesch, 2023; Alabrese, Fetzer, & Wang, 2024). A fraying global trade order amidst a populist backlash (Fajgelbaum, Goldberg, Kennedy, & Khandelwal, 2020), marked by growing and escalating trade disputes, further complicates the economic landscape (Ossa, 2014b; Fetzer & Schwarz, 2019). These disputes may have adverse economic consequences, as evidenced by cross-country analyses (Funke et al., 2023), and specific case studies like Brexit in the UK (Alabrese et al., 2024; Hassan, Hollander, Lent, & Tahoun, 2024). The COVID-19 pandemic has further highlighted these issues, emphasizing the need for resilient economic policies (Kaplan, Moll, & Violante, 2020).

Many countries are pursuing structural transformations away from hydrocarbon-dependent industries towards more sustainable models. These dual challenges raise important questions about the roles of the public sector and private firms in facilitating economic transitions, as well as debates on the governance of international trade in a period of increasing frictions (François & Woerz, 1999; Hoekman & Mattoo, 2006; Winters et al., 2004; Mulabdic, Osnago, & Ruta, 2017). For instance, Alfaro and Chor (2023)

document a shift in US imports from China to other low-wage countries and patterns of friend- and near-shoring as a response to COVID-related trade shocks. Furthermore, the literature also touches upon the role of service sector trade, analyzing its cost-benefit aspects and the repercussions on the UK's economic relationship with the EU (Baldwin & Weder di Mauro, 2019; Fetzer & Wang, 2020). Noteworthy discussions on the economic aftermath of the COVID-19 pandemic and the effects of policy uncertainty between major trading nations underline the significant role of geopolitical tensions in shaping trade networks and integration (Baldwin & Freeman, 2020; Baldwin & di Mauro, 2020; Barro, Ursúa, & Weng, 2020; Handley & Limão, 2017; Fetzer & Schwarz, 2019; Ossa, 2014a; Crowley, 2014).

These challenges arise in the context of a growing inward-looking perspective on trade policy. The structural change towards a service sector economy may redefine the role of the state as an economic platform provider that leverages its informational capacity to shape and direct economic development (Fetzer, Shaw, & Edenhofer, 2024). This has renewed interest in studies on the digital divide, sluggish technology adoption, and their impact on productivity (Juhász et al., 2023). Additionally, there is accelerated structural transformation away from goods to services sector trade, growing geopolitical tensions, and increasing public health risks due to threats such as antimicrobial resistance. Various literature has underscored the repercussions of increased trade frictions, including indirect costs to trade routes affected by Somali piracy (Besley, Fetzer, & Mueller, 2012). The global economy has faced numerous shocks including financial crises, debt crises, austerity measures, and war-induced energy price shocks such as those from the Ukraine conflict and the shale gas revolution. Examining the effect of politically motivated trade sanctions on industry transformation, sanctions on Russian firms and the corresponding policy reaction by the Russian state led to inefficient capital reallocation (Nigmatulina, 2023). Sanctions on firms in the sanctioning country, such as US firms with Chinese customers, also show lower profitability and a break-up of trade relationships (Crosignani, Han, Macchiavelli, & Silva, 2023). These developments have

refocused attention on how economies can enhance resilience against supply disruptions and boost economic security.

Firstly, in the domain of industrial policy and infant industry protection, our study underscores the importance of nurturing nascent industries to build economic resilience. The unique context of Qatar, with its limited initial industry and skewed trade dynamics, highlights how strategic industrial policies can foster local industries and enhance economic stability (Juhász, 2018; Allen & Donaldson, 2017).[3]

Secondly, this research adds to the literature on the economic consequences of geopolitical events. By comparing the Qatar blockade with other significant events such as trade wars and Brexit, we illustrate how the unique asymmetry of the blockade provides a distinct empirical test of geopolitical shocks. Unlike typical symmetric retaliation observed in other cases, Qatar's experience offers new insights into the economic impacts of unilateral trade barriers (Fajgelbaum et al., 2020; Fetzer & Schwarz, 2019; Becker et al., 2017).[4]

Thirdly, our findings contribute to the understanding of trade shocks. Empirical and theoretical contributions in this field emphasize the substitution effects and structural reorganization following such shocks. Our study shows how politically motivated trade sanctions can lead to inefficient capital reallocation, echoing broader themes in the literature (Caselli, Koren, Lisicky, & Tenreyro, 2020; Dhyne, Kikkawa, Mogstad, & Tintelnot, 2020; Oberfield, 2018; Nigmatulina, 2023; Crosignani et al., 2023).

Additionally, contemporary studies on trade highlight the nuanced impacts of industry reshuffling and productivity, significantly influenced by events like the COVID-19 pandemic and policy uncertainty. Our research aligns with these studies, examining

[3]Over the years, extensive research has been conducted into the domains of trade and industrial composition, with significant contributions from scholars such as Donaldson, Arkolakis, and Melitz. Notably, (Koren & Tenreyro, 2013) delved into technological diversification, exploring its implications and nuances in modern economics. Furthermore, (Kremer, 1993) highlights the Leontieff-nature of supply chains, suggesting the system is only as strong as its weakest linkage.

[4]Politically motivated trade barriers are a prevailing feature of many conflicts. For example, (Fetzer & Schwarz, 2019) studies the recent geopolitical trade barriers erected, while (Korovkin & Makarin, 2023) shows that the reduction in trade between Ukraine and Russia after the 2014 invasion is stronger in non-combat regions with fewer ethnic Russians, indicating destroyed trust and social capital.

the shifts in trade patterns and industrial adjustments under such pressures (François & Woerz, 1999; Hoekman & Mattoo, 2006; Winters et al., 2004; Mulabdic et al., 2017; Alfaro & Chor, 2023; Baldwin & Weder di Mauro, 2019; Fetzer & Wang, 2020; Baldwin & Freeman, 2020; Barro et al., 2020; Handley & Limão, 2017).

Furthermore, the challenges posed to global value chains by higher energy or transportation costs, and the importance of governance structures, are critical areas our study touches upon. By examining how these factors influence the resilience and adaptability of global production networks, we contribute to a deeper understanding of the dynamics within global value chains (Arezki, Fetzer, & Pisch, 2017; Womack, Jones, & Roos, 1990; Suzaki, 1987; Gereffi & Korzeniewicz, 1994; Humphrey & Schmitz, 2004).

At the firm level, our research explores theories of vertical integration and the balance between market transactions and internal production. This examination is essential for understanding how firms and economies can optimize their production processes and supply chain structures (Coase, 1937; Williamson, 1971; Grossman & Hart, 1986; Hart & Moore, 1990; Fujimoto, 1999; Alfaro et al., 2018; Alfaro, Antràs, Chor, & Conconi, 2019; Atalay, Hortacsu, Li, & Syverson, 2018).[5]

To model value chains, the literature centrally relies on input-output tables. Fally (2012) and Antràs, Chor, Fally, and Hillberry (2012) develop measures of "upstreamness" using US input-output tables at a granular HS6 level. Karbevska and Hidalgo (2023) instead use trade data from over 300 regions and a trade theoretical approach to establish product-level supply chain ties. These approaches are distinct from our classification. We construct supply chain networks using descriptions of product categories. This qualitative foundation yields a measure of supply chain relations independent of trade patterns observed in our data, alleviating endogeneity concerns.

Finally, this paper connects to both text-as-data and network econometrics. To our

[5]While our unit of analysis is at the national level, our ability to zoom into detailed product-level trade flows has a similar flavor to studies of on-shoring at the firm level. Although our focus is reduced form evidence, we appeal to the mechanisms outlined in these theories. Recent empirical work has also studied the role of vertical organization within and across firms. Additionally, we consider trade shocks and theoretical underpinnings from works such as (Elliott & Jackson, 2023).

knowledge, we are the first to use a frontier LLM to construct such a network. Others have used LLMs to study labour markets (Hansen et al., 2023). Perhaps the most closely related application of text-as-data methods to recover supply chain linkages comes from Frésard, Hoberg, and Phillips (2019), who utilize text data to construct a vertical network across publicly listed firms. For a more general overview of NLP methods, see (Ash & Hansen, 2023). Network data has been used widely in recent years. For an overview see De Paula (2017). For a discussion of empirical considerations when working with dyadic data, see Cameron and Miller (2014).

3 Data Sources and Models

In this section, we provide a brief overview of the various data sources used to build AIPNET and also to conduct our analysis on on-shoring, though we leave the specifics of how we use them to the very next section on how we build AIPNET.

3.1 Harmonised System (HS) Codes

To operationalize our production network, we define each product using one of the 5,648 Harmonised System (HS) product codes. The HS product codes are a hierarchical nomenclature maintained by the World Customs Organization (WCO). These classifications are adopted universally across countries. Each product is represented by a six-digit numerical code.[6] The WCO maintains a list and description of each 6-digit HS product, as well as higher-level 4-digit, 2-digit and 21 section groups. Throughout this paper, we utilized the HS Nomenclature 2017 edition[7], which can be found here.

[6]Some entities further refine these into more granular categorizations. For example, the US's International Trade Administration (ITA) uses a 10-digit code to classify import and export products, which extends the HS code structure

[7]The WCO periodically revise these codes, introducing new products and editing descriptions of existing products. The most recent edition is was released in 2022. Throughout this paper, we stuck to using the 2017 edition (which was the previous vintage prior to the 2022). We felt that using 2017 struck a balance between more up-to-date, but not so new that its adoption was not widespread. Another consideration is that the latest vintage of HS codes may feature less prominantly in our AI tools training corpus. In practice, the differences between the 2022 and 2017 edition are minimal, and cross walks are readily

3.2 Global Trade Data

We leverage a global trade dataset obtained from UN Comtrade, encompassing dyadic trade data for 120 leading economies worldwide, spanning from the year 2012 to 2022. This dataset covers all goods classified under the Harmonized System (HS) at the 4-digit level (HS4) on an annual basis. The dataset in its raw form includes approximately 1.58 million rows of data, structured by country, HS4 code, and year.[8] Given the identified input-output linkages between all HS6 product codes, we map this data to trade flows, resulting in a dataset with dimensions of 120 countries × 1,200 HS4 codes × 1,200 HS4 codes × 11 years, totaling 1.9 billion potential data points. This mapping captures the likely purpose or use of a trade transaction, distinguishing between final goods consumption and intermediate use in production processes.

3.3 Qatar Trade Data

Our study uses foreign trade data published by the Planning and Statistics Authority of Qatar.[9] For each month between January 2012 through June 2023, the data report value and volume (weight) of imports aggregated at the product category and country of origin level. The product categories follow the 8-digit Harmonised System (HS), embedded in the international 6-digit HS published in 2012 by the World Customs Organisation (WCO). We construct a balanced panel covering 102,715 combinations of product category and country of origin, giving 12.9 million observations across 10 years and 6 months. For exports, we similarly create a balanced panel covering 9,258 combinations of product category and target country, giving 1.3 million observations across 12 years and 6 months.[10]

available (e.g. can be found here) for those wanting to convert AIPNET to a different HS vintage .

[8] For computational reasons, we focus on the overall flows of imports into a country rather than the country-of-origin dimension.

[9] The data is available at https://www.psa.gov.qa/en/statistics1/ft/pages/default.aspx.

[10] As our treatment variable is defined at the product category level of imported goods, we restricted the export data to product categories that saw imports in 2016.

3.4 Validation sources

For validating AIPNET, we used four key data sources. First, we employed the United States' Bureau of Economic Analysis (BEA) Input-Output Tables (IOTs) and Supply-Use Tables (SUTs) from 2017, which record transactions and product flows across industries. These empirical tables, including the Use table and the Direct and Total Requirements tables, were compared to our network to validate production relationships.

Second, we utilized the product complexity index (PCI) developed by Stojkoski, Koch, and Hidalgo (2023), which ranks products based on the diversity and sophistication of the know-how required for their production.

Third, we used the measure of product 'upstreamness' proposed by Antràs et al. (2012) and Fally (2012), which indicates the average distance of industries from final consumption within the supply chain, providing insights into each industry's strategic positioning.

Fourth, we analyzed differences across product types using end-use categories from the UN's Broad Economic Categories (BEC) classification (Rev. 5), which maps HS6 codes to broad end-use categories: capital, consumption, and intermediate.[11] BEC classifications offer product-level end-use categorizations, while our measure provides product-dyad level vertical relationships. To compare our linkage type to BEC's product-level end-use, we determine the predominant (i.e., modal) linkage type of an HS product.

3.5 AI Model: GPT-4

GPT-4, developed by OpenAI, is a state-of-the-art foundational AI model renowned for its role in powering 'ChatGPT 4'. It features billions of parameters, enabling it to perform complex language understanding and generation tasks with high accuracy. GPT-4 is pre-trained on a diverse corpus that includes books, academic papers, websites, and

[11] We compare the "consumption" BEC category to our AIPNET's "final" goods, and the intermediate goods are categorized into "primary" and "processed," where we compare the "primary" ones to our "raw" materials.

other text sources, encompassing a wide range of topics and detailed descriptions of production processes and product characteristics. This extensive pre-training allows GPT-4 to have a nuanced understanding and human-level judgment in various contexts.

For AIPNET, we leveraged the model's capabilities through the File Retrieval Enabled Assistant (RAG) system, which enhances the model with specific data inputs. This method ensures precise and relevant information extraction, facilitating the construction of detailed network representations. The scalability and efficiency of GPT-4 make it an essential tool for our analysis, allowing us to process and integrate vast amounts of data effectively.

4 Building and Validating the AI-built Production Network (AIPNET)

In this section we introduce the AI-built Production Network, or AIPNET. We built AIPNET to address a number of problems with the existing production networks. First, there is very limited data which link products along the production process. What little exists is either very hard to get hold of (e.g. VAT firm-to-firm transactions), is highly aggregated (Input-Output Tables), or else is limited in terms of coverage (e.g. Compustat firm-to-firm sales). Third, these data products capture observed transactions rather than some latent technological process governing production. In some cases, this might be an advantage, but in other cases relying on observed transactions can censor the data (e.g. due to vertical integration), be subject to strategic manipulation (e.g. transfer pricing), or be explicitly correlated with the objects being subsequently studied within this network (a form of network endogeneity).

To overcome these measurement challenge, we built a network data product (AIPNET) which maps the input-output relationships across 5,648 Harmonized System (HS) product groups. Each product group features as a node in the network, with nodes connected via discrete and directed edges. Each edge connects a source node (a prod-

uct) which is used in the production of the target node (another product). We do this without relying on any direct measures of economic transactions. Instead, we utilise the latent production processes associated with each product, and back-out the full network structure from rich textual data describing these processes.

4.1 Graph Notation

Formally, AIPNET is a directed discrete graph $\mathbf{G} = (\mathbf{W}, N, L)$ which consists of a *triple*; an edge set $\mathbf{W}$, the set of product nodes N, and the mapping from all edges to their linkage type t. For two product nodes $i, j \in N$ let i be the input product node and j is the output product node, and let w_{ij} be an entry in edge matrix $\mathbf{W}$. If $w_{ij} = 1$ then the source product node is an input into the production process of the destination node j, otherwise $W_{ij} = 0$. Finally, L_{ij} classifies each non-empty edge into one of: capital (k), raw materials (r), or intermediate (m)[12]. We shall often denote the linkage type using a superscript on the entry in the edge matrix, i.e. $W_{ij}^{k} = 1$ denotes that i is used as a capital input in the production of j.

4.2 Examples

To fix ideas, consider some examples: The *printing press* (HS 8443.11) is used as a capital input in the production of *newspapers* (HS 4902.10). Various *enzymes* (HS 3507.90) are a crucial intermediate input used to produce *insulin* (HS 3003.31), and copper ore (HS 2603.00) is a raw material used to make copper cathodes (HS 7403.11), which then get turned into copper wire (HS 7408.11), which ultimately end up in things like computed tomography (CT) scanning equipment (HS 9022.12). Figure 1 provides some additional visualisations of these network structures[13] These examples highlight different types of goods: a consumer-facing non-durable good (Insulin), an essential capital input (Printing

[12] Definitions of all three here.

[13] Each figure presents a one-degree network (i.e., direct connections) of a single focal product. Node size is proportional to authority centrality, as detailed in Section 4.4.

Press), a final good often consumed by Government (Military Artillery Weapons), and a crucial raw material used in a broad range of downstream products (Copper Ores).

(Figure 1)

4.3 Extracting Input-Output Linkages using AI

Most people know that you need a printing press to print a newspaper. Far fewer people can list the enzymes used while synthesizing insulin, however this information is accessible in seconds through a simple web search. For most if not all of the product nodes contained within AIPNET, the set of input-output relationships are either quite obvious or a simple web-search away. The challenge one faces in building the network of input-output linkages over the full universe of HS product codes is not one of information availability, but rather one of efficient information synthesis at scale. This challenge is ideally suited to the latest pre-trained AI language models, whose training over vast corpora of documents, web-pages, books, transcripts, and myriad other sources gives them sufficient detail on just about every production process imaginable.

In order to build AIPNET, we first adopt a leading foundational AI model called GPT-4, best known as the model which powers 'ChatGPT 4'. The pre-training of GPT4 already spans the requisite information needed to detail the input-output structures, though we still had to overcome three key challenges in order to leverage this model effectively: First, the model needed to be tailored to our specific data extraction task. We did this through 'prompt-tuning', a method of providing custom instructions which compel the desired output. Second, the model was not sufficiently versed in the nomenclature of Harmonized System (HS) product codes.[14] To ensure the AI model consistently made accurate references to the HS nomenclature, we supplied it both the names, numerical values, and textual descriptions of all size-digit HS product codes available from the

[14]This was a large issue, as the model would hallucinate the numerical codes and incorrectly assign products to codes which did not match. It had clearly learnt the basic idea that codes were numerical and had technical-sounding names, but could not recover specifics.

World Customers Organization (WCO).[15]. Third, we needed to develop an iterative process by which the model could systematically fill in the relevant graph/network structure.

We summarise the overall pipeline of building AIPNET in Figure 2, which highlights the key steps involved. Appendix A further documents the considerations at each stage of the process, and how we operationalised the latest AI tools to populate the entire network structure over HS product codes. Some example subnetworks for specific product nodes, as retrieved from AIPNET in text form, can be found in appendix section A.3.

(Figure 2)

4.4 AIPNET visualisation

Figure 3 visualises AIPNET, where each node corresponds to a Harmonized System (HS) 6-digit product code, and edges represent vertical production relationships. The layout, derived using force-based layout algorithms, organizes nodes into clusters by predominant linkage type. We show nodes colored and clustered according to their linkage type: raw materials in yellow, intermediary inputs in grey, capital inputs in blue, and final goods in green. This panel introduces the graph's logical progression in an x-y dimensional framework, where nodes increase in size—indicating higher authority centrality—as we move from left to right and from bottom to top, especially evident in capital and final goods sectors.

(Figure 3)

4.5 Network Descriptive Statistics

Table 1 summarizes the structural properties of AIPNET at two levels of product aggregation: HS6 and HS4. At the HS6 level, the network includes 5,648 nodes and 55,719

[15]Specifically, we downloaded and formatted all the information found on www.wcoomd.org

edges, with an average degree of 20.2 and a low network density of 0.0018. This indicates a highly interconnected but sparse network typical of large-scale production systems. The global clustering coefficient is 0.0205, showing that direct connections are rare among goods linked to the same third good. Assortativity is near zero (0.0016), meaning no strong preference for nodes to connect with others of similar degree, and the network has two connected components, with the largest containing 5,646 nodes.

At the HS4 level, the network is more aggregated with 1,253 nodes and 40,710 edges. The average degree increases to 65.0, and the network density rises to 0.0260, indicating more direct connections among goods. The global clustering coefficient is higher at 0.1620, suggesting greater clustering at this broader level. Assortativity is slightly negative (-0.0843), showing a tendency for nodes to connect with nodes of different degrees. This network forms a single connected component, highlighting its integrated structure.

(Table 1)

These properties illustrate the rich complexity of production networks at different levels of detail. A full description is available in Appendix A.5, with heterogeneity analyzed by upstreamness and product complexity index (PCI) in Appendix A.6.

4.6 Validating AIPNET using Input-Output Tables

One commonly used source of information on the structure of production networks is the Input-Output Tables (IOTs) and Supply-Use Tables (SUTs) published by many national statistics authorities. The IOTs record transactions across industries, whereas the SUTs show the products and services being used and produced across each industry.[16] Conceptually, the IOTs/SUTs are based on a domestic economies transactions. This is vastly different to the way AIPNET was built, which instead utilises the vastness of the

[16]This is often refered to by statistical authorities as 'balancing the SUTs'. This involves compiling the unbalanced SUTs from raw data inputs, which span the three different views of total GDP, namely the production, expenditure, and income view. In theory, these three views of GDP should equate, and so the balancing procedure seeks to impose this accounting restriction by apportioning data across different products and industries in the economy.

textual pre-training in recent LLMs to recover relationships between traded products. Nonetheless, we compare the data driven vs text-driven objects for validation.

For this comparison, we collect data from the IOTs published by the United States' Bureau of Economic Analysis (BEA). The BEA periodically produces industry-level Input-Output tables derived from the economic census and complementary sources at the Department of Commerce (Horowitz & Planting, 2006, give detailed accounts of the methodology). We employ the 2017 version obtained from the Bureau of Economic Analysis, U.S. Department of Commerce (2022). These are the latest detailed versions of the Use table, the Total Requirements table, and the Direct Requirements table.

The *Use table* is a matrix of approximately 402 commodity-producing and 402 receiving industries. Thus, a square in the matrix reports the value of commodities produced by industry i consumed by industry j. The BEA-industry classification closely corresponds to the NAICS classification.

Requirement tables augment the Use tables with the Supply tables, which report the outputs of a given industry and its end-users. With that, the BEA infers the share of inputs from industry i used to produce a dollar output of industry j. The *Direct Requirement table* accounts for immediate inputs while *Total Requirement table* additionally accounts for inputs required in upstream industries. Overall, the Requirement tables, especially the Direct Requirement table, come closest to describing the inputs required for producing an industry's goods. Thus, these are the empirical BEA measurements that come closest to what our network measures.

To bring our network to the BEA-industry level, we use the correspondence table for 6-digit HS codes and BEA-industry codes by Antràs et al. (2012). Our 6-digit code network is generally more granular with 5'121 product codes and assigns a binary variable, taking the value 1 for connected dyads. As multiple product dyads often map into a single industry dyad, we take an average of the binary connection values in our network. We then standardize both the I-O-table values and the network scores. A drawback of aggregating our network using the partly outdated and incomplete correspondence table

is considerable loss. We remain with approximately 205 BEA industries.

Our comparison of AIPNET to the US official economic structure is performed using the below regression model:

$$Y_{i,j} = \beta N_{i,j} + U_i + D_j + \epsilon_{j,i} \tag{1}$$

where $Y_{i,j}$ denotes the inputs produced in industry i by industry j according to the BEA Input-Output tables. $N_{i,j}$ is an aggregated industry-level score and indicates whether, according to our network, industry i's output is a required input for industry j's production. U_i and D_j are either sector-specific intercepts for the sectors of industries i and j or industry-specific intercepts for the industries i and j.[17]

The binscatter plots in figure 4 visualise the strong positive relationship between the empirical networks derived from Input-Output tables and our network. In line with our prediction, the Network score explains the variation best in the Requirement tables, specifically the Direct Requirements table. While the Use Value responds only marginally, albeit significantly, to an increase in the Network score, the requirement shares increase by approximately 0.16 standard deviations for total and direct requirements. Thus, our assumption that the network is able to model production relationships which manifest in empirical accounts of inter-industry trade appears credible.

Appendix Table A.4 reports the regression outputs of equation 1. We regress the standardized Input-Output values on the standardized network scores without fixed effects in columns (1), (4), and (7), with upstream and downstream sector-fixed effects in columns (2), (5), and (8) as well as with industry-fixed effects in the remaining columns. The coefficient can be interpreted as the standard deviation increases in the Input-Output value as our Network score increases by one standard deviation.

(Figure 4)

[17]The BEA categorizes industries into 23 sectors.

4.7 Validating AIPNET using Other Product-level Network Statistics

In the section we explore the relationships between AIPNET and two widely utilised product-level production network statistics. The first is the product complexity index (PCI) developed by (Stojkoski et al., 2023).[18] The second is the measure of product 'upstreamness' proposed by (Antràs et al., 2012; Fally, 2012).[19] We compare the node authority centrality of each product node in AIPNET to both the PCI and 'upstreamness' measures.[20]

Figure 5 depicts bin-scatter plots comparing authority centrality from the AIPNET network against both PCI and 'upstreamness'. This strong linear relationship between these measures suggests that products which are central in the AIPNET production network tend to be those with higher complexity, possibly indicating that more sophisticated and technologically advanced products also play crucial roles in the network's structure.

(Figure 5)

[18]The PCI ranks the diversity and sophistication of the productive know-how required to produce a product. Products with a high PCI value (the most complex products that only a few countries can produce) include electronics and chemicals. Products with a low PCI value (the least complex product that nearly all countries can produce) include raw materials and simple agricultural products. In our analysis, we average yearly PCI data from 2008 to 2022 for HS6 and HS4 level products, allowing us to assess the aggregate complexity of products over time.

[19]Upstreamness measures the average distance of industries from final consumption within the supply chain (Antràs et al., 2012; Fally, 2012). This measure contextualizes each industry's position in the sequential production process. Higher values of upstreamness signify a greater distance from final consumer use, implying a predominant role in the earlier stages of production chains. This metric is crucial for understanding the strategic positioning of sectors within the entire production landscape, providing insights into how industries are interconnected and the flow of goods from raw materials to finished products.

[20]Derived from hyperlink-induced topic search (HITS) algorithm originally used in the analysis of inbound link structures on the web, Authority Centrality is employed here to evaluate the importance of products in the production network. Unlike other centrality measures such as Degree, Closeness, or Betweenness, Authority Centrality specifically quantifies the "draw" or attractiveness of a node within a directed network. It is particularly pertinent for our analysis as it helps identify key products that act as critical nodes—those which receive a high number of connections from other 'hub' nodes within the network. This characteristic makes Authority Centrality especially relevant for understanding the global supply chain, as it highlights products that, while possibly not central in a traditional geographic or volume-centric view, hold significant sway due to their critical positioning in the production processes. The average Authority Centrality for all HS6 products is 0.18, while all upstream products average at 0.17. Notably, capital goods exhibit a significantly higher average centrality of 0.30, followed by intermediary goods at 0.17, and raw materials at 0.11. This is intuitive as we expect a product's centrality to increase as the nature of product becomes more involved. The result is very similar with HS4 products or with use of medians rather than mean.

Conversely, there is a negative correlation between Upstreamness and Authority Centrality (subfigure 5b). This finding could imply that products closer to the final stages of production chains are more likely to be central in our production network model. It reflects the notion that while raw and intermediary inputs (which are typically more upstream) are essential, the critical control points in the network—often related to final product assembly or sophisticated processing stages—hold more centrality as defined by Authority measures.

These relationships are also robust to the granularity of products. Results are robust to various transformations of the variables: Z-score transformation or Inverse hyperbolic sine transformation. See Appendix table A.3 for details of these regressions at both six- and four-digit HS levels.

Network representation We can visualise the relationship between authority centrality from AIPNET with some of these other measures. In Figure 6 we present a multi-panel visualization of the production network, where each node corresponds to a Harmonized System (HS) 6-digit product code, and edges represent vertical production relationships. Panel (a) serves as the baseline plot, and is reproduced from figure 4.4. Once again, this panel introduces the graph's logical progression in an x-y dimensional framework, where nodes increase in size—indicating higher authority centrality—as we move from left to right and from bottom to top, especially evident in capital and final goods sectors. Subfigure (b) retains this layout but changes node colors according to UN's Broad Economic Categories (BEC) classification (Rev. 5), revealing the missing granularity within each linkage type and highlighting classification mismatches, particularly in non-capital categories.. Subfigure (c) transitions to coloring nodes by Upstreamness from red (low) to blue (high), visually emphasizing the negative relationship between authority centrality and upstreamness. Finally, subfigure (d) colors nodes based on the Product Complexity Index (PCI), from red (low) to blue (high), underscoring a trend where larger nodes, indicative of higher centrality, generally display higher PCI, suggesting a discernible

correlation between node centrality and complexity within the economic network.

(Figure 6)

4.8 Validation of AIPNET with Permuted Networks

To further validate the robustness of AIPNET, we conducted three exercises involving permuted networks. These exercises assess the network's structure and its explanatory power for various economic measures. The exercises are: (1) stratified permutation, (2) perturbation intensity, and (3) temperature parameter robustness. Each exercise employs a specific methodology to test different aspects of AIPNET's robustness.

Stratified Permutation To validate AIPNET, we compared it against stratified permuted networks. These networks were created by randomly reassigning connections within the constraints of HS2 product categories while preserving the original degree distribution. This method ensures each node retains its in-degree and out-degree, maintaining the overall connectivity pattern while altering specific connections. This approach is akin to block-level randomization, ensuring that some hierarchical structure is preserved.

For each permuted network, we calculated the authority centrality for each product node. We then performed regressions of various economic measures against the true and permuted networks. For the Direct Requirements from the IO tables, we performed separate regressions of the direct requirement values on AIPNET connections for each permuted network. For PCI and upstreamness, we calculated the authority centrality for each permuted network and compared these centrality scores with PCI and upstreamness data, recording the R^2 values and regression coefficients for each permuted network.

In Figure 7, we present the results of this validation process. Subfigure 7a shows the distribution of R^2 values from regressions of Direct Requirement IO table values against AIPNET connections for the permuted networks, with the true network's R^2

value highlighted in red. This demonstrates that the true network's R^2 value is an outlier compared to the distribution of R^2 values from the permuted networks, indicating significantly stronger explanatory power for Direct Requirements.

Subfigure 7b presents the kernel density plot of R^2 values from regressions of PCI on AIPNET authority centrality, with the blue-shaded density representing the distribution of R^2 values from the permuted networks and the red dashed line marking the R^2 value from the true network. Similarly, Subfigure 7c displays the kernel density plot of R^2 values from regressions of Upstreamness against AIPNET authority centrality, with the true network's R^2 highlighted in red. In both cases, the true network's R^2 value is an outlier compared to the permuted networks' R^2 values, underscoring the significant role of AIPNET authority centrality in explaining both PCI and Upstreamness in the true network.

These results collectively validate AIPNET. The consistent outlier status of the true network's R^2 values across different economic measures provides strong evidence that the relationships captured by the true network are not due to random chance but reflect meaningful economic connections.

(Figure 7)

Perturbations to AIPNET To further examine the robustness of AIPNET, we systematically perturbed the network 1000 times by varying the intensity of edge rewiring from 1% to 100%, in steps of 0.1%. For each intensity level, we rewired the network using the Erdos-Renyi random graph model, ensuring the network retains its structural properties while introducing controlled randomness. This approach aligns with the principles of the Erdos-Renyi random graph model (Erdos, Rényi, et al., 1960), where edges are added between nodes with a certain probability (dictated by perturbation intensity). In our case, each edge in the original network has a probability corresponding to the perturbation intensity of being rewired, creating a randomized version of the network while preserving the number of edges.

For the IO tables, we performed separate regressions of the direct requirement values on AIPNET connections for each perturbed network. For PCI and upstreamness, we calculated the authority centrality for each perturbed network and compared these centrality scores with PCI and upstreamness data, recording the coefficients and the coefficient of variation (CV) for each level of perturbation. The coefficient measures the strength of the relationship between the network connections and the economic measures, while the CV indicates the relative variability of the coefficient estimates.

Panel I of Figure 8 shows the coefficients for the IO Table (Direct), PCI, and Upstreamness as perturbation intensity increases. Panel II displays the corresponding CV for the same measures on a logarithmic scale. As perturbation intensity increases, the coefficients for all three measures approach zero, indicating decreased explanatory power, while the CV increases, reflecting higher relative variability. This demonstrates that AIPNET's structure captures meaningful economic relationships that degrade predictably with increased noise, validating its robustness and sensitivity to perturbations. Refer to Appendix Figure A.1 for illustrations of the network perturbations at 25% and 75% intensity levels.

(Figure 8)

Temperature Parameter Robustness To assess the robustness of AIPNET under different model configurations, we systematically varied the temperature settings (0%, 25%, 50%, and 100%) and compared the generated networks to the baseline network with a temperature of 0%. The primary metrics of comparison are the overlap of edges (binary: true or false) and, conditional on overlap, whether there is agreement on the linkage type of edges (capital, raw, intermediary).

The temperature parameter in language models controls how deterministic the model output is. A temperature setting of 0 makes the model highly deterministic, often resulting in repeated phrases, while higher temperatures introduce more variability and

randomness in the generated outputs[21].

To conduct this exercise, we randomly selected 100 HS6 nodes from the full set of HS6 nodes used to create our network. For each node, we prompted the RAG assistant 10 times for each temperature setting with non-zero temperature (i.e., 25%, 50%, and 100%). This resulted in 100 HS6 codes times 10 iterations times 3 temperature settings. For the temperature setting of 0, we prompted once for all 100 HS6 codes since this setting is deterministic and does not require multiple iterations. The 10 iterations for non-zero temperatures provide a sample over which we can compute the summary statistics of relationships. Our goal is to analyze the overlaps and agreement as described.

As shown in Figure 9, the results indicate that conditional on overlapping edges, the mean proportion of agreement remains relatively consistent across different temperatures, with a very slight decline as the temperature increases. Specifically, the 25% and 50% temperatures exhibit the highest mean proportion of agreement, followed by 0% and then 100%. This suggests that lower and medium temperatures produce more reliable results in terms of agreement with the baseline network.

Additionally, the number of overlapping edges is highest at 25%, slightly decreasing at 50%, and further decreasing at 100%. This indicates that higher temperatures result in less overlap with the deterministic network (temperature of 0%), likely due to increased variability and randomness in the responses.

To further explore the effect of maximum randomness (temperature 100%), we analyzed the modal network, which represents the most frequent edges across all generated networks at this temperature. The modal network achieved a percentage overlap of 63%, significantly higher than the average of 38.5%. The linkage type agreement, conditional on overlap, slightly decreased to 72.5% from 73.9%.

These findings highlight that while higher temperatures introduce more variability, the generated networks still maintain a considerable degree of similarity to the base-

[21]While exploring how the temperature parameter influences graph structure is interesting, note that this is quite different from hallucinations. Hallucination refers to cases when a model makes a statement absent in its training data. Higher temperatures do not eliminate hallucinations; they simply make the model's outputs less deterministic.

line network, especially when considering the modal network. This robustness check demonstrates that AIPNET's performance is relatively stable across different temperature settings. The full summary statistics can be found in the Appendix Table A.1.

(Figure 9)

5 Supply Shocks and On-shoring

We begin by studying patterns in trade along AIPNET production linkages. To do so, we build a quasi dyadic data structure that emulates trade data as if we observe trade-flows disaggregated in a *use-specific* fashion. The key intuition is that while traditional trade statistics only observe the gross import/export flows between each country-pair and good, the binary linkages that are captured in AIPNET allow the inferring of the potential use of each import as an input for either domestic input as an intermediary use or for final goods consumption.

We leverage this data first in a fully reduced-form fashion documenting that, over time, imports of goods that serve as capital inputs in particular strongly increase. This shift is particularly visible from 2016 onwards for capital goods. Constructing a more direct measure of supply shocks capturing more permanent price shocks for downstream goods, we note that such shocks are significant drivers of imports of upstream goods.

5.1 Global Trade Data

We leverage a global trade dataset that encompasses dyadic trade data for 120 leading economies worldwide, spanning from the year 2012 to 2022, obtained from UN Comtrade. It covers all goods classified under the Harmonized System (HS) at the 4-digit level (HS4), on an annual basis.[22] That is, the dataset in its raw form has a dimensionality covering 120 countries $\times$ 1,200 HS4 goods $\times$ 11 years, or around 1.58 million rows of

[22]We ignore the dimension of country-of-origin of imports and focus on the overall flows of imports into a country for computational reasons.

data[23].

Given that we have identified input-output linkages between all HS 6 product codes, we map this data to trade flows. This results in the data having dimensions of 120 (countries) $\times$ 1,200 (HS4 codes) $\times$ 1,200 (HS4 codes) $\times$ 11 (years) = 1.9 billion potential data points. The implicit assumption is that this data captures the likely purpose or *use* of a trade transaction, with potential uses being either final goods consumption or use as an intermediate good in some other production process. For example, rice may be imported and nearly directly sold to end consumers without much processing, or it could be further processed to make rice pudding. While we do not observe the specific use of each import transaction from the aggregated trade data, patterns and signatures of likely purposes should be detectable. As countries develop economically, we expect to see increased imports of capital equipment, in particular, which supports the production of other goods.

5.2 Non-parametric pattern in import's across supply chain

We begin with a reduced-form and non-parametric analysis. We study – over time – how imports of upstream goods evolve over time along value chains. This analysis uses a fully-dyadic dataset to investigate the patterns of trade for goods involved in input/output production relationships. Specifically, we observe the imports of "unfinished" or "upstream" goods into countries, identified through the AIPNET linkage indicator. This indicator marks whether an upstream good serves as an input in the production of a downstream good.

[23]The ideal trade dataset would include purpose or activity-specific import data, observing imports linked to the production of specific goods. This would allow us to see the input j used in the production of finished good i from country c in year t, denoted as y_{ijct}. However, publicly shared data typically provides total imports without linking them to their specific or intended use, showing only y_{ict} and y_{jct}, where goods i and j may not be linked in an input/output relationship. Nevertheless, we have strong reasons to believe that some imports of good j may occur as part of an input in the production of good i.

Specification We study this entirely non-parametrically through estimating the following baseline specification:

$$\text{Import}_{u_{hs4},c,t} = \beta_t \times W_{u_{hs4},f_{hs4}} + \alpha_{u_{hs4},f_{hs4},c} + \eta_{u_{hs2},c,t} + \epsilon_{u_{hs2},f_{hs2}} \tag{2}$$

Here, the dependent variable is the import of upstream 4-digit goods u_{hs4} into country c in year t. $W_{u_{hs4},f_{hs4}}$ is our binary linkage indicator that captures whether a specific upstream good u_{hs4} serves as an upstream good (i.e., input, capital good or raw material) in the production of a downstream good f_{hs4}. For example, rice may serve as an upstream good to produce rice pudding in a food processing plant.

This binary indicator comes directly from AIPNET, that is:

$$W_{u_{hs4},f_{hs4}} = \begin{cases} 1 & \text{if input } u_{hs4} \text{ is a capital, raw or intermediate input for } f_{hs4} \\ 0 & \text{otherwise} \end{cases}$$

Our baseline specification adjusts for dyad by country specific fixed effects, $\alpha_{u_{hs4},f_{hs4},c}$, which accounts for idiosyncratically higher levels of imports for each potential use of an upstream good u_{hs4}. Note that while the level of the trade data is not specific at the transaction or the specific *use*, we expect to see, for example, notable level differences in trade along existing value chains that implicitly capture the underlying use of a downstream good.

We also adjust for country- and HS2-digit specific non-linear time trends, $\eta_{u_{hs2},c,t}$. These capture non-linear country-specific time trends in demand of imports for broad classes of goods (2-digit HS level). These measures capture terms-of-trade shocks more generally, account for the country-specific domestic economic cycle and broad measures of time-varying preferences or tastes.

We estimate the above specification flexibly to obtain a vector of coefficients β_t capturing the evolution of imports of goods that have a supply-chain linkage, $W_{u_{hs4},f_{hs4}} = 1$ vis-a-vis those that do not. This allows us to study to what extent there are differential

trends in imports of goods along value chains over time to allow us to detect potential trend-breaks.

Results The results from this analysis are presented in Figure 10. The left Panel A focuses on the incidence of imports (i.e. Import > 0), while the right panel focuses on the import volume measure, specifically the log of Imports. We observe that from 2016 onwards there has been a notable change in trend suggesting increased imports of goods that have I/O linkages, suggesting potential localisation developments.

(Figure 10)

Linkage type We conduct a pooled estimation to study how imports of value-chain linked goods have changed after 2016, considering different linkage types. The following specification estimates linkage-type specific heterogeneity using a subscript for linkage type:

$$\text{Import}_{u_{hs4},c,t} = \beta_l \times I(t > 2016) \times W_{u_{hs4},f_{hs4},l} + \alpha_{u_{hs4},f_{hs4},c} + \eta_{u_{hs2},c,t} + \epsilon_{u_{hs2},f_{hs2}} \tag{3}$$

The specification builds upon the baseline specification 2, adding an interaction term $I(t > 2016)$ to the pool the effects post 2016. We also add the linkage type l dimensionality to the binary linkage indicator.

In Figure 11, we present the results from this pooled estimation, depicting a coefficient plot of β_l. This figure allows us to understand the differential impacts of supply-chain linkages on import patterns post-2016, highlighting the specific roles of raw materials, intermediary inputs, and capital goods.

(Figure 11)

We observe notable heterogeneity: on the extensive margin of any trade (panel A), we note that this dimension is particularly responsive to capital goods. That is, there

are more likely to be any capital goods imports in value-chain links post-2016. This is not surprising given that we would expect capital goods to be less frequently traded and imported. However, it is important to note that since we focus on the 120 large economies, the extensive margin of any trade is particularly suitable for smaller countries. On the intensive margin (panel B), we see that increases in imports post-2016 along supply chains are particularly prevalent for intermediary and capital goods.

The focus of the analysis on a reduced-form post 2016 estimation is motivated by the non-parametric difference-in-differences exercise. In the next part we impose some structure by specifically focusing on supply shocks as a potential driver of the dynamic that is observed since 2016.

5.3 Persistent price shocks and localization

In order to study the impact of downstream supply shocks on upstream imports, we need to measure or capture what may constitute a price shock. We do this by studying trade data from 2002 to 2022 and extract (persistent) price shocks from the trade data.

Measuring persistent price shocks to finished goods We use unit-price indices capturing the ratio of the import value and the import volume.[24]

In a first step we remove idiosyncratic good and country-specific level differences ($\nu_{d_{hs4},c}$) in the import price indices $p_{d_{hs4},c,t}$. $\nu_{d_{hs4},c}$ may capture time-invariant country-specific price levels. We also remove broader good group specific non-linear price shocks ($\eta_{d_{hs2},t}$), which may capture general supply- or demand imbalances within similar class of goods. That is we estimate:

$$p_{d_{hs4},c,t} = \nu_{d_{hs4},c} + \eta_{d_{hs2},t} \tag{4}$$

We then obtain the residuals from this regression, denoted as $\hat{\varepsilon}_{d_{hs4},c,t}$, and code an

[24]This measure may be distorted by year-on-year changes in quality in the respective import bundle. Our price-shock definition specifically looks for structural changes in prices that persist idiosyncratic changes.

outlier if a specific good d_{hs4} has an above-median positive residual. We create a binary indicator:

$$\mathbb{I}_{\hat{\varepsilon},t} = \mathbb{I}\left(\hat{\varepsilon}_{d_{hs4},c,t} > \text{median}(\hat{\varepsilon}_{d_{hs4},c,t}) \cap \hat{\varepsilon}_{d_{hs4},c,t} > 0\right) \tag{5}$$

We classify a persistent positive price shock as a sequence of positive above-country and good-specific median price residuals for three consecutive periods:

$$\text{Shock}_{d_{hs4},c,t} = \begin{cases} 1 & \text{if } \mathbb{I}_{\hat{\varepsilon},t} = 1, \mathbb{I}_{\hat{\varepsilon},t-1} = 1, \mathbb{I}_{\hat{\varepsilon},t-2} = 1 \\ 0 & \text{otherwise} \end{cases} \tag{6}$$

We present the results in Figure 12, which illustrate the trends and geographic distribution of persistent price shocks. Panel A shows that from 2016 onwards, there has been a notable increase in the number of finished goods experiencing persistent positive price shocks. This trend indicates a significant shift in the price dynamics of finished goods in the global market. Panel B maps the geographic distribution of the count of these supply shocks post-2016, highlighting that these shocks are not uniformly distributed but are concentrated in specific countries and regions.

(Figure 12)

Impact of persistent price increases on imports of linked raw, intermediate and capital goods We now focus on the time-variation in persistent price shocks that implicitly embed structure:

$$\text{Import}_{u_{hs4},c,t} = \nu \times \text{Shock}_{f_{hs4},c,t} \times W_{u_{hs4},f_{hs4}} + \xi \times \text{Shock}_{f_{hs4},c,t} + \alpha_{u_{hs4},f_{hs4},c} + \eta_{u_{hs2},c,t} + \epsilon_{u_{hs2},f_{hs2}} \tag{7}$$

Here, the coefficient ν captures the differential effects on imports of upstream (unfinished) goods linked to downstream (finished) goods that have experienced a supply

shock. The coefficient ξ captures the direct effect of the price shock on finished goods, which may be confounded by or correlated with other country-level shocks (e.g., terms-of-trade shocks). In the case of onshoring or adaptation, we would expect $\nu > 0$, even if $\xi 0$.

Table 2 shows the impact of persistent supply shocks affecting downstream goods prices on imports of upstream goods. Column 1 is our main specification, which includes country-by-HS4 fixed effects and non-linear country-specific time trends for broad HS2 categories of goods. We find a statistically significant positive coefficient for the interaction term "AIPNET Link $\times$ Supply Shock" (0.0034), indicating that a persistent price increase in downstream goods leads to an increase in imports of linked upstream goods. This suggests that when the price of a finished good (e.g., gingerbread) increases persistently, there is a corresponding increase in the imports of intermediate goods or machinery used in its production (e.g., machinery for baking).

(Table 2)

The observed pattern suggests a clear linkage between persistent price increases in downstream goods and an increase in the imports of upstream goods, reinforcing the notion of onshoring or adaptation in response to supply shocks. We can speculate on the origin of these price shocks, but rather, we study their impact on patterns of trade.

Robustness Appendix Table A.5 presents regression results documenting the impact of persistent price shocks on downstream goods on upstream imports. The exercise explores robustness of the main effects to different definitions of the supply shock. Column (1) to (3) explore different definitions of the main supply shock measure that uses the regression filtering that was described in equation 4. Column (1) presents the main estimation. Column (2) defines the supply shock as a binary shock that persists at least 3 lags excluding the contemporaneous year. Column (3) classifies a shock based on a persistence in supply shock for four consecutive years. Columns (4) and (5) uses a Markov

switching model to identify shocks. Column (6) to (8) add the idiosyncratic outlier definition for the contemporaneous, and lagged years interacted with the AIPNET linkage dummy to document that the effects are not confounding idiosyncratic price shocks but rather capture structural or longer price shocks.

Effects by Linkage Type The results by linkage type are presented in Figure 13.

What is noteworthy is a pattern that we already observe. The effects appear strongest on intermediary goods imports, suggesting that supply shocks lead to substitution of imports along the value chain. This implies that firms adapt to shocks by importing more intermediary goods and raw materials as a temporary measure, allowing them to ”buy time” for further adjustments.

(Figure 13)

This pattern is not as strongly pronounced and clear in comparison to the post-2016 analysis by linkage type (i.e., in figure 11), which suggested the strongest effects for capital goods imports. This indicates that the supply shocks identified through our price shock filtering capture only a part of the story. The substitution effects observed here suggest a complex adaptation mechanism where firms adjust their import strategies based on the type of linkage and the nature of the shock.

5.4 Linking non-parametric reduced form findings to supply shock findings

Since 2016, marking the onset of wider deglobalization with geopolitical events such as the UK's vote for Brexit and the US election of Donald Trump, there has been a notable increase in the imports of connected upstream goods. This suggests that countries may have been adjusting their trade strategies to enhance local production capabilities.

These changes reflect an adaptation to the changing global trade environment, with increases in imports of capital and intermediate inputs, possibly driven by persistent

price shocks and the need for localized production amidst the perceived instability of global trade systems.

We observed that there is a notable increase in imports of supply-chain linked goods that starts from 2016 onwards across countries. We further documented that post-2016 there has been an increase in supply shocks that operate in a similar fashion along the supply chain.

The reduced form non-parametric findings for the post-2016 interaction and the exploitation of measured supply shocks retrieved from import price indices suggest that there may be a narrative overlap: countries exposed to post-2016 supply shocks are also those that saw an increase in supply-chain linked imports post-2016.

We can empirically test this hypothesis by estimating both regressions country-by-country. First, consider the following specification:

$$\text{Import}_{u_{hs4},c,t} = \beta_c \times \mathbb{1}(t > 2016) \times W_{u_{hs4},f_{hs4}} + \alpha_{u,f,c} + \eta_{u_{hs2},c,t} + \epsilon_{u_{hs2},f_{hs2}} \tag{8}$$

Here, by pooling the post-2016 regression coefficients (β_c), we estimate the differential impact across countries to examine the extent to which we see a pattern of imports consistent with the localization of (some) value chains.

We can now estimate both equation 8 and equation 7 to obtain a vector of reduced form estimates $\widehat{\beta}_c$ and $\widehat{\nu}_c$ and compare the estimated coefficients.

We present the results from this analysis in Table 3. The results show that the non-parametric post-2016 coefficients —- which we can think of as a bundle of narratives -— are to some extent explained by the supply shock story.

(Table 3)

To supplement this result, we present the map of distributions of the estimated elasticities across countries in Appendix Figure A.2. We also present a country-level scatterplot to visualize the relationship between $\widehat{\beta}_c$ and $\widehat{\nu}_c$ in Appendix Figure A.3.

The R^2 in Table 3 is unconditionally around 7%. This means our country-level supply shock elasticities explain 7% of the variation in the country-level post-2016 non-parametric elasticities. While this may seem modest, it is not negligible given the inherent noise in the data. This indicates that supply shocks are likely a non-negligible driver of the effects observed post-2016.

The trade war and the breakdown or fraying of the rules-based trading system following Brexit and Trump's election have resulted in countries benefiting from development through the import of capital goods.

6 Causal Evidence of On-shoring

The previous section documents trade patterns in granular cross-country trade data. We observed there was a significant shift pointing towards an increase in imports of upstream goods along value chains that we have measured in AIPNET. We further observed that this pattern, to a non-negligible extent may be linked to (persistent) supply shocks that became more prevalent since 2016. Given the exercise is cross-country, there may be concerns about causality. To complement the cross-country exercise we next present evidence that relaxes many identification assumption studying an economic blockade.

6.1 Context, measurement and descriptive evidence

The context of the 2017 diplomatic tensions between Qatar, Saudi Arabia, and other neighboring countries provides a near-perfect natural experiment to study onshoring. The conflict, which escalated into a trade blockade in June 2017, offers a unique opportunity to analyze how such geopolitical events influence trade patterns and drive economic localization. Qatar was highly reliant on agricultural and manufactured products from Saudi Arabia, with most imports shipped through Saudi Arabian ports.

In June 2017, a coalition of countries led by Saudi Arabia abruptly escalated the political conflict and imposed a trade blockade on Qatar. This blockade was eventually

lifted in January 2021. The timing of the blockade, along with the unique characteristics of Qatar's economy, makes this a compelling natural experiment. Qatar's GDP is less than 1% of the global GDP, making it a relatively small and open economy. Additionally, the Qatari Riyal is pegged to the USD, eliminating nominal exchange rate effects. Furthermore, Qatar's economy is resource-based with limited industrial or agricultural production capacity prior to the blockade.

We utilize the timing of the June 2017 diplomatic and economic blockade of Qatar by surrounding Gulf countries.[25] The key empirical data point used is the timing of the blockade, which we apply through a difference-in-difference analysis. We combine this with product-level exposure to this event, which is defined based on country-of-origin in the Qatari trade data (data used is described in section 3.3). We illustrate the pre-blockade trade patterns and the changes induced by the blockade in Appendix Figures A.4 and A.5.

Measurement of blockade Exposure To measure the initial impact of the blockade on Qatari imports, we construct an exposure measurement defined according to the volume or value of final goods coming from those countries which ceased trading with Qatar on June 5, 2017. We define a country c as first belonging to the set of all countries so that $c \in C$. Next, define the subset of all blockading countries as $B = \{UAE, KSA, Egypt, Bahrain\} \subset C$. Denote a product-level HS Code (or simply each 'good') as j. We define how exposed the importation of this good was to the blockade as:

$$BlockadeExposure_j = \frac{\sum_{c \in B} Imports_{j,c}}{\sum_{c \in C} Imports_{j,c}} \tag{9}$$

where j indicates a good, c indicates the origin country, and $Imports$ is the quantity or value of imports in 2016, before the blockade. $BlockadeExposure_j$ is bounded on the unit interval, taking a value of 1 if all imports of this good j were imported from blockading

[25] Appendix Figure A.8 shows a map of the countries that participated in the blockade in orange, which comprise the main quartet: Saudi Arabia, UAE, Bahrain, and Egypt, alongside some smaller allies such as Mauritania, Djibouti, and the Maldives.

countries B.

For each 8-digit product, we compute the share of imports prior to the blockade that is sourced from blockading countries in total imports. This allows us to estimate a simple difference-in-differences with a dosage effect, exploiting variation in exposure to the blockade across products j. The size of the supply shock depends significantly on good-specific blockade exposure, as there is substantial heterogeneity across products in their exposure to the blockade from blockading countries. Appendix Table A.7 lists the top 30 imports by volume across HS2 sections affected by the blockade.

Descriptive Evidence We document the blockade's impact on Qatar, highlighting two key facts: the blockade drove a large shift in trade patterns from blockading countries to the rest of the world and acted as a supply shock, leading to a 25 basis-point price increase and a 30 basis-point fall in trade volumes.

Appendix figure A.6 shows the rapid shift in import trade patterns that occurred after the blockade was unexpectedly introduced. Subfigure A.6a shows the total import trade value for all goods which are 'blockade-exposed', which we define as any HS 8-digit product code where the majority of import value in 2016 came from blockading countries. We see that the flow of trade abruptly falls after the introduction of the blockade, and a similar sized increase in trade value sourced from non-blocking countries. Subfigure A.6b shows the same analysis for all products, revealing a similar shift and highlighting how total trade volumes remained fairly stable.

Figure 14 shows how prices and trade volumes (i.e. weight-volume) were affected after the blockade. Both figures depict an index constructed using 2016 as the base year. In both subfigures, we consider only those goods which are blockade-exposed. Each index is calculated by first calculating the HS 8-digit product level index. In each half-yearly period, we then aggregate across products using a weighted mean, weighted using the total value of trade for each product in 2016. Panel A depicts the abrupt 25 basis point increase in blockade-exposed products and that this price increase was also

accompanied by a 30 basis-point fall in trade volumes. While these patterns are striking in and of themselves, we next outline an econometric design to test for the effects of blockade exposure–the share of 2016 imports sourced from blockading countries—on trade prices, expenditures, and volumes. The heterogeneous effects of the blockade are espoused in Panel B, which break both price and volume changes across broad HS section categories.

(Figure 14)

We provide illustrative examples of the on-shoring response to the blockade in Appendix Figure A.7. The subfigures depict the stock of up-stream capital and the import value of down-stream products these capital items can be employed to product. For example, subfigure A.7a shows the dramatic rise in dairy-producing machinery imported in response to the blockade, accompanied by the decline in dairy imports. While stylistic, these figures illustrate the mechanism we test for in the remainder of this paper.

6.2 Empirical Design

In this section, we describe how we estimate the effect of the blockade on own-product import prices, trade values, and trade volumes. We further consider the impact on the importation of vertically related products, which are necessary in the domestic production of each good. Across all these outcomes, our treatment measure is the product-level $BlockadeExposure$, outlined in Section 6.1.[26]

Direct Effect of Blockade Exposure Consider our baseline specification:

$$log(Y_{j,t}) = \beta \ PostJune2017_t \times BlockadeExposure_j + \alpha_j + \theta_t + \epsilon_{j,t} \tag{10}$$

[26]Recall our $BlockadeExposure$ measure is the fraction of each focal product's total trade value which was sourced from blockading countries in 2016

where j is a product, defined at the HS 8-digit level, t represents each time period, PostJune2017_t is a dummy variable which equals 1 for all year-months after June of 2017, $\text{BlockadeExposure}_j$ is a product's fraction of 2016 trade value that arrived from blockading countries, and α_j and θ_t are product and time fixed effects.[27]

The coefficient of interest is β, which represents the elasticity of our outcome measure with respect to the product-specific exposure to the blockade. A 1% increase in exposure leads to a β% increase in $Y_{j,t}$. The above specification can be further decomposed in order to measure the coefficient of interest, β, over time:

$$\log(Y_{j,t}) = \sum_{t}^{T} (\beta_t \times \theta_t \times \text{BlockadeExposure}j) + \alpha j + \theta_t + \epsilon_{i,t} \tag{11}$$

where again j is a product, defined at the HS 8-digit level, t represents each year-month, the sequences of $\{\beta_t\}_{t=1}^{T}$ contain the elasticity of product-specific exposure to the blockade on Y_{it} for each time period, including prior to and after the end of the blockade.

Lastly, we can decompose the specification across countries in order to recover heterogeneous changes in trade patterns across trading partners:

$$\begin{aligned}\log(Y_{j,c,t}) = {} & \beta \times \text{PostJune2017}_t \times \text{BlockadeExposure}_j \times \text{Blockading}_c \\ & + \gamma \times \text{PostJune2017}_t \times \text{BlockadeExposure}_j \times \text{NonBlockading}_c \\ & + \alpha_{j,c} + \theta_{t,c} + \epsilon_{j,c,t}\end{aligned} \tag{12}$$

where again j is a product, defined at the HS 8-digit level, c represents the trading partner (country), t indexes month and year, β contains the elasticity of product-specific exposure to the blockade on Y_{jct} for trade with countries that participated in the blockade and γ contains the same elasticity for trade with other countries.

[27] We also introduce alternative controls and fixed effects outlined in section 6.4, but we omit them from the formula for brevity.

6.3 Dyadic Regression Specification to measure on-shoring

Finally, we consider how trade patterns for upstream goods such as capital and intermediary inputs are impacted by the blockade exposure of downstream goods. Here we use a dyadic regression specification, where each observation is paired with a single upstream good j and a single downstream good i. Each product is related in our supply-chain network representation.[28] The aim of the regression is to assess the impact of downstream exposure on the importation of upstream capital and intermediaries, using specification:

$$\begin{aligned}\log(Y_{j,i,t}) = \beta \times \text{PostJune2017}_t \times \text{BlockadeExposure}_j \\ + \gamma \times \text{PostJune2017}_t \times \text{DownstreamBlockadeExposure}_{ij} \\ + \alpha_{j,i} + \theta_t + \epsilon_{j,i,t}\end{aligned} \tag{13}$$

where j is an upstream product, defined at the HS 8-digit level, i is an upstream product, defined at the HS 8-digit level, t represents each year-month. Fixed effects $\alpha_{j,i}$ and θ_t control for dyad-specific and year-month unobservables, respectively. We control for the potential direct effects of exposure for upstream good j by including $\text{BlockadeExposure}_j$, so as to ensure the estimates of γ recover only the on-shoring response.[29]

Since we are using dyadic data to represent a network structure, we cluster standard errors in Equation 13 both at the upstream product and downstream product level. Since our network is directed, we argue this is sufficient to avoid network-auto-correlation (see (Cameron & Miller, 2014)).

[28] See Section 4 for an overview of how we construct this network using our Large Language Model approach.

[29] Without this control, it is possible that we have omitted variable bias due to the fact that vertically related goods are correlated in their blockade exposure.

6.4 Results

6.4.1 Direct Effect of Blockade Exposure on Trade Patterns

We first show the results from a product-level difference-in-difference estimation approach outlined in Equation 10. Here, we use data for each 8-digit product in each month, collapsed across all countries. Our treatment is the blockade exposure of each good, defined as the share of import value sourced from blockading countries in 2016. Table 4 reports results across two different levels of fixed-effect saturation. Panel 4a includes 8-digit HS product level fixed effects, along with month dummies to account for seasonality, whereas 4b additionally uses year-month fixed effects, interacted with 6-digit product codes. We find that the blockade is consistent with a large supply shock. Column (1) shows that for each additional percentage of exposure, post-blockade prices increased by around 0.35%. Columns (2) and (3) show that a one percent increase in exposure drove down import values and volumes by between 1.5-2.7%. Column (4) shows the probability of a non-zero trading month also fell by between 0.11 and 0.19 percent for each additional unit of exposure. Finally, above pre-blockade levels of monthly trade were also reduced by blockade exposure, as shown in Column (5).

(Table 4)

We visualize the difference-in-difference setting for these direct effects of blockade exposure in Figure 15. We show that there is an abrupt and persistent increase in prices, and decrease in trade expenditures for goods which are more exposure to the blockade.

(Figure 15)

Appendix table A.6 corresponds to difference-in-differences-in-differences regression described in equation (13) of export data before the beginning and after the end of the blockade in January 2021. The results suggest that Qatar did not compensate for the long-term fall in imports by reducing exports to non-blockading countries. However,

the blockade had a lasting effect on trade relationships between the blockading countries and Qatar.

6.4.2 Effect of the Blockade on On-Shoring

Having established that the product-level blockade exposure induced a sizable supply shock in the previous subsection, we now turn to the key piece of analysis in this section. Table 5 uses a dyadic regression specification, where we consider product-pairs at the monthly frequency. We again use blockade exposure as our primary causal shock variable, but not differentiate between the blockade exposure of the upstream good (direct exposure) relative to the blockade exposure of the downstream good in each dyad. Panels (a) and (b) provide alternative degrees of fixed effect saturation, with the former controlling for dyadic fixed effects as well as a month dummy to absorb seasonality, and the latter additionally ads year-month controls. We run these specifications for up-stream goods which fall into Sections 1, 10, 15, 16, and 19 of HS product nomenclature, which represent the majority of raw material inputs and capital equipment.

(Table 5)

We find that there is significant evidence of 'on-shoring', namely that the down-stream exposure actually predicts an increase in imports of upstream goods. While the average treatment effect of down-stream exposure is dominated by the direct effect, we still see that one additional percentage of down-stream exposure increases imports by around a third of a percentage point. That this is significant and positive is strong evidence of on-shoring, especially given the onerous controls and likely attrition bias present due to sample pooling.

To further decompose the on-shoring response, we consider a more heterogeneous regression specification which allows for differential effects of down-stream blockade exposure on up-stream capital inputs vs intermediary inputs. Table 6 shows the results of this specification. We find that the on-shoring response is stronger for up-stream capital

inputs compared to intermediary inputs by a factor of 2. Even in this specification, we still find a significant positive effect of down-stream exposure across both input types.

(Table 6)

7 Conclusion

The resurgence of industrial policy, trade restrictions, and on-shoring is evident worldwide, driven by recent supply shocks, including the global pandemic and heightened geopolitical tensions. This paper introduces the AI-built Production Network (AIPNET), mapping input-output relationships across 5,648 Harmonized System (HS) product groups using large language models (LLMs).

Our analysis using AIPNET reveals a decrease in global imports of downstream goods relative to upstream inputs, indicative of production process localization. Persistent supply shocks after 2016 are identified as a key driver of these changes, with the strongest effects observed for capital goods imports, highlighting investments in domestic manufacturing capacity.

To causally identify the impact of trade shocks on on-shoring, we examine the blockade of Qatar in 2017. This quasi-experimental case study shows that a 5 percentage point increase in the price of a downstream product led to a 3 percentage point increase in imports of linked upstream goods.

AIPNET provides a valuable tool for understanding the evolving dynamics of global trade and production networks. Future research can extend this network to explore additional regions and shocks, enhancing our understanding of on-shoring and industrial transformation.

References

Alabrese, E., Fetzer, T., & Wang, S. (2024). Leveling up, by pushing down? *mimeo*(486).

Alfaro, L., Antràs, P., Chor, D., & Conconi, P. (2019, April). Internalizing global value chains: A Firm-Level analysis. *J. Polit. Econ.*, *127*(2), 508–559.

Alfaro, L., Bloom, N., Conconi, P., Fadinger, H., Legros, P., Newman, A. F., ... Wernerfelt, B. (2018). *Come together: Firm boundaries and delegation*. https://core.ac.uk/download/pdf/159070284.pdf. (Accessed: 2023-9-11)

Alfaro, L., & Chor, D. (2023, September). Global supply chains: The looming "great reallocation" [Working Paper]. (31661). Retrieved from http://www.nber.org/papers/w31661 doi: 10.3386/w31661

Allen, T., & Donaldson, D. (2017). The Geography of Path Dependence.

Antràs, P., Chor, D., Fally, T., & Hillberry, R. (2012, May). Measuring the upstreamness of production and trade flows. *American Economic Review*, *102*(3), 412-16. Retrieved from https://www.aeaweb.org/articles?id=10.1257/aer.102.3.412 doi: 10.1257/aer.102.3.412

Arezki, R., Fetzer, T., & Pisch, F. (2017, jul). On the comparative advantage of U.S. manufacturing: Evidence from the shale gas revolution. *Journal of International Economics*, *107*, 34–59. Retrieved from https://linkinghub.elsevier.com/retrieve/pii/S0022199617300284 doi: 10.1016/j.jinteco.2017.03.002

Ash, E., & Hansen, S. (2023, July). Text algorithms in economics. *Annu. Rev. Econom.*.

Atalay, E., Hortacsu, A., Li, M. J., & Syverson, C. (2018). How wide is the firm border? *SSRN Electron. J.*.

Auclert, A., Malmberg, H., Martenet, F., & Rognlie, M. (2021). Demographics, Wealth, and Global Imbalances in the Twenty-First Century. *SSRN Electronic Journal*. doi: 10.2139/ssrn.3906779

Baldwin, R., & di Mauro, B. W. (Eds.). (2020). *Economics in the time of covid-19*. CEPR Press.

Baldwin, R., & Freeman, R. (2020). *Supply chain contagion waves: Thinking ahead on manufacturing contagion and reinfection from the COVID concussion. VoxEU. org, 1 april.*

Baldwin, R., & Weder di Mauro, B. (2019). *The economics of brexit: A cost-benefit analysis of the uk's economic relationship with the eu*. VoxEU.org Book.

Barro, R. J., Ursúa, J. F., & Weng, J. (2020). *The coronavirus and the great influenza pandemic: Lessons from the "spanish flu" for the coronavirus's potential effects on mortality and economic activity* (Tech. Rep.). National Bureau of Economic Research.

Bauer, M. D., & Rudebusch, G. D. (2021, sep). The Rising Cost of Climate Change: Evidence from the Bond Market. *The Review of Economics and Statistics*, 1–45. Retrieved from https://direct.mit.edu/rest/article/doi/10.1162/rest_a_01109/107405/The-Rising-Cost-of-Climate-Change-Evidence-from doi: 10.1162/rest_a_01109

Becker, S. O., Fetzer, T., & Novy, D. (2017, oct). Who voted for Brexit? A comprehensive district-level analysis. *Economic Policy*, *32*(92), 601–650. Retrieved from http://www2.warwick.ac.uk/fac/soc/economics/research/centres/cage/manage/publications/305-2016_becker_fetzer_novy.pdfhttp://academic.oup.com/economicpolicy/article/32/92/601/4459491/Who-voted-for-Brexit-A-comprehensive-districtlevel doi: 10.1093/epolic/eix012

Besley, T., Fetzer, T., & Mueller, H. (2012). The Welfare Cost of Lawlessness: Evidence from Somali Piracy. *Journal of the European Economics Association*, *13*(2), 203–239.

Bureau of Economic Analysis, U.S. Department of Commerce. (2022). *BEA Data Archive: Gross Domestic Product by Industry and Input-Output Statistics.* Retrieved from https://www.bea.gov/itable/ (Accessed on April 21, 2024)

Cameron, C. A., & Miller, D. L. (2014). *Robust inference with dyadic data*. https://cameron.econ.ucdavis.edu/dyadic_cameron_miller_june2014.pdf. (Accessed: 2023-9-11)

Caselli, F., Koren, M., Lisicky, M., & Tenreyro, S. (2020, February). Diversification through trade. *Q. J. Econ.*, *135*(1), 449–502.

Coase, R. (1937). The theory of the firm. *Economica*.

Crosignani, M., Han, L., Macchiavelli, M., & Silva, A. F. (2023). Geopolitical risk and decoupling: Evidence from u.s. export controls [Working Paper]. Retrieved from https://ssrn.com/abstract=4563485

Crowley, M. A. (2014). Trade wars: The exaggerated impact of trade in economic debate. *The World Economy*, *37*(1), 29–42.

De Paula, A. (2017). Econometrics of network models. In *Advances in economics and econometrics: Theory and applications, eleventh world congress* (pp. 268–323). books.google.com.

Dhyne, E., Kikkawa, A. K., Mogstad, M., & Tintelnot, F. (2020, October). Trade and domestic production networks. *Rev. Econ. Stud.*, *88*(2), 643–668.

Elliott, M., & Jackson, M. O. (2023). Supply chain disruptions, the structure of production networks, and the impact of globalization. *Available at SSRN*.

Erdos, P., Rényi, A., et al. (1960). On the evolution of random graphs. *Publ. math. inst. hung. acad. sci*, *5*(1), 17–60.

Fajgelbaum, P. D., Goldberg, P. K., Kennedy, P. J., & Khandelwal, A. K. (2020, feb). The Return to Protectionism. *Quarterly Journal of Economics*, *135*(1), 1–55. Retrieved from http://www.nber.org/papers/w25638.pdfhttps://academic.oup.com/qje/article/135/1/1/5626442 doi: 10.1093/qje/qjz036

Fally, T. (2012). Production staging: Measurement and facts. *Working Paper*.

Fetzer, T., & Schwarz, C. (2019). Tariffs and Politics: Evidence from Trump's Trade Wars. *SSRN Electronic Journal*. Retrieved from https://www.ssrn.com/abstract=3349000 doi: 10.2139/ssrn.3349000

Fetzer, T., Shaw, C., & Edenhofer, J. (2024). Informational Boundaries of the State. *CEPR Working Paper*.

Fetzer, T., & Wang, S. (2020). Measuring the Regional Economic Cost of Brexit: Evidence up to 2019. *CAGE Working Paper*(486).

François, J., & Woerz, J. (1999). The impact of trade on intra-industry reallocations and aggregate industry productivity. *Econometrica*, *67*(6), 1395–1426.

Frésard, L., Hoberg, G., & Phillips, G. M. (2019, September). Innovation activities and integration through vertical acquisitions. *Rev. Financ. Stud.*, *33*(7), 2937–2976.

Fujimoto, T. (1999). The evolution of a manufacturing system at toyota. *Oxford University Press*.

Funke, M., Schularick, M., & Trebesch, C. (2023, dec). Populist Leaders and the Economy. *American Economic Review*, *113*(12), 3249–3288. Retrieved from https://pubs.aeaweb.org/doi/10.1257/aer.20202045 doi: 10.1257/aer.20202045

Gaubert, C., Kline, P., Vergara, D., & Yagan, D. (2021). Trends in US Spatial Inequality: Concentrating Affluence and a Democratization of Poverty. *AEA Papers and Proceedings*, *111*, 520–525. doi: 10.1257/pandp.20211075

Gereffi, G., & Korzeniewicz, M. (1994). *Commodity chains and global capitalism*. Praeger.

Grossman, S. J., & Hart, O. D. (1986). The costs and benefits of ownership: A theory of vertical and lateral integration. *J. Polit. Econ.*.

Handley, K., & Limão, N. (2017). Policy uncertainty, trade, and welfare: Theory and evidence for china and the united states. *American Economic Review*, *107*(9), 2731–2783.

Hansen, S., Lambert, P. J., Bloom, N., Davis, S. J., Sadun, R., & Taska, B. (2023, March). *Remote work across jobs, companies, and space* (No. 31007).

Hart, O., & Moore, J. (1990, December). Property rights and the nature of the firm. *J. Polit. Econ.*, *98*(6), 1119–1158.

Hassan, T. A., Hollander, S., Lent, L. V., & Tahoun, A. (2024, feb). The Global Impact of Brexit Uncertainty. *The Journal of Finance*, *79*(1), 413–458. Retrieved from https://onlinelibrary.wiley.com/doi/10.1111/jofi.13293 doi: 10.1111/jofi.13293

Hoekman, B., & Mattoo, A. (2006). Liberalizing trade in services: a survey. *The World Bank Research Observer*, *22*(2), 139–167.

Hong, H., Karolyi, G. A., & Scheinkman, J. A. (2020). Climate finance. *Review of Financial Studies*, *33*(3), 1011–1023. doi: 10.1093/rfs/hhz146

Horowitz, K. J., & Planting, M. A. (2006). *Concepts and methods of the u.s.*

input-output accounts. U.S. Bureau of Economic Analysis, U.S. Department of Commerce. Retrieved from https://www.bea.gov/sites/default/files/methodologies/IOmanual_092906.pdf (Updated in April 2009)

Humphrey, J., & Schmitz, H. (2004). The governance of global value chains. *Review of International Political Economy*, *12*(1), 78–104.

Juhász, R. (2018). Temporary Protection and Technology Adoption: Evidence from the Napoleonic Blockade. *America Economic Review*, 1–108. Retrieved from http://eprints.lse.ac.uk/60697/ doi: 10.1257/aer.20151730

Juhász, R., Squicciarini, M., & Voigtländer, N. (2023). Technology Adoption and Productivity Growth: Evidence from Industrialization in France. *forthcoming, Journal of Political Economy*. doi: 10.2139/ssrn.3649867

Kaplan, G., Moll, B., & Violante, G. L. (2020). The Great Lockdown and the Big Stimulus: Tracing the Pandemic Possibility Frontier for the U.S. *NBER Working Paper Series*.

Karbevska, L., & Hidalgo, C. A. (2023). Mapping global value chains at the product level. *arXiv.org*.

Kehoe, T. J., Ruhl, K. J., & Steinberg, J. B. (2018). Global imbalances and structural change in the United States. *Journal of Political Economy*, *126*(2), 761–796. doi: 10.1086/696279

Koren, M., & Tenreyro, S. (2013, February). Technological diversification. *Am. Econ. Rev.*, *103*(1), 378–414.

Korovkin, V., & Makarin, A. (2023, January). Conflict and intergroup trade: Evidence from the 2014 russia-ukraine crisis. *American Economic Review*, *113*(1), 34-70. Retrieved from https://www.aeaweb.org/articles?id=10.1257/aer.20191701 doi: 10.1257/aer.20191701

Kremer, M. (1993, August). The o-ring theory of economic development. *Q. J. Econ.*, *108*(3), 551–575.

Mulabdic, A., Osnago, A., & Ruta, M. (2017). Trade and worker deskilling. *Journal of Development Economics*, *132*, 58–73.

Nigmatulina, D. (2023). Sanctions and misallocation. how sanctioned firms won and russia lost [Working Paper].

Oberfield, E. (2018). A theory of input-output architecture. *Econometrica*, *86*(2), 559–589.

Ossa, R. (2014a). Trade wars and trade talks with data. *American Economic Review*, *104*(12), 4104–4146.

Ossa, R. (2014b, dec). Trade Wars and Trade Talks with Data. *American Economic Review*, *104*(12), 4104–4146. Retrieved from https://www.journals.uchicago.edu/doi/10.1086/261999http://pubs.aeaweb.org/doi/10.1257/aer.104.12.4104 doi: 10.1257/aer.104.12.4104

Stojkoski, V., Koch, P., & Hidalgo, C. A. (2023). Multidimensional economic complexity and inclusive green growth. *Communications Earth & Environment*, *4*(1), 130.

Suzaki, K. (1987). The new manufacturing challenge: Techniques for continuous improvement. *Free Press*.

Tol, R. S. J. (2009, apr). The Economic Effects of Climate Change. *Journal of Economic Perspectives*, *23*(2), 29–51. Retrieved from https://pubs.aeaweb.org/doi/10.1257/jep.23.2.29 doi: 10.1257/jep.23.2.29

Williamson, O. E. (1971). The vertical integration of production: Market failure considerations. *Am. Econ. Rev.*, *61*(2), 112–123.

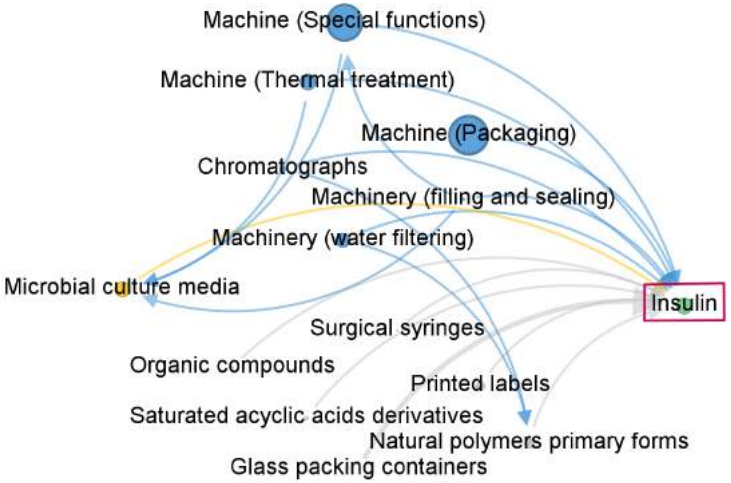
Winters, L. A., et al. (2004). *Trade and poverty in the developing world*. Centre for Economic Policy Research.

Womack, J. P., Jones, D. T., & Roos, D. (1990). *The machine that changed the world*. Rawson Associates.

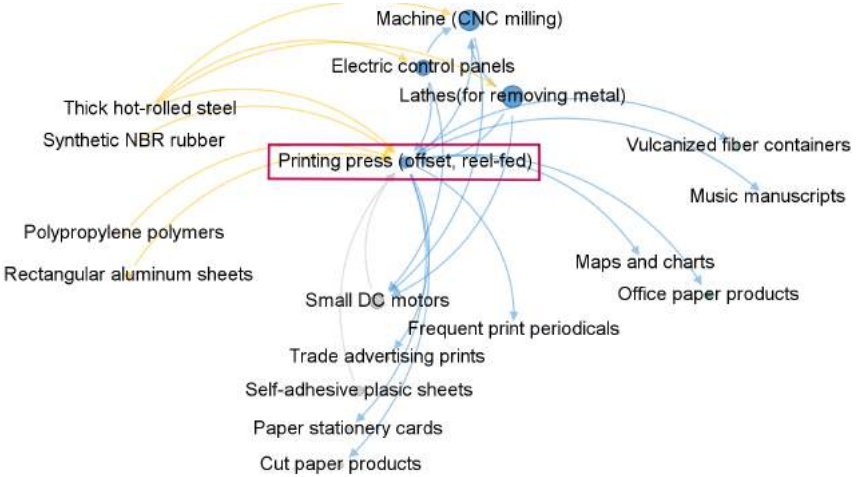
8 Main Figures and Tables

Figure 1: Illustrative examples

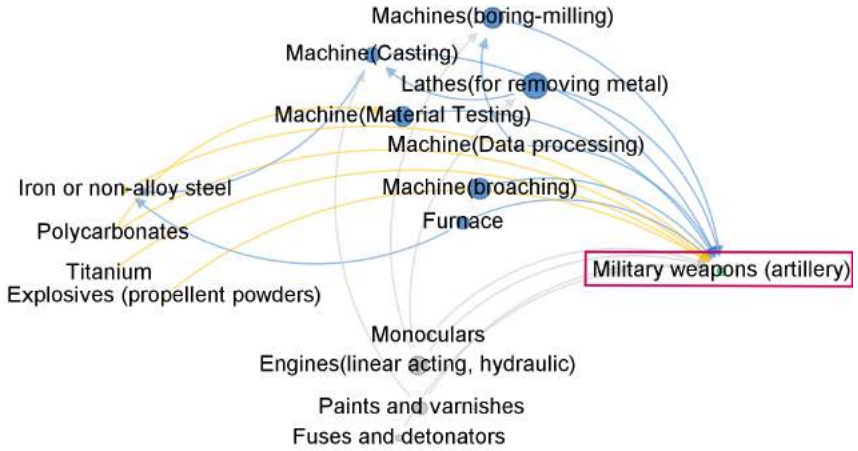
(a) Insulin (HS: 3003.31)



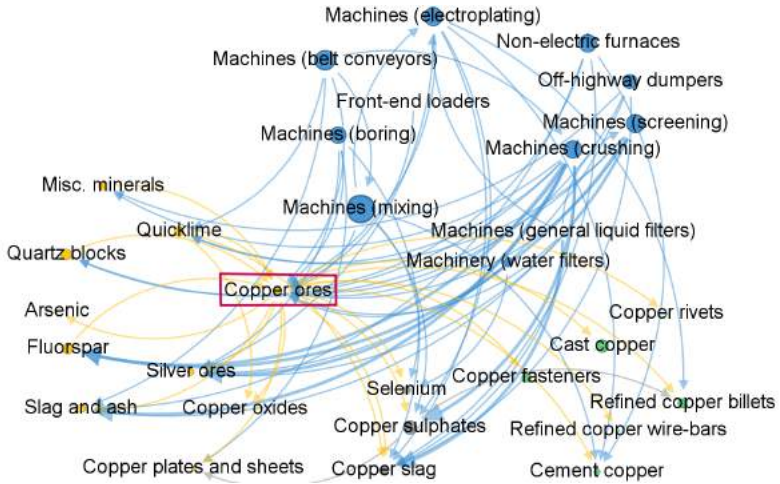
(b) Printing Press (HS: 8443.11)



(c) Military Artillery Weapons (HS: 9301.10)

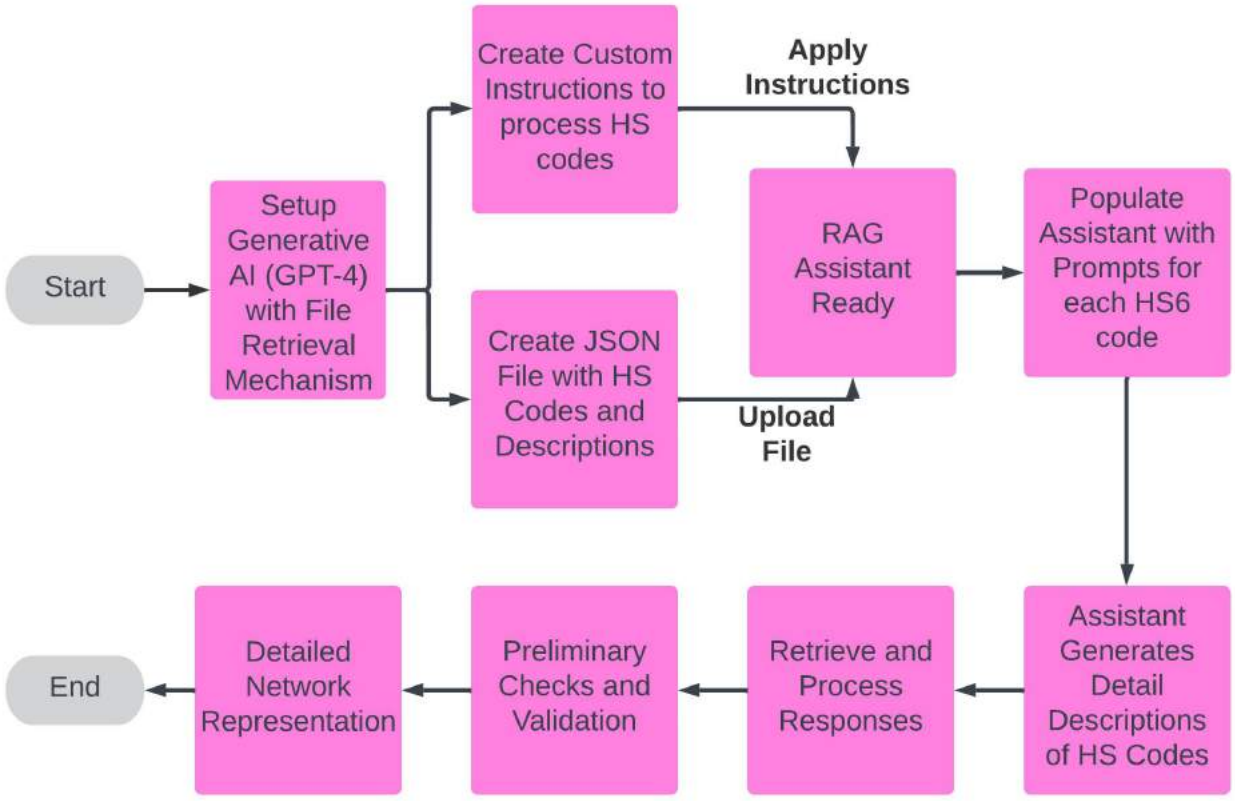


(d) Copper Ores (HS 2603.00)



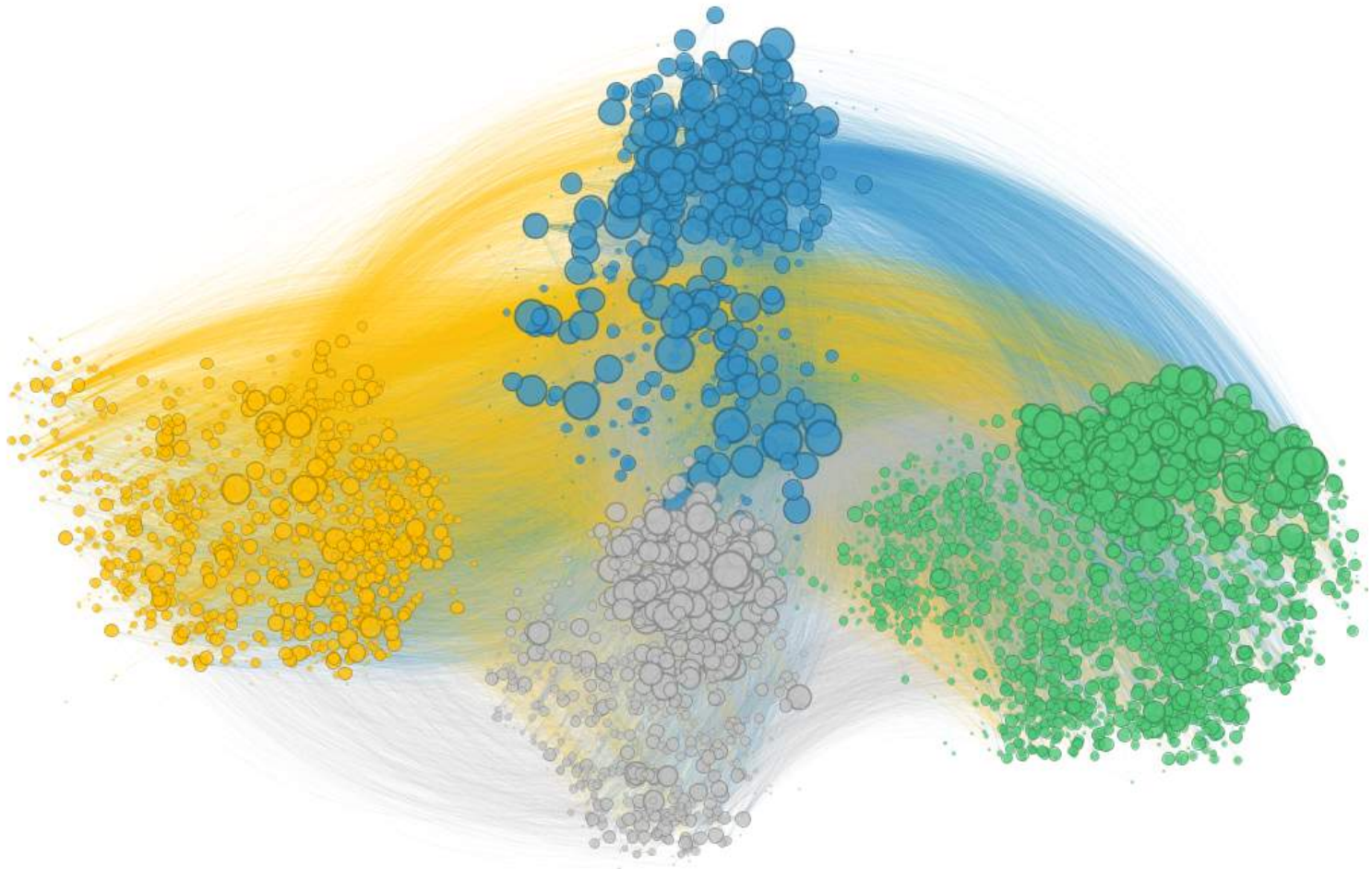
Note: Each panel presents a **one-degree ego network** of the focal product in AIPNET. Each node represent a single six-digit HS product code, based on the 2017 nomenclature published by WCO, available here. Code descriptions have been abbreviated for brevity. The full set of HS Code linkages can be found in appendix Table. Nodes are colored by their predominant linkage type: yellow for raw materials, grey for intermediary inputs, blue for capital inputs, and green for final goods. The focal node in each sub-figure is enclosed in a red box. Focal nodes Edges are colored by the source node. Node size is proportional to authority centrality (for definition see section 4.7). Note that while this is a one-degree network around the focal good, we have included edges between one-degree nodes. For instance, Furnace is required directly for Military Weapons and also for iron or non-alloy steel, which is needed for those weapons.

Figure 2: Flowchart of steps to build AIPNET retrieval augmented generation assistant



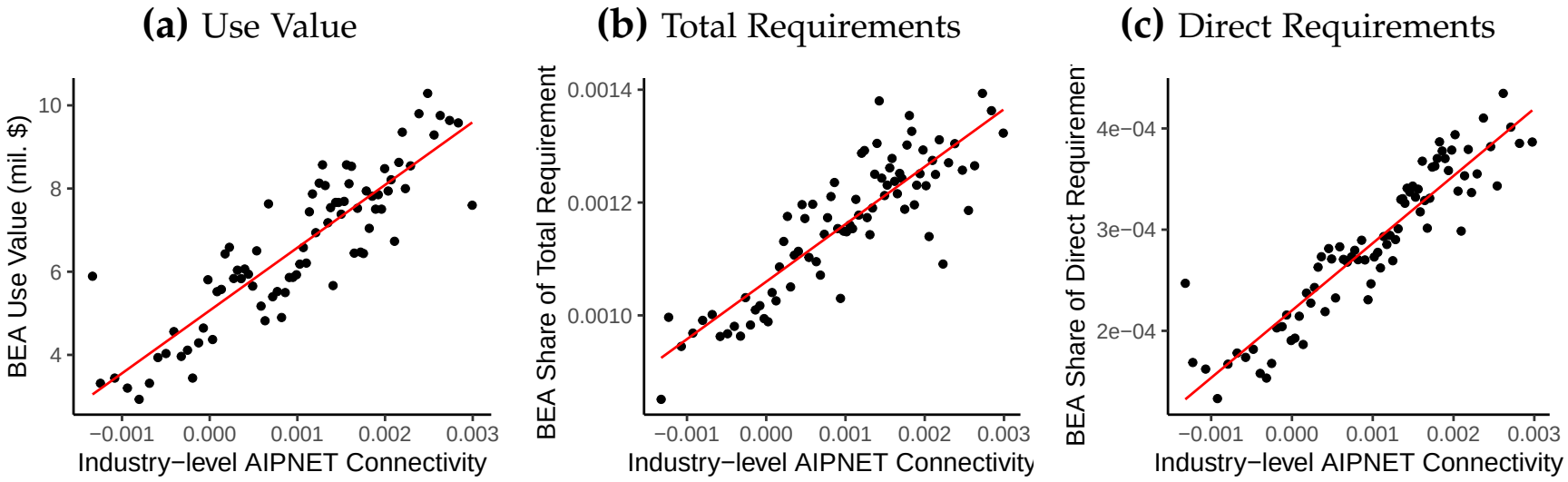
Note: This flowchart provides an overview of the AIPNET process. It begins with setting up the Generative AI (GPT-4) with a file retrieval mechanism. A file containing (Harmonized System) HS codes and descriptions is created and uploaded to the assistant. Custom instructions are created to process HS codes, which are then applied to ready the (Retrieval Augmented Generation) RAG assistant. The assistant is populated with prompts for each HS6 code, leading to the generation of detailed descriptions of HS codes. Responses are retrieved and processed, followed by preliminary checks and validation. The final output is a detailed network representation between HS products.

Figure 3: AI-built Production Network (AIPNET) visualization



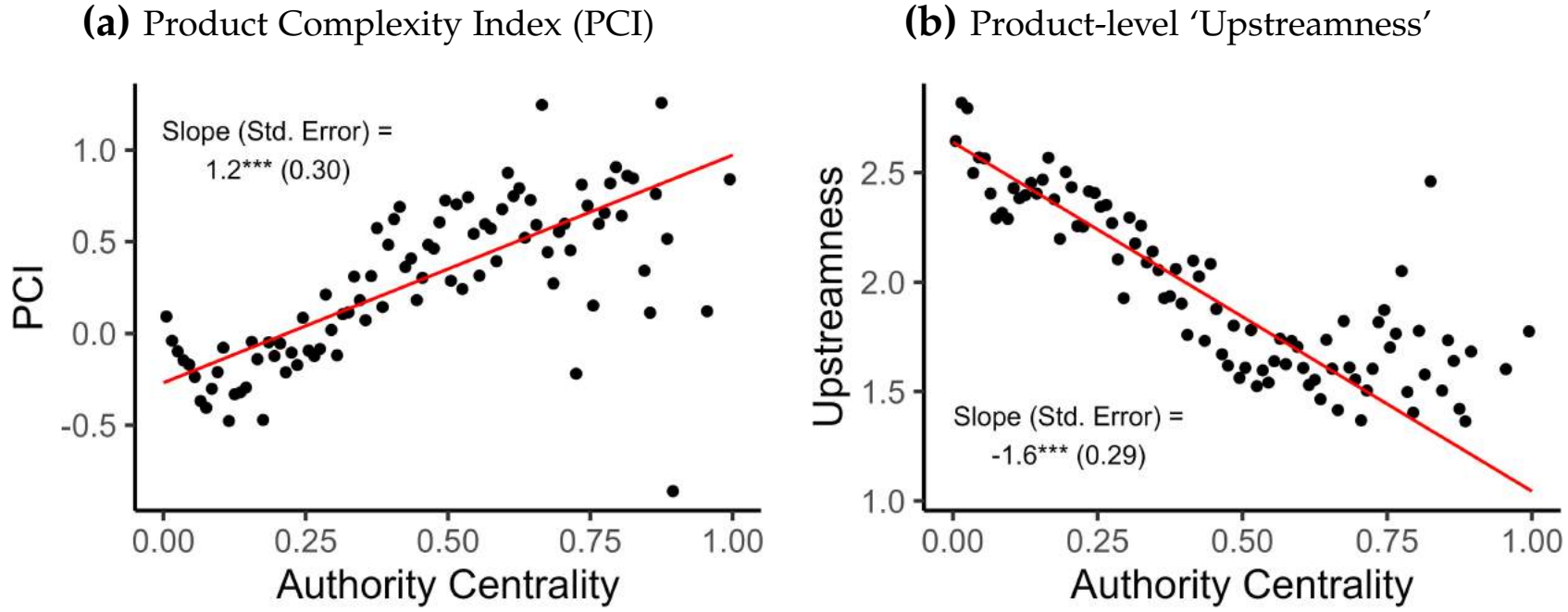
Note: This figure presents a visualization of the production network, where each node corresponds to a Harmonized System (HS) 6-digit product code, and edges represent vertical production relationships. The layout, derived using force-based layout algorithms, organizes nodes into clusters by predominant linkage type. We show nodes colored and clustered according to their linkage type: raw materials in yellow, intermediary inputs in grey, capital inputs in blue, and final goods in green. This panel introduces the graph's logical progression in an x-y dimensional framework, where nodes increase in size—indicating higher authority centrality—as we move from left to right and from bottom to top, especially evident in capital and final goods sectors.

Figure 4: AIPNET has strong relationship with US Input-Output Table structure



Note: The binscatter plots compare our network to (a) the BEA Use table, (b) Total Requirements, and (c) Direct Requirements. Using industry fixed effects, we residualize both standardized Input-Output table values and standardized network scores resulting from aggregating the HS 6-digit level network to the BEA-industry level. We exclude observations with residuals in the top and bottom 1% in either dimension. We create 100 bins based on the Network score, averaging horizontal and vertical variables. The blue dotted line is a LOESS fit, and the red line fits a linear model on the binned observations.

Figure 5: AIPNET centrality strongly predicts widely used production-network statistics

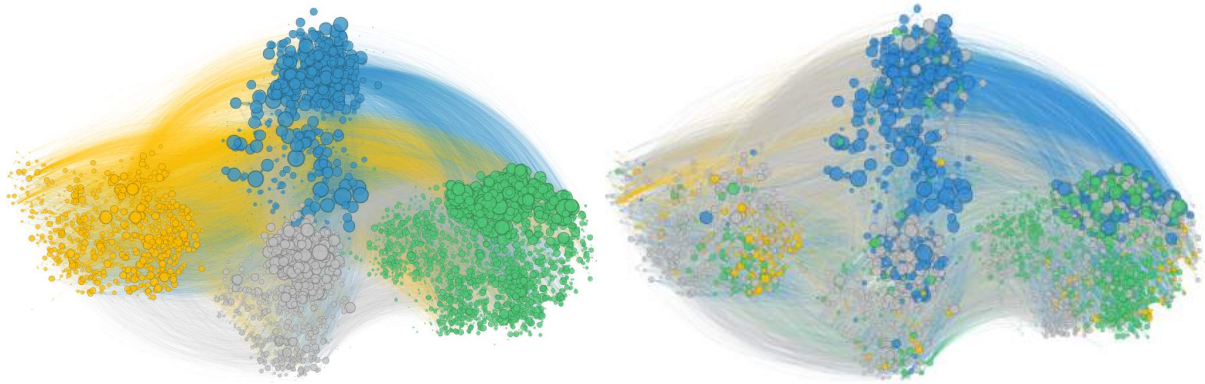


Note: This figure depicts two binscatters comparing AIPNET network structure to external measures of production network statistics. In both figures, we compare product-specific node authority centrality on the x-axis, calculated using the AIPNET discrete directed network structure, as described in section 4.7. Subfigure (a) compares this to product-level measures of the Product Complexity Index (PCI), simple arithmetic average over all years up to 2022, developed by (Stojkoski et al., 2023), using 2,074 HS six-digit codes (the intersection of both measures for which data was available). Subfigure (b) compares this to product-level measures of 'upstreamness' developed by (Antràs et al., 2012; Fally, 2012), using 4,435 HS six-digit products representing the intersection of AIPNET and 'upstreamness' measures. Both figures show an ordinary-least-squares line of best. The slope coeffient (standard error) when regressing PCI and 'Upstreamness' on AIPNET authority centrality were 1.2^{***} (0.09) (Figure a) and -1.6^{***} (0.08), respectively. *** denotes significance at the 0.001 level. The OLS coefficients were generated with HS 2-digit product level clustered standard errors. See Appendix table A.3 for details of this regression at both six- and four-digit HS levels.

Figure 6: Network of Product-level Production Network constructed using AI

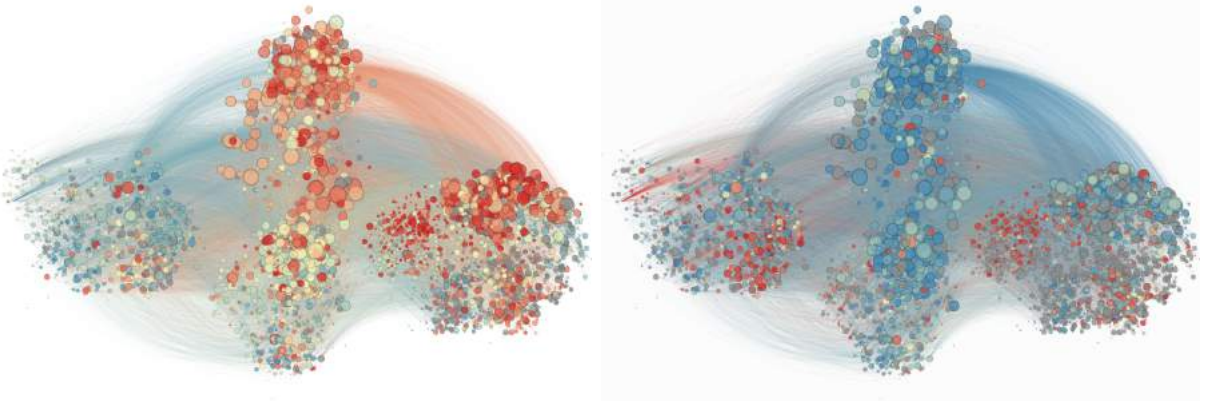
(a) Predominant Link Type (AIP-NET)

(b) Predominant Link Type (BEC classification)



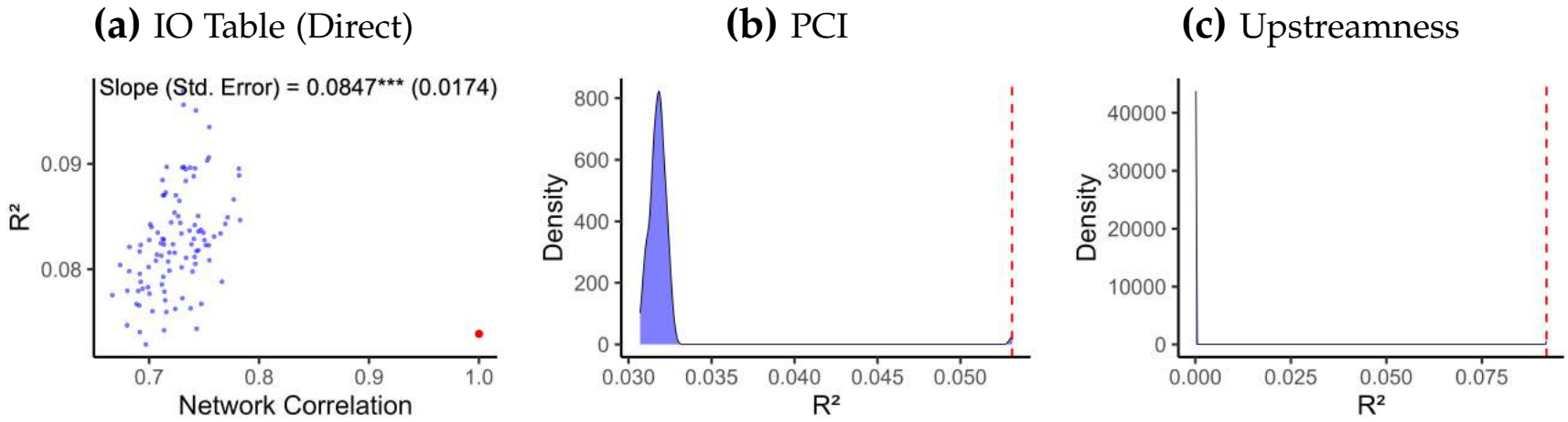
(c) Upstreamness from (Antràs et al., 2012)

(d) Product Complexity Index



Note: This figure presents a multi-panel visualization of the production network, where each node corresponds to a Harmonized System (HS) 6-digit product code, and edges represent vertical production relationships. The layout, derived using force-based layout algorithms, organizes nodes into clusters by predominant linkage type. **Panel (a)** serves as the baseline plot, showing nodes colored and clustered according to their linkage type: raw materials in yellow, intermediary inputs in grey, capital inputs in blue, and final goods in green. This panel introduces the graph's logical progression in an x-y dimensional framework, where nodes increase in size—indicating higher authority centrality—as we move from left to right and from bottom to top, especially evident in capital and final goods sectors. **Panel (b)** retains this layout but changes node colors according to UN's Broad Economic Categories (BEC) classification (Rev. 5), revealing the missing granularity within each linkage type and highlighting classification mismatches, particularly in non-capital categories. **Panel (c)** transitions to coloring nodes by Upstreamness from red (low) to blue (high), visually emphasizing the negative relationship between authority centrality and upstreamness. Finally, **panel (d)** colors nodes based on the Product Complexity Index (PCI), from red (low) to blue (high), underscoring a trend where larger nodes, indicative of higher centrality, generally display higher PCI, suggesting a discernible correlation between node centrality and complexity within the economic network.

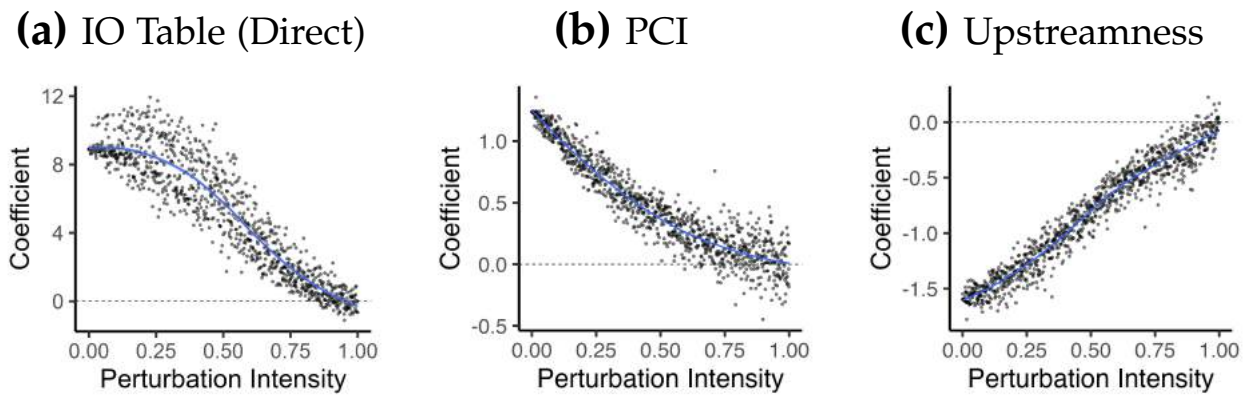
Figure 7: Validation of AIPNET with Stratified Permutations of AIPNET



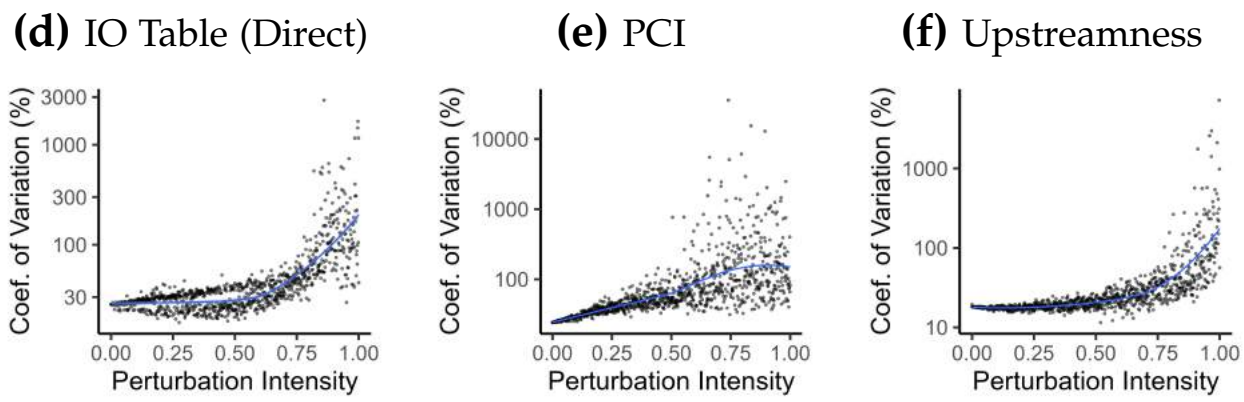
Note: This figure compares the explanatory power of AIPNET (true network) against 100 stratified permuted networks for different economic measures. The permuted networks are created by randomly reassigning connections within the constraints of HS2 product categories, ensuring that some hierarchical structure is preserved while maintaining the original degree distribution. Subfigure 7a shows the distribution of R^2 values from regressions of Direct Requirement IO table values against AIPNET connections for the permuted networks. The true network's R^2 value is highlighted in red, indicating it stands out as an outlier compared to the permuted networks. Subfigure 7b presents the kernel density plot of R^2 values from regressions of PCI on AIPNET authority centrality, with the true network's R^2 marked by a red dashed line. Subfigure 7c illustrates the kernel density of R^2 values from regressions of Upstreamness against AIPNET authority centrality, also highlighting the true network's R^2 with a red dashed line. These plots demonstrate that the true network's R^2 values are outliers compared to the permuted networks, indicating a significantly stronger explanatory power of the true network across all measures.

Figure 8: Validation of AIPNET with Monotonic Perturbation of Edges

Panel I: Coefficient by Perturbation Intensity

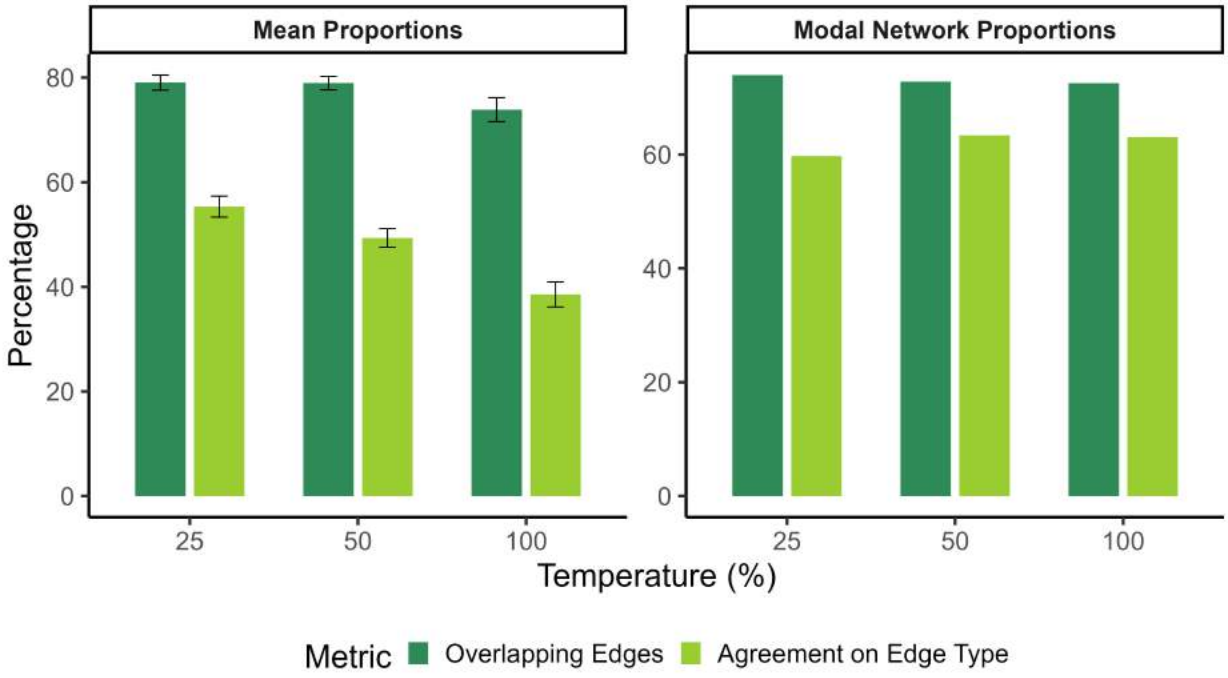


Panel II: Coefficient of Variation (%) by Perturbation Intensity



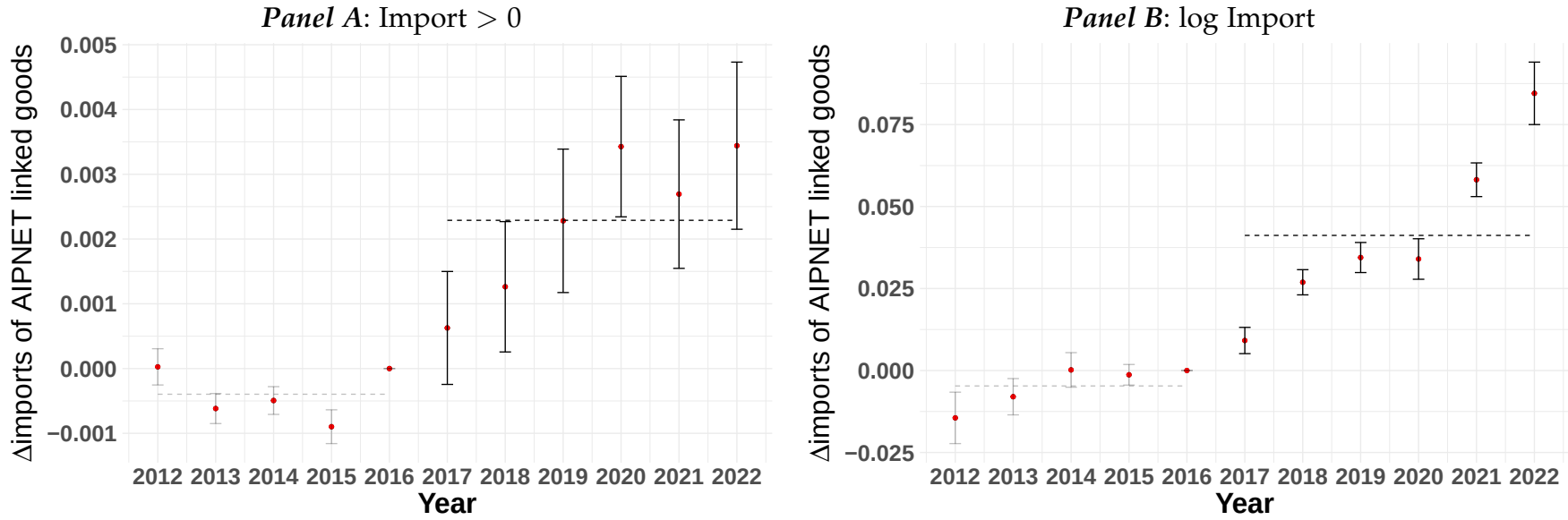
Note: This figure illustrates the impact of perturbation intensity on the coefficients and coefficient of variation (CV) from regressions of different economic measures against AIPNET connections. Panel I shows the coefficients for the IO Table (Direct), PCI, and Upstreamness as perturbation intensity increases. Panel II displays the corresponding CV for the same measures on a logarithmic scale. To conduct this exercise, we systematically perturbed the network by varying the intensity of edge rewiring from 1% to 100%, in steps of 0.1%. For each intensity level, we rewired the network using the Erdos-Renyi random graph model. This method adds edges between nodes with a certain probability (dictated by the perturbation intensity), thereby creating a randomized version of the network while preserving the number of edges. For the IO tables, we performed separate regressions of the direct requirement values on AIPNET connections for each perturbed network. For PCI and upstreamness, we calculated the authority centrality for each perturbed network and compared these centrality scores with PCI (Product Complexity Index) and upstreamness data. We then performed regressions of PCI and upstreamness on authority centrality, recording the coefficients and CV for each level of perturbation. Our analysis reveals that the coefficients decrease monotonically as the perturbation intensity increases, indicating reduced explanatory power. Concurrently, the CV increases, indicating greater relative variability in the estimates. These findings highlight the sensitivity of the network to noise and validate its robustness in capturing meaningful economic relationships.

Figure 9: Proportion of Overlapping Edges and Agreement by Temperature Setting



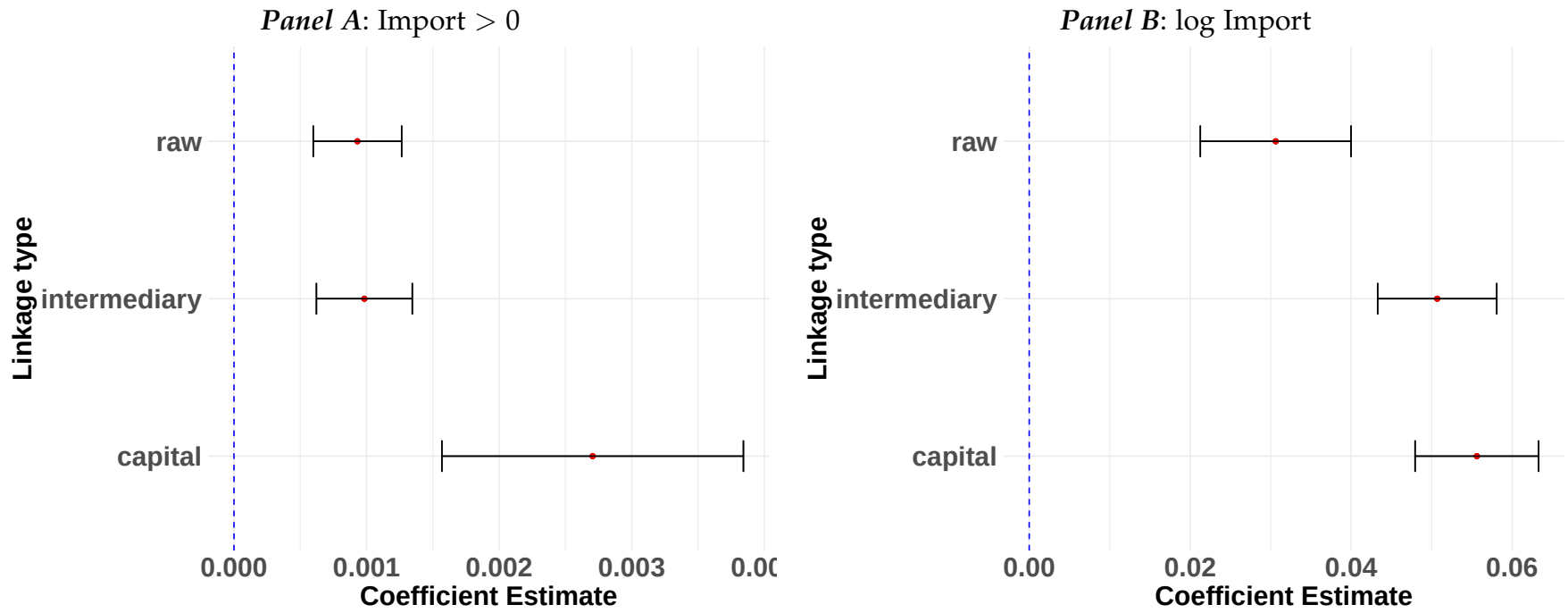
Notes: This figure illustrates the proportion of overlapping edges and the agreement on edge types across different temperature settings (25%, 50%, and 100%) compared to the baseline deterministic network from the temperature setting of 0%. To conduct this exercise, we randomly selected 100 HS6 nodes from the full set used to create our network. For each node, the RAG assistant was prompted 10 times for each non-zero temperature setting (25%, 50%, 100%), resulting in 100 HS6 codes times 10 iterations times 3 temperature settings. For the temperature setting of 0, we prompted once for all 100 HS6 codes since it is deterministic. This process provides a sample over which the summary statistics of relationships were computed. The left facet represents the mean proportions, and the right facet represents the modal network proportions, calculated as the most frequent edges across all generated networks at each specified temperature. The mean proportions include error bars indicating the standard deviation. Higher temperatures introduce more variability and randomness in the network's responses, as reflected in the decreasing overlap percentages with increased temperature. Specifically, the mean proportion of overlapping edges is highest at 25%, slightly decreasing at 50%, and further decreasing at 100%. The agreement on edge type remains relatively consistent across different temperatures, with a slight decline as the temperature increases. The modal network results show that despite higher temperatures introducing more variability, the generated networks still maintain a considerable degree of similarity to the baseline network. The modal network achieved a percentage overlap of 63% at 100%, significantly higher than the average of 38.5%. The linkage type agreement, conditional on overlap, slightly decreased to 72.5% from 73.9%. For more detailed summary statistics, refer to the appendix table A.1.

Figure 10: Trends in unfinished goods imports for goods that have I/O linkages to finished goods relative to goods that have no AIPNET linkage



Notes: Figure plots differential trends in import value and volume of downstream goods that have an AIPNET I/O linkage $W_{ij} = 1$ with some upstream goods relative to goods that do not have an AIPNET linkage, i.e. goods for which $W_{ij} = 0$. The dataset that is used for the estimation is a fully dyadic panel with 120 (countries) x 1200 (HS4 goods) x 1200 (HS4 goods) x 12 (years) = 2 billion observations. The regressions include country-by-dyad and country by HS2 by year fixed effects. Panel A documents the increase in the incidence of imports, while Panel B measures the log of imports as dependent variable. The omitted category is the year 2016. We note that from 2016 onwards there has been a notable change in trend suggesting increased imports of goods that have I/O linkages.

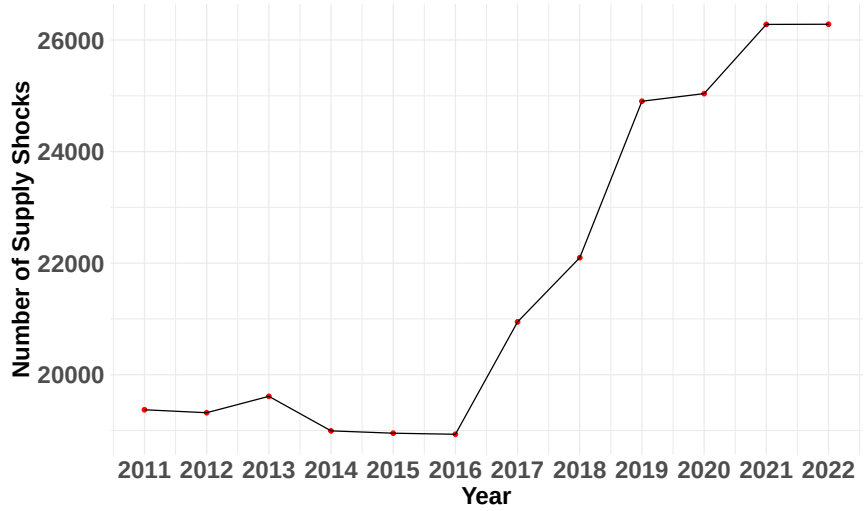
Figure 11: Patterns of import of AIPNET linked goods on extensive and intensive margins post 2016



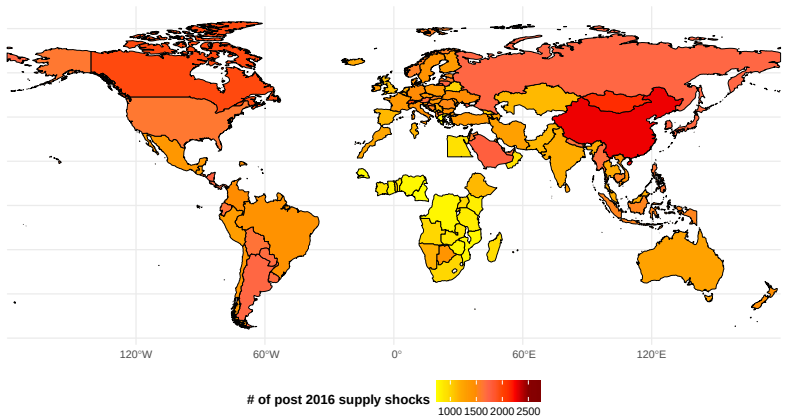
Notes: Figure plots differential trends in import value and volume of unfinished goods that have an AIPNET I/O linkage with some finished goods. We note that from 2016 onwards there has been a notable change in trend suggesting increased imports of goods that have I/O linkages suggesting potential localisation developments.

Figure 12: Persistent price shocks of finished goods and imports of unfinished goods

Panel A: number of price shocks

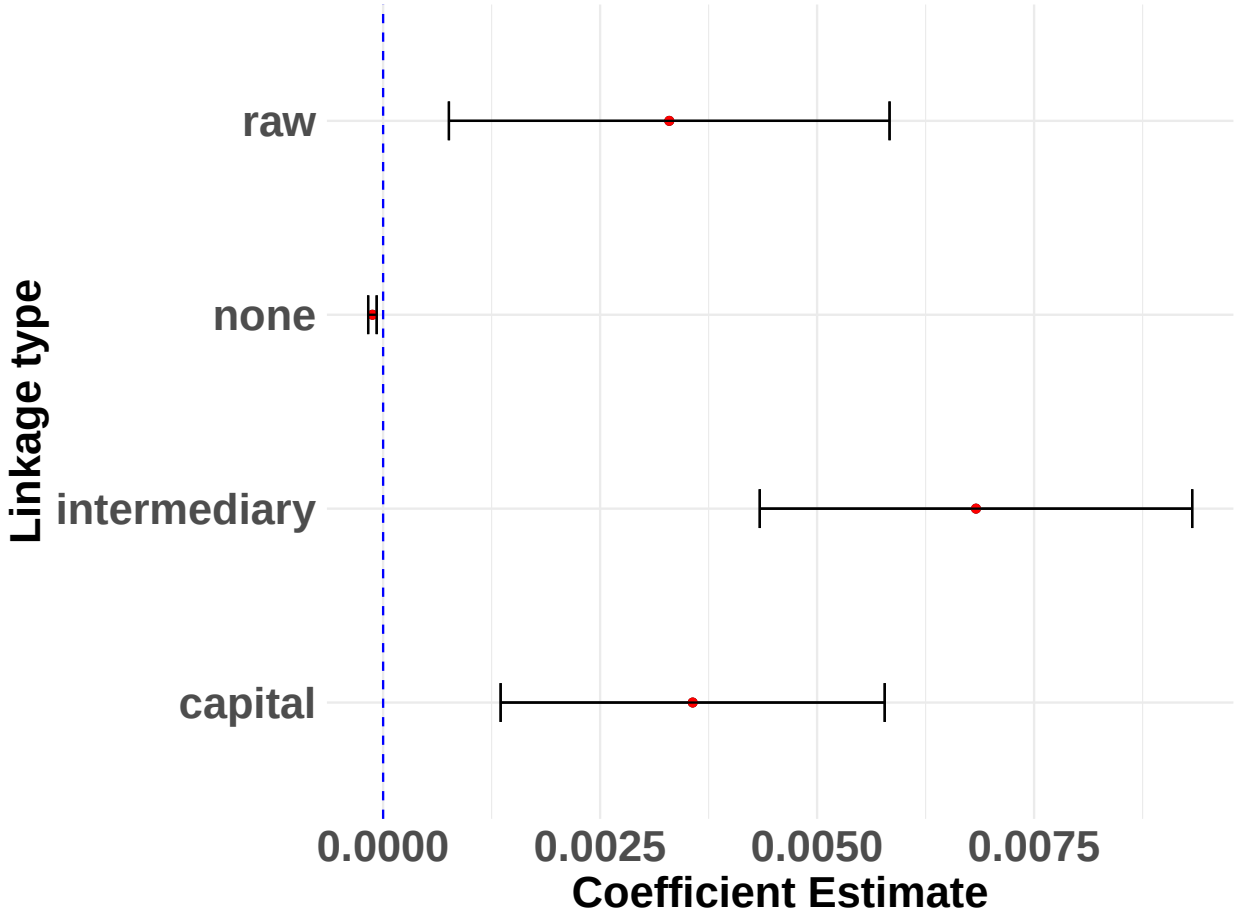


Panel B: geographic distribution of post 2016 supply shocks



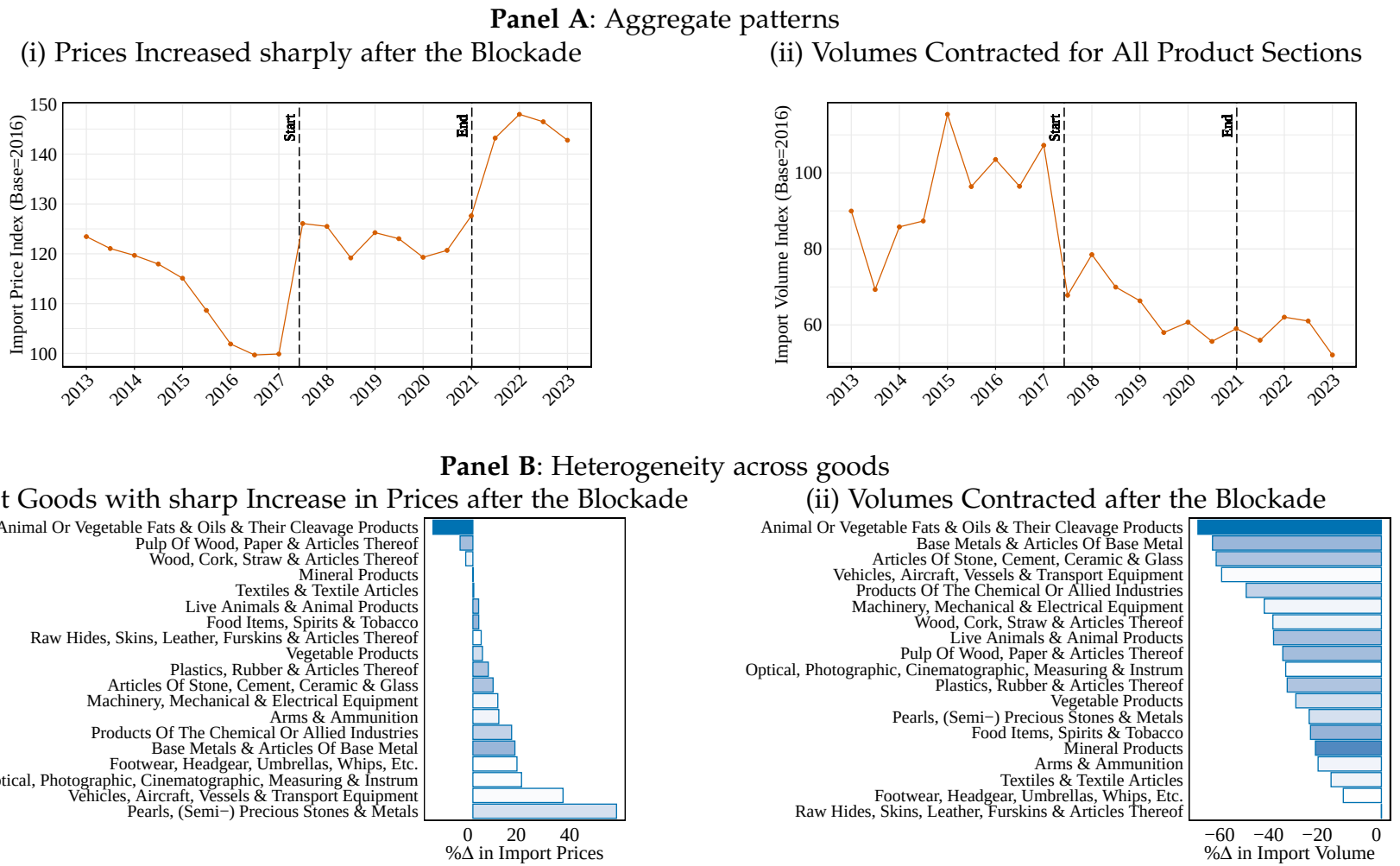
Notes: Figure plots the number of finished goods over time that record a positive and persistent price shock across all 120 main countries. We note that from 2016 onwards the number of finished goods for which there is a positive persistent price increase has increased drastically.

Figure 13: Persistent price shocks of finished goods and imports of unfinished goods by supply linkage type



Notes: This figure shows the impact of persistent price shocks of finished goods on (log) imports of unfinished goods, categorized by supply linkage type. The analysis indicates that the strongest effects are observed in intermediary goods imports, highlighting the substitution of imports along the value chain in response to supply shocks.

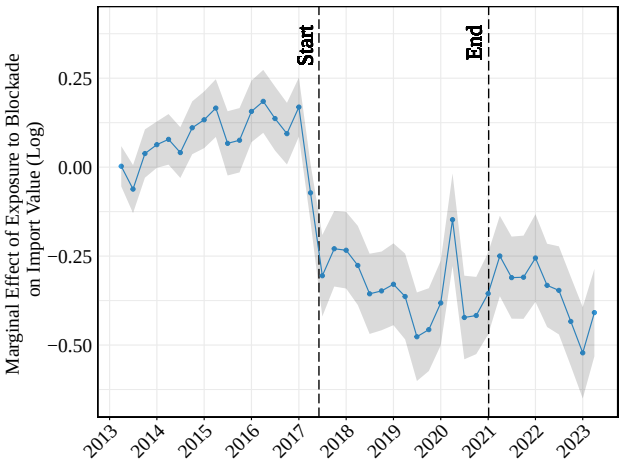
Figure 14: Blockade Caused a Supply Shock for Trade-Exposed Products



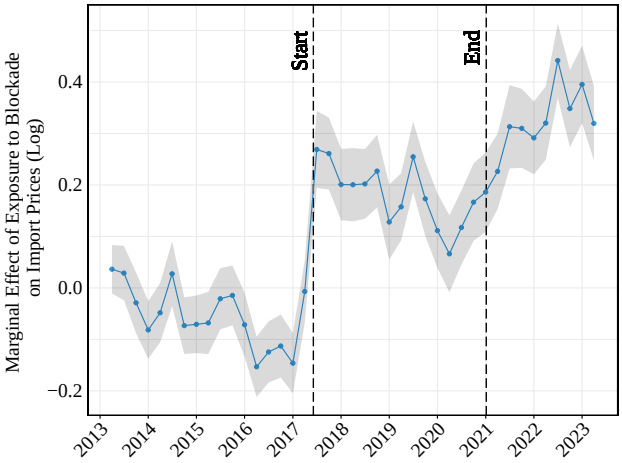
Note: This figure shows the impact of the blockade on 'blockade exposed' goods and the heterogeneity across product sections. Panel A (a) displays a composite price index and (b) a composite volume index, both weighted by 2016 trade values. Vertical black dashed lines mark the start and end of the blockade. Panel B (c) shows percentage changes in average prices and (d) in total trade volumes between 2015-2016 and 2018-2019, with gradients indicating import value shares from blockading countries. "Works of art, collectors' pieces and antiques" is excluded for clarity.

Figure 15: Impact of the Blockade on Trade Patterns and Prices

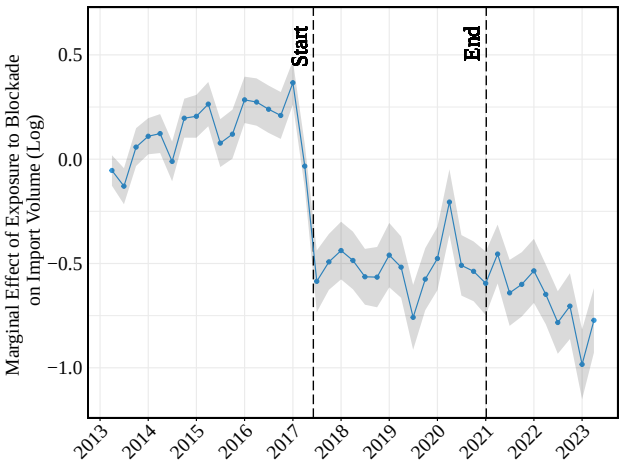
(a) Expenditures



(b) Prices



(c) Volumes



Note: Notes.

Table 1: Network Properties

Property	HS6 Values	HS4 Values
No. of Nodes	5,648	1,253
No. of Edges	55,719	40,710
Average Degree	20.2043	64.9801
Network Density	0.0018	0.0260
Global Clustering Coefficient	0.0205	0.1620
Assortativity	0.0016	-0.0843
No. of Connected Components	2	1
Size of Largest Connected Component	5,646	1,253

Note: This table summarizes the key structural properties of the AIPNET at two levels of product aggregation: HS6 and HS4. The HS6 network includes 5,648 nodes and 55,719 directed edges, while the HS4 network comprises 1,253 nodes and 40,710 directed edges. The average degree, indicating the average number of direct connections per node, is 20.2043 for HS6 and 64.9801 for HS4. Network density, representing the proportion of possible connections that are actual connections, is 0.0018 for HS6 and 0.0260 for HS4. The global clustering coefficient, measuring the likelihood that nodes cluster together, is 0.0205 for HS6 and 0.1620 for HS4. Assortativity, which indicates the tendency of nodes to connect with similar degree nodes, is 0.0016 for HS6 and -0.0843 for HS4. The number of connected components, showing the count of isolated sub-networks, is 2 for HS6 and 1 for HS4, with the largest connected component containing 5,646 and 1,253 nodes for HS6 and HS4, respectively.

Table 2: Impact of persistent supply shocks affecting downstream goods prices on imports of upstream goods

	(1)	(2)	(3)	(4)
Panel A: **log(Import value)**				
AIPNET Link × Supply Shock	0.0034***	0.0035***	0.0046***	0.0044***
	(0.0006)	(0.0006)	(0.0009)	(0.0008)
No. of estimated FE	496,626	642,960	178,401,817	178,548,151
R^2	0.94444	0.94448	0.94477	0.94522
Observations	1,844,701,890	1,844,701,890	1,844,701,890	1,844,701,890
Panel B: **Import $>$ 0**				
AIPNET Link × Supply Shock	0.0002***	0.0002***	0.0003***	0.0003***
	(6×10^{-5})	(6.02×10^{-5})	(8.08×10^{-5})	(7.92×10^{-5})
No. of estimated FE	500,098	649,258	182,003,723	182,152,883
R^2	0.75003	0.75017	0.75176	0.75321
Observations	1,941,321,071	1,941,321,071	1,941,321,071	1,941,321,071
Regression specification:				
Country x HS4	X	X		
Country x HS2 Downstream x Year	X	X	X	X
Country x Dyad			X	X
Country x HS4 Downstream x log(upstream import) trend		X		X

Notes: Table presents regression results documenting the impact of persistent price shocks on downstream goods on upstream imports. Standard errors provided in parentheses are clustered at the HS2 by HS2 pair level with stars indicating *** p <0.01, ** p <0.05, and * p <0.1.

Table 3: Narrative Linkage: Exploration of Heterogeneous Treatment Effects by Country

DV: $\widehat{\beta_c}$ vector	(1)	(2)	(3)
Supply Shock estimates $\widehat{\nu_c}$ vector	1.001***	1.304*	1.217**
	(0.3396)	(0.4866)	(0.4793)
No. of estimated FE	0	5	7
R^2	0.07317	0.35100	0.35763
Observations	112	112	112
Other controls	None	Continent FE	Region FE

Notes: Table presents regression results documenting the impact of persistent price shocks on downstream goods on upstream imports. Standard errors provided in parentheses are clustered at the HS2 by HS2 pair level. Stars indicate significance levels: *** p <0.01, ** p <0.05, and * p <0.1.

Table 4: Effects of Product-level Blockade Exposure on Imports

(a) Controls for HS8 Product and Seasonality

Dependent Variables:	(1) Import Price (Log)	(2) Import Value (Log)	(3) Import Volume (Log)	(4) Nonzero Trade (Binary)	(5) High Trade (Binary)
Variables					
Blockade Exposure	0.35***	-1.6***	-1.5***	-0.11***	-0.07***
	(0.04)	(0.22)	(0.20)	(0.01)	(0.01)
Fit statistics					
Observations	661,664	941,472	941,472	941,472	941,472
R^2	0.759	0.586	0.601	0.532	0.589

(b) Controls for HS8 Product and HS6 Product×Year-Month

Dependent Variables:	(1) Import Price (Log)	(2) Import Value (Log)	(3) Import Volume (Log)	(4) Nonzero Trade (Binary)	(5) High Trade (Binary)
Variables					
Blockade Exposure	0.35***	-2.7***	-2.4***	-0.19***	-0.08***
	(0.05)	(0.26)	(0.23)	(0.02)	(0.01)
Fit statistics					
Observations	661,664	941,472	941,472	941,472	941,472
R^2	0.818	0.659	0.672	0.614	0.665

Note: This table reports results from running the regression defined in Section 6.2 Equation (10). We test for the effect of 'Blockade Exposure', measured for each HS8 product as the proportion of the total value of trade that came from blockading countries in 2016. This is interacted with an indicator variable denoting the start of the blockade. The data used is at the monthly frequency of imports for each HS8 product. Columns (2) and (3) use the inverse-hyperbolic-sine transform to approximate log. Column (4) and (5) use as outcomes binary indicators for non-zero trade and high-trade respectively, where the latter equals 1 if trade volumes for that product in that year-month exceeded the 2016 average. Panel (a) contains fixed effects for HS8 product codes and dummy variables for each month to control for seasonality. Panel (a) adds an additional fixed effect for time (year-month dummies), which are interacted with HS6 Product Codes. Standard errors (clustered by HS4 product code) in parentheses. Significance Codes: ***: 0.01, **: 0.05, *: 0.1.

Table 5: Dyadic Regressions of Downstream Blockade Exposure

(a) Fixed Effects for Dyad (HS8×HS8) and Seasonality

Dependent Variables:	(1)	(2)	(3)	(4)	(5)	(6)
	Import Value (Log)			Import Volume (Log)		
BlockadeDummy	0.80***	0.47***	0.77***	0.60***	0.31**	0.56***
	(0.17)	(0.16)	(0.17)	(0.13)	(0.14)	(0.13)
Blockade Exposure (Direct)	-1.8**		-1.9**	-1.6**		-1.6**
	(0.87)		(0.87)	(0.73)		(0.73)
Blockade Exposure (Down-stream)		0.24	0.36**		0.23*	0.33**
		(0.17)	(0.16)		(0.14)	(0.14)
Observations	3,025,008	3,025,008	3,025,008	3,025,008	3,025,008	3,025,008
R^2	0.611	0.609	0.611	0.643	0.642	0.643

(b) Fixed Effects for Dyad (HS8×HS8) and Year-Month

Dependent Variables:	(1)	(2)	(3)	(4)	(5)	(6)
	Import Value (Log)			Import Volume (Log)		
Blockade Exposure (Direct)	-1.8**		-1.9**	-1.6**		-1.6**
	(0.85)		(0.85)	(0.71)		(0.71)
Blockade Exposure (Down-stream)		0.20	0.36**		0.18	0.32**
		(0.16)	(0.16)		(0.13)	(0.14)
Observations	3,025,008	3,025,008	3,025,008	3,025,008	3,025,008	3,025,008
R^2	0.612	0.611	0.612	0.645	0.643	0.645

Note: This table reports results from running the dyadic regression defined in Section 6.2 Equation (13). We test for the effect of 'Blockade Exposure' on Import patterns of up-stream HS8 products. 'Direct Exposure' measures the focal upstream goods proportion of total value of trade that came from blockading countries in 2016. 'Down-stream Blockade Exposure' measures the exposure of the down-stream product. We interact exposure with an indicator variable denoting the start of the blockade. We run these specifications for up-stream goods which fall into Sections 1, 10, 15, 16, and 19 of HS product nomenclature, which represents the majority of raw material inputs and capital equipment. Panel (a) contains fixed effects for HS8 product codes and dummy variables for each month, to control for seasonality. Panel (b) adds an additional fixed effect for time (year-month dummies), which are interacted with HS6 Product Codes. We cluster standard errors to account for correlation on both sides of the dyadic pairs. Dyadic-clustered standard-errors in parentheses. Significance Codes: ***: 0.01, **: 0.05, *: 0.1.

Table 6: Dyadic Regressions of Direct and Downstream Blockade Exposure

Dependent Variables:	(1) Import Value (Log)	(2) Import Value (Log)	(3) Import Volume (Log)	(4) Import Volume (Log)
Variables				
Blockade Exposure (Direct)	-	-1.9**	-	-1.6**
		(0.85)		(0.71)
Blockade Exposure (Down-stream) ×Capital Input	0.59*	0.61*	0.45*	0.47*
	(0.32)	(0.32)	(0.25)	(0.26)
Blockade Exposure (Down-stream) ×Intermediate Input	0.11	0.32*	0.12	0.29*
	(0.20)	(0.19)	(0.16)	(0.16)
Fixed-effects				
Dyad (HS8×HS8)	Yes	Yes	Yes	Yes
Year-Month	Yes	Yes	Yes	Yes
Fit statistics				
Observations	3,048,318	3,048,318	3,048,318	3,048,318
R^2	0.611	0.613	0.644	0.645

Note: This table reports results from running the dyadic regression defined in Section 6.2 Equation (13). We test for the effect of 'Blockade Exposure' on Import patterns of up-stream HS8 products. 'Direct Exposure' measures the focal upstream goods proportion of the total value of trade that came from blockading countries in 2016. 'Down-stream Blockade Exposure' measures the exposure of the down-stream product. We interact exposure with an indicator variable denoting the start of the blockade. Compared to Table 5, we further interact the effect of Downstream Exposure based on whether the up-stream good is a capital input or an intermediary input. We cluster standard errors to account for correlation on both sides of the dyadic pairs. Dyadic-clustered standard-errors in parentheses. Significance Codes: ***: 0.01, **: 0.05, *: 0.1.

A Detailed Description of AI-built Production Network (AIPNET)

In this section, we provide additional details on the construction of AIPNET at the six-digit level (HS6). The construction of the four-digit level (HS4) network follows a very similar methodology. We present the final network representations for both the HS6 and HS4 level networks.

First, LLMs establish linkages beyond simple Natural Language Processing (NLP) methods, which typically depend on keyword overlap. Pre-trained on extensive datasets, including detailed descriptions of production processes and product characteristics from sources like Wikipedia, LLMs bring a nuanced understanding of language that enables them to apply human-level judgment at scale. For instance, the Wikipedia entries for 'Electrical energy' and 'Dairy' are just two examples of the rich content informing LLM training, enhancing their ability to discern vertical relationships between products.[30]

Second, deploying LLMs is cost-effective and scalable. Third, their use results in high accuracy. Fourth, LLMs operate based on knowledge, not merely empirical patterns. While firm-to-firm or cross-industry market transactions data can be invaluable for empirically defining supply chains, such data may miss vital links due to vertical integration or transaction-cost barriers that obscure production relationships not visible through market transactions. Similarly, input/output tables are only as comprehensive as the data spanning all industries/products they are based on.

The process begins with setting up the generative AI with a file retrieval mechanism. A file containing HS codes and descriptions is created and uploaded to the assistant. Custom instructions are created to process HS codes, which are then applied to ready the RAG assistant. The assistant is populated with prompts for each HS6 code, leading

[30]One important source for training LLMs is Wikipedia. This source alone provides highly informative content on the production process of many goods, for example, the entries for 'Electrical energy' and 'Dairy'. Countless sources such as these enter the LLMs training data. The net result is an ability to apply human-level judgment, at scale, when determining vertical relationships between products.

it to generate detailed descriptions of HS codes. Responses are retrieved and processed, followed by preliminary checks and validation. Finally, a detailed network representation is constructed. This sequence is visually summarized in Figure 2, which provides a flowchart of the entire process. The remainder of this section will describe this process, along with properties of the retrieved network and comparisons with existing network-inspired measures and correlation with input-output tables.

These instructions also direct the AI model to utilise the additional data we load into the models context using RAG (see next section). This ensures that the assistant makes semantic connections between products within the predefined product space.

The JSON file uploaded to assistant is based on publicly available 2017 HS codes and their descriptions. It contains entries at 2-digit, 4-digit, and 6-digit levels, each with an 'index' for unique identification and hierarchical descriptions that combine all levels into a single line, such as the entry for code '0101.21' which describes it within the broader 2-digit level category of "Animals; live," narrowing down to the 6-digit level of "Horses; live, pure-bred breeding animals." This structured format allows for efficient data retrieval and precise cross-referencing between the hierarchies of product codes.

The full system instructions are provided in appendix section A.1. These instructions guide the assistant to structure its responses into four main sections: (i) Introduction, which details the general context of the product group; (ii) Capital Inputs, focusing on the machinery, buildings, equipment, and technology used in production; (iii) Raw Inputs, describing the necessary natural resources and unprocessed goods; and (iv) Intermediary Inputs, outlining the required semi-finished goods, components, or services. Each section mandates the inclusion of relevant HS codes at 2-, 4-, or 6-digit levels, enhancing the precision and relevancy of the information provided. This structured approach not only ensures the production of factual and professionally-toned descriptions but also facilitates the mapping of interdependencies within the production chains. The assistant was directed to prioritize inputs that are widely recognized as crucial, thereby minimizing ambiguities and focusing on economically significant production methods.

A.1 Full System Instructions

In the design of the system instructions for the assistant, our primary goal was to ensure clarity, consistency, and depth in the responses pertaining to various product groups within the Harmonized System (HS). Each product group is detailed in four main sections: Introduction, Capital Inputs, Raw Inputs, and Intermediary Inputs. These sections are not merely informational but are structured to enhance the assistant's ability to identify and describe the essential components and their interdependencies within the production chains.

Introduction: This section sets the general context for the product group. It includes a broad overview that facilitates an understanding of the subsequent, more specific details.

Capital Inputs: Focuses specifically on the machinery, buildings, equipment, and technology used in production. This section is crucial as it details the infrastructure without which the production process cannot commence.

Raw Inputs: Describes the essential natural resources and unprocessed goods required for the production process. This section emphasizes the foundational materials that are transformed through various industrial processes.

Intermediary Inputs: Outlines the semi-finished goods, components, or services that are necessary for completing the production of final goods. This section highlights the connective elements within the production chain that link raw materials to final products.

To guide the assistant effectively, the instructions explicitly require the inclusion of relevant HS codes at the 2-, 4-, or 6-digit levels. This specificity not only enhances the precision of the information provided but also aids in mapping the detailed interdependencies within the production chains. Such structured instructions ensure that the descriptions are not only factual and professionally toned but also uniformly detailed across all sections.

To further refine the assistant's responses, we employed specific directives:

1. Explicit Mention of Products: The term ”Explicit” in the instructions ensures that products are mentioned directly with their HS codes, and not merely implied through descriptions. This direct referencing is critical for clear and unambiguous communication of information.

2. Explicit Mention of Products: The term ”Explicit” in the instructions ensures that products are mentioned directly with their HS codes, and not merely implied through descriptions. This direct referencing is critical for clear and unambiguous communication of information.

3. Consistent Retrieval of HS Codes: The directive to enclose HS codes within triple hashes (e.g., `3289.08###`) standardizes the text format, allowing for consistent retrieval and processing of these codes through string operations.

4. Detail-Oriented Descriptions: By describing the assistant as ”very detail-oriented” and requesting ”very comprehensive descriptions,” we set a high standard for the depth and quality of the content. This encourages the production of extensive material that can significantly enhance the user's understanding of the product categories.

5. Encouraging Detailed Descriptions: To ensure detailed descriptions and consistency in referencing HS codes, we specifically ask for a substantial amount of relevant detail (suggested 500 words) and explicit listing of all related 4-digit and 6-digit HS Codes. This not only increases the detail within each section but also ensures uniformity in the assistant's behavior regarding the reference to HS codes.

These carefully crafted instructions are designed to maximize the efficiency and effectiveness of the assistant in delivering high-quality, detailed descriptions that are essential for professionals dealing with HS-coded products. The full system instructions, provided below, embody these principles and are a testament to our commitment to precision and utility in informational content.

Here are the full system instructions:

> You are a very detailed-oriented assistant with expertise in the 2012 Harmonized System (HS) product codes and production processes. Your resources include a JSON file detailing all HS product codes at the 2-digit, 4-digit, and 6-digit levels, with each entry containing 'code' and 'description' fields.
>
> When given a 6-digit HS Code, produce a very comprehensive description of the production process for that product group. Use the JSON file to reference all pertinent HS codes and describe the process using the following structure:
>
> 1. Introduction: Offer a brief overview of the product group related to the given 6-digit HS Code. 2. Capital Inputs: Detail the machinery, buildings, equipment, and technology used in production. Provide lots of relevant detail (500 words) and explicitly list any related 6-digit HS Codes (e.g., `###4008.21###` for plates, sheets and strip). 3. Raw Inputs: Describe the natural resources and unprocessed goods required. Provide lots of relevant detail (500 words) and explicitly list any related 6-digit HS Codes (e.g., `###2925.11###` for saccharin and its salts). 4. Intermediary Inputs: Explain the need for semi-finished goods, components, or services. Provide lots of relevant detail (500 words) and explicitly list any related 6-digit HS Codes (e.g., `###0810.10###` for strawberries).
>
> Ensure that referenced HS codes are directly related to the focal product's production process. If multiple production methods exist, focus on the most common or economically significant ones. The description should be very detailed, factual, and presented in a clear and professional tone.
>
> Before responding to each prompt, parse the entire JSON file to understand the universe of HS codes and accurately cross-reference them in your descriptions. If any ambiguities arise, prioritize inputs that are well recognized as essential for the production process. When referring to an HS code, include

it within three hashes (e.g. `###5702.49###`).

Prompt:

HS-Code: '*HS6 code*'. Description: '*HS6 code description*'.

A.2 JSON file

The JSON file used in our project is a crucial resource designed to support the detailed analysis of global trade relationships based on the Harmonized System (HS) of product coding. This file contains meticulously organized data on HS codes at three levels of specificity: 2-digit (HS2), 4-digit (HS4), and 6-digit (HS6), which are critical for comprehensive data retrieval and detailed analysis. Each entry in the JSON file includes an 'index' which assigns a unique identifier to each product, alongside HS2, HS4, and HS6 fields that categorize products into increasingly specific groups. The 'description' field provides a concatenated narrative that links all three levels of product classification in one line, presenting a clear hierarchical structure from broad categories to specific items.

For example, the entry for '0101.21' not only gives the code but also describes it as part of broader categories—indicating that it pertains to "Animals; live" at the broadest level, narrows down to "Horses, asses, mules and hinnies; live" at an intermediate level, and specifies "Horses; live, pure-bred breeding animals" at the most detailed level. This structure allows for an intuitive understanding of the context and specificity of each code, facilitating precise analysis and enabling efficient cross-referencing within the dataset.

The design of this file provides significant benefits for our analysis, allowing for the quick identification of product groups and their detailed descriptions within the global trade schema. The hierarchical linking of descriptions ensures that users can understand the relation and context of specific items within broader categories, critical for tasks requiring detailed product knowledge and trade analysis. However, this approach also has limitations. The reliance on hierarchical, pre-defined categories may not capture all

nuances of product differences or emerging categories that do not fit neatly within the established HS structure. Furthermore, the brief nature of descriptions, typically 1-2 sentences, while efficient, may not provide enough detail for an in-depth understanding without further research.

This JSON file was chosen for its structured approach to data organization, which aligns well with the needs of our project to map and analyze complex trade relationships accurately and efficiently.

A.3 Examples and full responses

In this section, we provide full responses by our assistant for two closely related codes: (1) HS Code 2716.00, ”Electrical Energy” and (2) HS code 8541.40 for solar panels, specifically ”Electrical apparatus; photosensitive, including photovoltaic cells, whether or not assembled in modules or made up into panels, light-emitting diodes (LED)”.

For instance, HS Code 2716.00, which refers to ”Electrical Energy,” showcases the depth of the assistant's capabilities. The production inputs for electrical energy are categorized into capital, raw, and intermediary inputs. Capital inputs include Thermal Power Plants with components like steam boilers (HS: 8402.01), gas turbines (HS: 8406.81), and AC generators (HS: 8591.54); Nuclear Power Plants featuring nuclear reactors (HS: 8401.30) and cooling systems (HS: 8419.50); and Renewable Energy Systems comprising wind turbines (HS: 8602.31), solar panels (HS: 8541.40), and hydraulic turbines (HS: 8410.11). Raw inputs involve fossil fuels such as anthracite coal (HS: 2701.11), natural gas (HS: 2711.11), and crude oil (HS: 2709.00), alongside enriched uranium (HS: 2844.20) for nuclear power plants, and natural resources like sunlight, wind, and water for renewable energy. Intermediary inputs include electrical transformers (HS: 8504.23), circuit breakers (HS: 8535.21), and insulators (HS: 8546.20). The full response (included below) also included some explicit restraint and uncertainty in mentioning a definitive code. This further aids in minimizing the risk of false positives, as it reflects, for instance, the diverse pathways available in electricity generation.

Moreover, electrical energy is a raw input to 14 other products and an intermediary to 68 products. Notably, the most common intermediary input across the network is related to packaging, particularly "Paper and paperboard; cartons, boxes, and cases, of corrugated paper or paperboard" (HS: 4819.10), which appears in 533 downstream products. Petroleum products (HS: 2710.19) follow closely, featured in 9% of downstream products. The most predominant capital input is "Machinery for packing or wrapping" (HS: 8422.40), found in 13% of downstream products. The predominant raw input is from the Iron and Steel category, particularly "Iron or non-alloy steel; flat-rolled, of a width of 600mm or more, hot-rolled, without patterns in relief" (HS: 7208.51), which appears in 8% of downstream products.

Out of the total HS6 products cataloged, 3092 (55%) function as upstream products in at least one category. Among these, 44% primarily serve as raw materials, 32% as intermediary goods, and 22% as capital inputs, with 41% appearing in multiple categories. Such distinctions, facilitated by the file-retrieval "grounding," allow the AI model to make precise identifications about what versions of a product serve as upstream goods, like "Dog or cat food; not for retail sale" (HS: 2309.90) categorized as a raw input for 70 products and as an intermediary for 26 products, whereas "Dog or cat food; for retail sale" (HS: 2309.10) is not considered an upstream good.

Full response for Electrical Energy (HS: 2716.00) The response for HS Code 2716.00, "Electrical Energy" is the following:

> Given the HS Code 2716.00, which pertains to 'Electrical Energy,' a comprehensive description of the production process is outlined below. This involves a high-level overview of how electrical energy is generated, the capital inputs, raw materials, and intermediary inputs necessary for producing electrical energy.
>
> **Introduction:** The production of electrical energy primarily involves converting energy from various sources, such as fossil fuels, nuclear power, or re-

newable resources, into electricity. Electricity generation is a complex process, which can vary significantly depending on the energy source. For simplicity, this description focuses on the most common methods of electricity production: thermal (coal, gas, oil), nuclear, and renewable (hydro, wind, solar).

Capital Inputs:

1. **Thermal Power Plants:** - **Boilers** are used to generate steam by heating water. The steam produced is then directed to turn turbines. HS Code: `###8402.11###` for steam or other vapor generating boilers. - **Turbines** convert the kinetic energy of steam or wind into mechanical energy, which drives the generators. HS Code: `###8406.81###` for gas turbines. - **Generators** convert mechanical energy into electrical energy. HS Code: `###8501.64###` for AC generators (alternators).

2. **Nuclear Power Plants:** - **Nuclear Reactors** generate heat through nuclear fission. This heat is used to produce steam for turbines. HS Code: `###8401.30###` for nuclear reactors. - **Cooling Systems** are essential for removing excess heat from the reactor core. HS Code: `###8419.50###` for heat exchange units.

3. **Renewable Energy Systems:** - **Wind Turbines** capture kinetic energy from the wind. HS Code: `###8502.31###` for generating sets with wind-powered generators. - **Solar Panels (Photovoltaic Systems)** convert sunlight directly into electricity. HS Code: `###8541.40###` for photosensitive semiconductor devices including photovoltaic cells. - **Hydroelectric Power Plants** use water flow to drive turbines. They require significant civil engineering for dam construction. HS Code: `###8410.11###` for hydraulic turbines and water wheels.

Full response for Solar PV (HS: 8541.40) The response for HS Code 8541.40, "Electrical apparatus; photosensitive, including photovoltaic cells, whether or not assembled in modules or made up into panels, light-emitting diodes (LED)" is the following:

Given the task, I'll now proceed to describe the production process for the HS Code **8541.40**, which pertains to **"Electrical apparatus; photosensitive, including photovoltaic cells, whether or not assembled in modules or made up into panels, light-emitting diodes (LED)"**.

Introduction: This product group involves a wide range of electrical devices that are sensitive to light, including photovoltaic (solar) cells and light-emitting diodes (LEDs). The production of these devices integrates advanced material science and electronic engineering to create components capable of converting light into electricity or using electrical energy to produce light, respectively.

Capital Inputs:

Machinery and Equipment: 1. **Clean Rooms and Controlled Environments** - Specialized rooms designed to minimize the presence of particulates. They feature advanced air filtration systems ###8414.80###, temperature and humidity control ###8415.90###, and static-free environments. 2. **Photolithography Equipment** - Utilized in the patterning of the photovoltaic cells and LEDs to create intricate circuit designs. This includes ultraviolet (UV) light sources ###8539.49###, mask aligners, and stepper machines. 3. **Chemical Vapor Deposition (CVD) Systems** - Machines that deposit thin films onto substrates to create semiconductor layers, critical for both LEDs and photovoltaic cells ###8419.89###. 4. **Doping Equipment** - Used to introduce impurities into semiconductors to modulate their electrical properties ###8479.89###. 5. **Scribing and Cutting Equipment** - Laser-based systems for cutting silicon wafers and separating cells or LEDs ###8456.10###. 6. **Testing and Inspection Systems** - Including electroluminescence (EL) imaging systems ###9031.49### and solar simulator machines for performance testing ###9032.89###.

Raw Inputs:

Natural Resources and Unprocessed Goods: 1. **Silicon** - The primary raw material for both photovoltaic cells and LEDs, used in the form of ingots or polycrystalline masses ###2804.69###. 2. **Rare Earth Metals** - Elements like gallium ###8104.30### and arsenide ###2846.90### are crucial for LED production to determine color and efficiency. 3. **Glass Substrates** - For the encapsulation and protection of photovoltaic panels ###7005.29###. 4. **Chemicals for Semiconductor Processing** - Includes hydrochloric acid ###2806.10###, sulfuric acid ###2807.00###, and phosphorous dopants ###2804.70###.

Intermediary Inputs:

Semi-Finished Goods, Components, or Services: 1. **Wafers** - Pre-processed silicon wafers ###3818.00### ready for doping and layering in the production of photovoltaic cells and LEDs. 2. **Sputtering Targets** - Metals and alloys ###7106.91### used in the deposition processes to create conductive and transparent layers. 3. **Encapsulation Materials** - Epoxy resins ###3907.30### and silicones ###3910.00### used for protecting LEDs and sealing photovoltaic modules. 4. **Electrical Contacts and Interconnects** - Copper ribbons ###7409.11### and silver pastes ###3215.10### for making electrical connections within the devices. 5. **Flexible Circuits** - For advanced LED installations, flexible printed circuits ###8534.00### provide structural support and electrical connectivity.

This illustrative description combines detailed information on capital and raw inputs, along with intermediary requirements, dedicated to the production of photosensitive electrical apparatus, under the HS Code **8541.40**. The HS Codes mentioned are hypothetical examples to illustrate how the actual codes could be interwoven into the comprehensive description of the production process.

A.4 Implementation Details

Implementation Process The operational setup for processing the Harmonized System (HS) codes was executed using OpenAI's official Python package. Initial steps involved uploading a JSON file, containing a comprehensive list of HS codes and their descriptions, to the assistant API client. This upload served as the foundation for the interactions that followed. Each HS code, accompanied by its description, was submitted as a separate "message" within a "thread" in the OpenAI playground UI. In OpenAI's ecosystem, a "thread" symbolizes an ongoing conversation, while a "message" encapsulates the text and any attached files, allowing dynamic interaction with the system. The format for each message was consistent, structured as:

HS-Code: '*HS6 code*'. Description: '*HS6 code description*'

The process of uploading these messages took approximately 30 minutes. The assistant then processed all the messages within one hour, generating responses accordingly. An additional 30 minutes was required to retrieve the generated responses back to our local system. In total, the procedure, including the time spent on post-processing to segregate codes from the provided sections, spanned about 2-3 hours. This demonstrates a significant efficiency in processing speed, with expectations of further improvements in the future.

Processing Responses and Summary Statistics Appendix table A.8 provides a clear overview of the number of HS6 codes retrieved per section, alongside character and word counts, illustrating the depth and scope of the responses generated by the assistant. Notable differences emerge across the types of inputs—capital, raw, and intermediary. Responses pertaining to capital inputs notably feature a higher median and maximum number of HS6 codes cited (median = 5, max = 21), suggesting a richer and more complex referencing of codes compared to the raw (median = 3, max = 14) and intermediary (median = 3, max = 13) sections. This indicates a more detailed exploration of capital

goods within the industry contexts. Unsurprisingly then, the character and word counts are significantly higher in the capital inputs section, with averages of 1811 characters and 244.5 words, respectively, reflecting the depth and breadth required to describe these inputs adequately. In contrast, the raw and intermediary inputs sections manifest lower counts, pointing to shorter descriptions. The introduction section occasionally contains lengthy responses, likely due to the necessity to provide a comprehensive context for the sections that follow. These variations illustrate the assistant's adeptness at adjusting the level of detail according to the nature of the input, which underscores its capacity to handle context-specific informational demands

Sample Checks and Evaluation To ensure the accuracy and reliability of the assistant's responses, following evaluative checks were conducted:

- Verification tests to determine whether the assistant could correctly identify which row numbers specific product codes were located in.
- Capability tests to assess if the assistant could accurately describe a random set of 6-digit product codes, including the corresponding 4-digit and 2-digit codes they are part of.

These tests confirmed that the assistant could effectively 'understand' and 'interpret' the hierarchical tree structure of the HS classification system when queried. This functionality is highly beneficial and confirms the system's operational efficacy. In our evaluation we analyzed the cost-benefit ratio of this implementation. The system minimized the occurrence of fictitious products or definitions, effectively reducing the potential for false positives. However, there remains a risk of false negatives—instances where existing upstream relationships might not be mentioned.

The use of RAG (Retrieval-Augmented Generation) has notably reduced costs and dependency on extensively hand-coded examples, which alternative approaches like a fine-tuned model would require. This model permits more focused attention and a

streamlined process at lower costs. Future improvements could include adjustments to the model's temperature settings, now available as part of the RAG assistant, which were not an option in our earlier implementations in March 2024. Another future enhancement could involve running simulations with increased randomness to obtain more robust confidence weights for each network linkage through bootstrapping, although this is currently cost-prohibitive.

A.5 Network Properties

We further quantify the structural properties of our directed network, which maps the vertical supply chain relationships from raw materials through intermediary and capital inputs to final goods. At the HS6 level, the network comprises 5,648 nodes and 55,719 directed edges, illustrating a rich and complex set of interactions among HS-coded goods in various stages of production. The average degree at this level, a measure of the average number of direct connections per node, is 20.2. This high number reflects the dense interconnectivity typical of production networks, where nodes (representing goods) often link to multiple other nodes along the supply chain.

In contrast, the HS4 level network consists of 1,253 nodes and 40,710 directed edges. The average degree at the HS4 level is significantly higher at 64.98, indicating that nodes at this aggregation level are much more interconnected. The broader categories of goods (HS4) encapsulate a wider array of interactions compared to the more specific HS6 categories.

Network density, quantifying the proportion of potential directed connections that are actual connections, is 0.002 at the HS6 level and 0.0260 at the HS4 level. The higher density at the HS4 level implies a slightly more tightly-knit network, where a greater proportion of potential connections are realized. This indicates that, at a more aggregated level, goods are slightly more likely to be directly connected, reflecting the more generalized nature of HS4 categories. In absolute terms, network density at both HS6 and HS4 is low. In the context of large-scale economic networks, this density indicates

a selective pattern of connections typical in production systems, where each good is not directly linked to every other good. For comparison, random networks of similar size might exhibit higher densities, but the strategic and structured nature of supply chain relationships inherently limits the number of feasible connections, emphasizing the network's efficiency and specialization. This sparsity is a hallmark of supply networks, where the direct interactions are dictated by the production and supply requirements.

The Global Clustering Coefficient is 0.0205 for the HS6 network, indicating a low level of clustering. This metric reflects the low probability that two goods directly connected to a third good are also connected to each other—a common characteristic in supply chains, where production pathways typically follow linear rather than cyclic patterns. At the HS4 level, the Global Clustering Coefficient is higher at 0.162, suggesting that broader categories tend to form more clusters. This higher clustering reflects the general interdependence within broader product categories.

Assortativity, at 0.0016 for the HS6 network, is near zero, indicating that nodes do not preferentially connect with other nodes of similar degree. At the HS4 level, the assortativity is -0.0843, showing a slight tendency for nodes to connect with other nodes of differing degrees. This negative assortativity at the HS4 level highlights a more diverse and hierarchical network structure at broader product categorization.

Assortativity, at 0.0016 for the HS6 network, is near zero, indicating that nodes do not preferentially connect with other nodes of similar degree. This feature is typical in production networks where both low-degree raw materials and high-degree capital goods might be essential inputs for another node, highlighting the diverse and hierarchical nature of supply chains. At the HS4 level, the assortativity is -0.0843, showing a slight tendency for nodes to connect with other nodes of differing degrees. This negative assortativity at the HS4 level highlihts the hierarchical and varied nature of supply chains even more strongly, as broader product categories encompass a wide range of interactions from basic raw materials to complex capital goods.

The HS6 network demonstrates robust connectivity with only two connected com-

ponents; the largest contains 5,646 nodes. This overwhelming dominance of a single component underscores the extensive integration within the network, showing that the vast majority of goods are part of a giant component that spans nearly the entire network. In comparison, the HS4 network is a single connected component, indicating even greater integration and robustness at this higher aggregation level. Such connectivity is crucial for the stability and resilience of the supply chain, ensuring that disruptions in one part of the network can potentially be mitigated through alternative pathways.

These properties provide insightful topological perspectives into the network's structure and are pivotal for understanding the flow of goods, their interdependencies, and the overarching complexity of the economic system modeled by this network. For detailed metrics categorized by linkage type, HS section, and other properties, refer to Tables A.9, A.10, and A.11 in the appendix.

A.6 Network properties: heterogeneity

This section of the appendix provides a detailed exploration of the network's heterogeneity by examining its structural properties segmented by predominant types of upstream goods, HS sections, and categories defined by Upstreamness and Product Complexity Index (PCI). The findings from these analyses are summarized in Tables A.9, A.10, and A.11, which offer a granular view of the network's characteristics at both the HS6 and HS4 levels.

Key Findings The detailed breakdown by predominant type of upstream good (Table A.9) shows distinct differences in network properties. At the HS6 level, capital goods have fewer nodes but a higher average degree and network density compared to raw materials, indicating a more interconnected subset of nodes. This suggests that capital goods are central to multiple production pathways, reflecting their critical role in manufacturing processes. The global clustering coefficient is highest for capital goods, hinting at a tightly-knit cluster of nodes that frequently interact. At the HS4 level, these trends

are amplified, with capital goods showing a substantially higher average degree and network density, emphasizing their importance even more.

HS section analysis (Table A.10) reveals that sectors like Machines and Chemicals not only have a high number of nodes but also exhibit the highest number of edges and average degree at both HS6 and HS4 levels, underlining their pivotal role in the network. Interestingly, the Machines section shows a positive assortativity at the HS4 level, which is unusual in such networks, suggesting that high-degree nodes tend to connect with other high-degree nodes, possibly indicating specialized clusters within this sector. This is less pronounced at the HS6 level, where the assortativity is closer to zero.

The categorization by Upstreamness and PCI (Table A.11) offers insights into the functional and complexity-related stratification within the network. At both HS6 and HS4 levels, nodes classified under high Upstreamness and high PCI typically show a higher average degree and network density, suggesting these goods are crucial in the network's flow and are complex in their production requirements. Notably, the differences between high and low categories are more marked at the HS4 level, indicating a sharper distinction in network roles and complexities at broader categorizations.

Implications for Network Understanding These findings emphasize the network's structural diversity, where different types of goods and sectors exhibit unique network characteristics. Such heterogeneity is crucial for understanding the resilience and vulnerability of the network. For example, the high integration of capital goods could mean that disruptions in this sector might have wide-reaching impacts across the network. HS4 level highlight even stronger interdependencies and specialization, particularly for capital goods and complex products.

Biases and Limitations While these tables provide profound insights, it is essential to acknowledge that they are based on sub-samples of the entire network, which can introduce biases. Sub-sampling might overemphasize certain pathways or relationships, especially if the sub-samples are not representative of the entire network. In economic

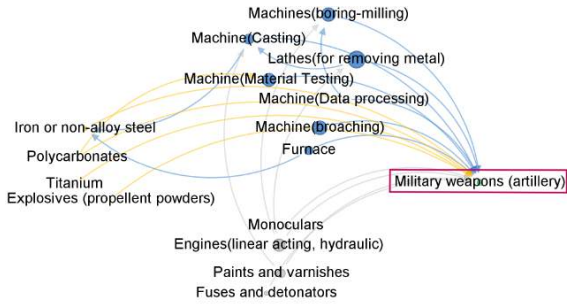
networks, such biases might mask or exaggerate the importance of certain nodes or connections, leading to skewed interpretations.

Despite these limitations, the analysis still offers valuable lessons about the complexity and connectivity of different network sections. It highlights the critical areas where the network is most densely connected and potentially most susceptible to cascading failures. Understanding these aspects helps in designing more robust systems and in strategic planning for mitigating risks associated with network disruptions. The comparison between HS6 and HS4 levels underscores the importance of analyzing networks at multiple levels of granularity to fully appreciate the underlying economic dynamics and interdependencies.

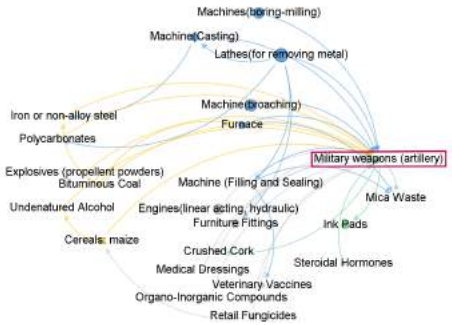
Appendix Figures and Tables

Figure A.1: Example of permuted networks: Military Artillery Weapons

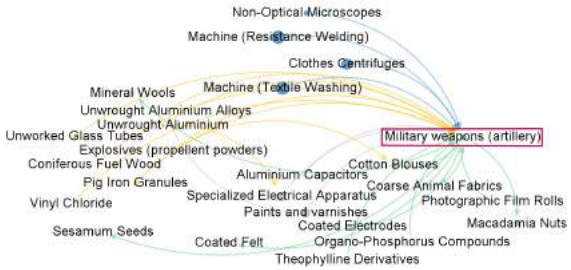
(a) Original example



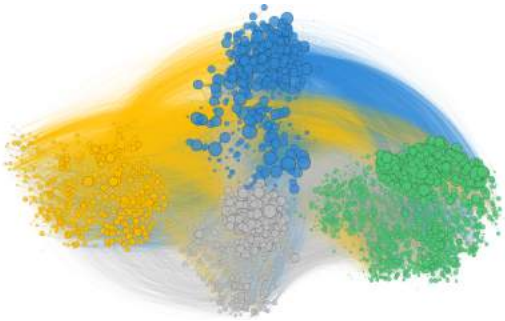
(b) 25% edges rewired



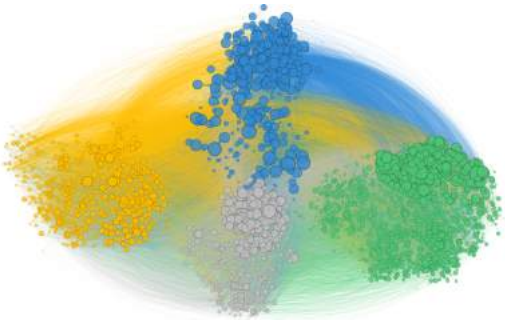
(c) 75% edges rewired



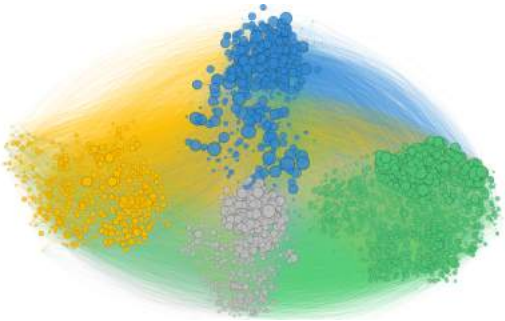
(d) Original full network



(e) 25% edges rewired (full)



(f) 75% edges rewired (full)



Note: Each panel presents a **one-degree ego network** or the **full network** from AIPNET. The **ego network** focuses on Military Artillery Weapons (HS: 9301.10), showing direct and indirect connections to related products. The **full network** visualizes the entire production network. Nodes represent six-digit HS product codes based on the 2017 nomenclature published by WCO, available here. Code descriptions are abbreviated for brevity. Nodes are colored by linkage type: yellow for raw materials, grey for intermediary inputs, blue for capital inputs, and green for final goods. The focal node in each ego network subfigure is enclosed in a red box, with edges colored by the source node. Node size indicates authority centrality (see section 4.7 for definition). While these are one-degree networks around the focal product, edges between one-degree nodes are also included. This figure illustrates the effects of perturbations on the network structure, with 25% and 75% of edges rewired randomly following the Erdos-Renyi model, as described in 4.8. Panels a-c are more intuitive, showing an increasing number of random connections as pertubation intensity increase, e.g., artillery weapons used to make macadamia nuts. Panels d-f show the aggregate pattern: a significantly more diffuse set of connections. These visualizations help to understand how the network is affected by edge rewiring. For detailed results on perturbation impacts, refer to Figure 8.

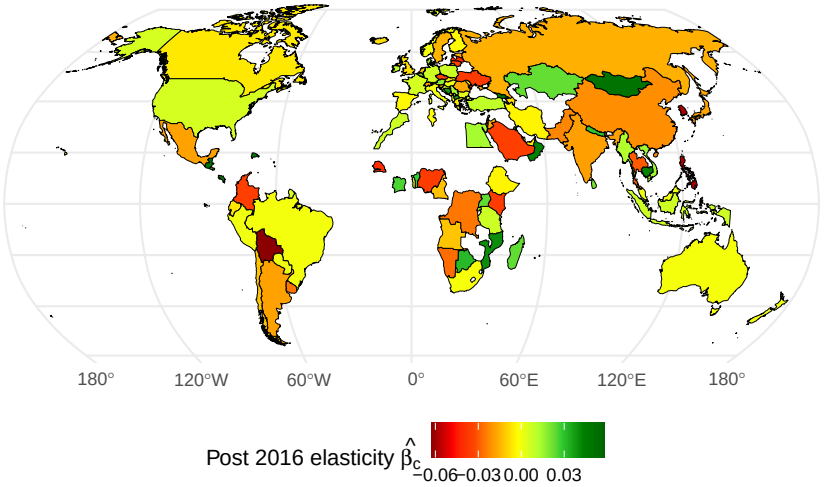
Table A.1: Summary Statistics by Temperature Setting Compared to Baseline (0%)

	Temperature		
	25%	**50%**	**100%**
% Overlapping Edges			
Min	51.7	46.7	35.4
Max	57.6	52.2	42.2
Median	56.0	49.2	38.1
Mean	55.3	49.3	38.5
SD	2.0	1.8	2.4
% Agreement on Edge Type			
Min	76.0	76.2	69.8
Max	81.1	80.8	76.9
Median	79.2	79.1	74.7
Mean	79.0	78.9	73.9
SD	1.4	1.3	2.3
Modal Network			
% Overlapping Edges	59.7	63.4	63.1
% Agreement on Edge Type	73.9	72.8	72.5

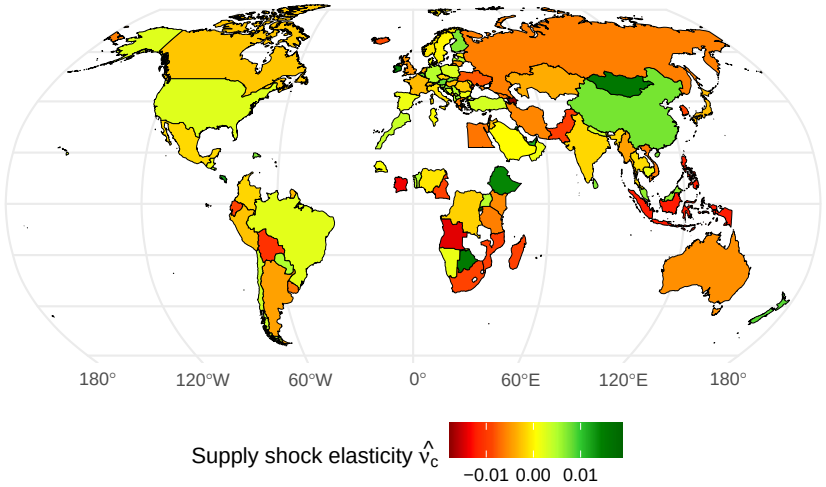
Notes: This table presents the summary statistics for the AIPNET network under different temperature settings compared to the baseline (0%). The percentage of overlapping edges indicates the proportion of edges in the generated networks that match the baseline network. The percentage agreement on edge type measures the conditional agreement on the type of overlapping edges (capital, raw, intermediary). The modal network statistics represent the most frequent edges and their agreement across all generated networks at each specified temperature. All values are reported in percentage terms. To conduct this exercise, we randomly selected 100 HS6 nodes from the full set used to create our network. For each node, the RAG assistant was prompted 10 times for each non-zero temperature setting (25%, 50%, 100%), resulting in 100 HS6 codes times 10 iterations times 3 temperature settings. For the temperature setting of 0, we prompted once for all 100 HS6 codes since it is deterministic. This process provides a sample over which the summary statistics of relationships were computed.

Figure A.2: Distribution of Estimated Elasticities from the Reduced-Form and Supply Shock Exercises Across Countries

Panel A: Post 2016 estimated elasticity $\widehat{\beta}_c$ of price shocks

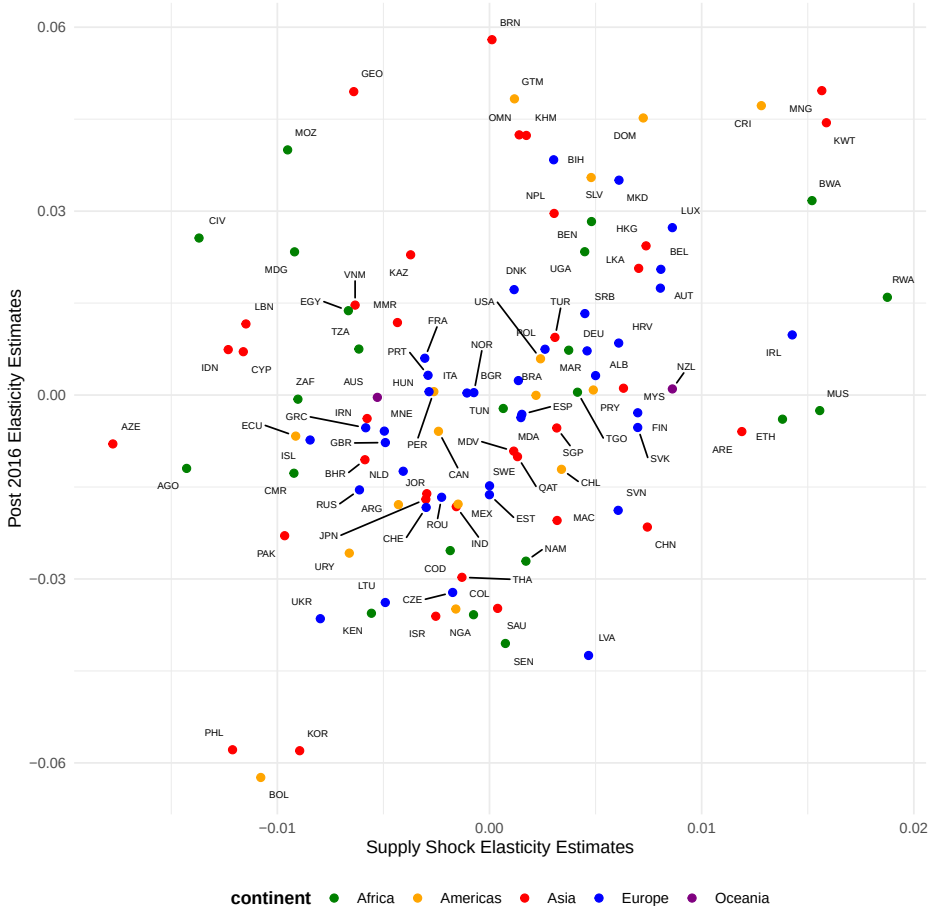


Panel B: Estimated supply shock elasticity $\widehat{\nu}_c$



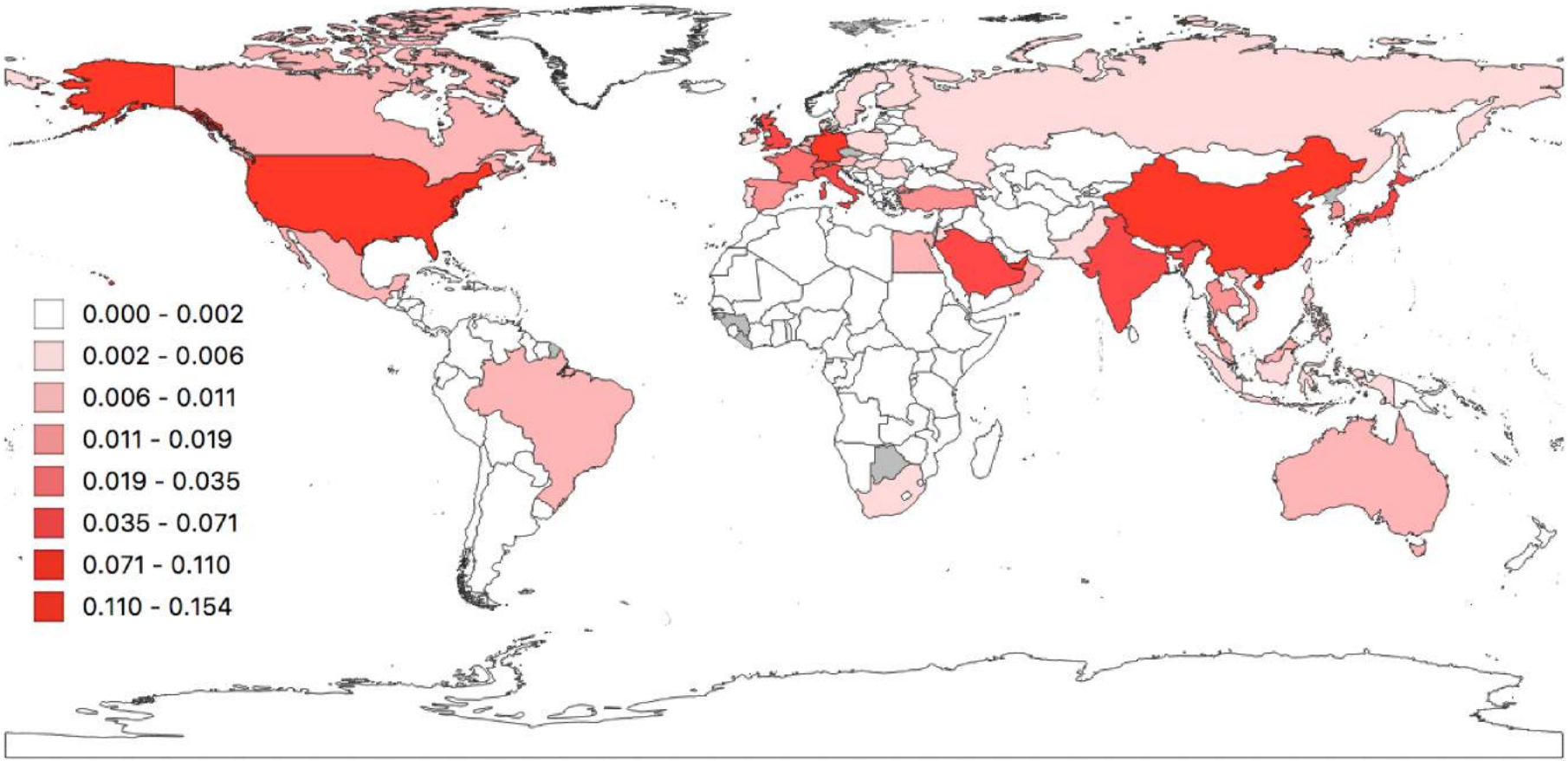
Notes: This figure presents the geographic distribution of estimated elasticities across countries. Panel A shows the post-2016 estimated elasticity of price shocks ($\widehat{\beta}_c$), while Panel B depicts the estimated supply shock elasticity ($\widehat{\nu}_c$).

Figure A.3: Scatterplot of $\widehat{\beta}_c$ against $\widehat{\nu}_c$



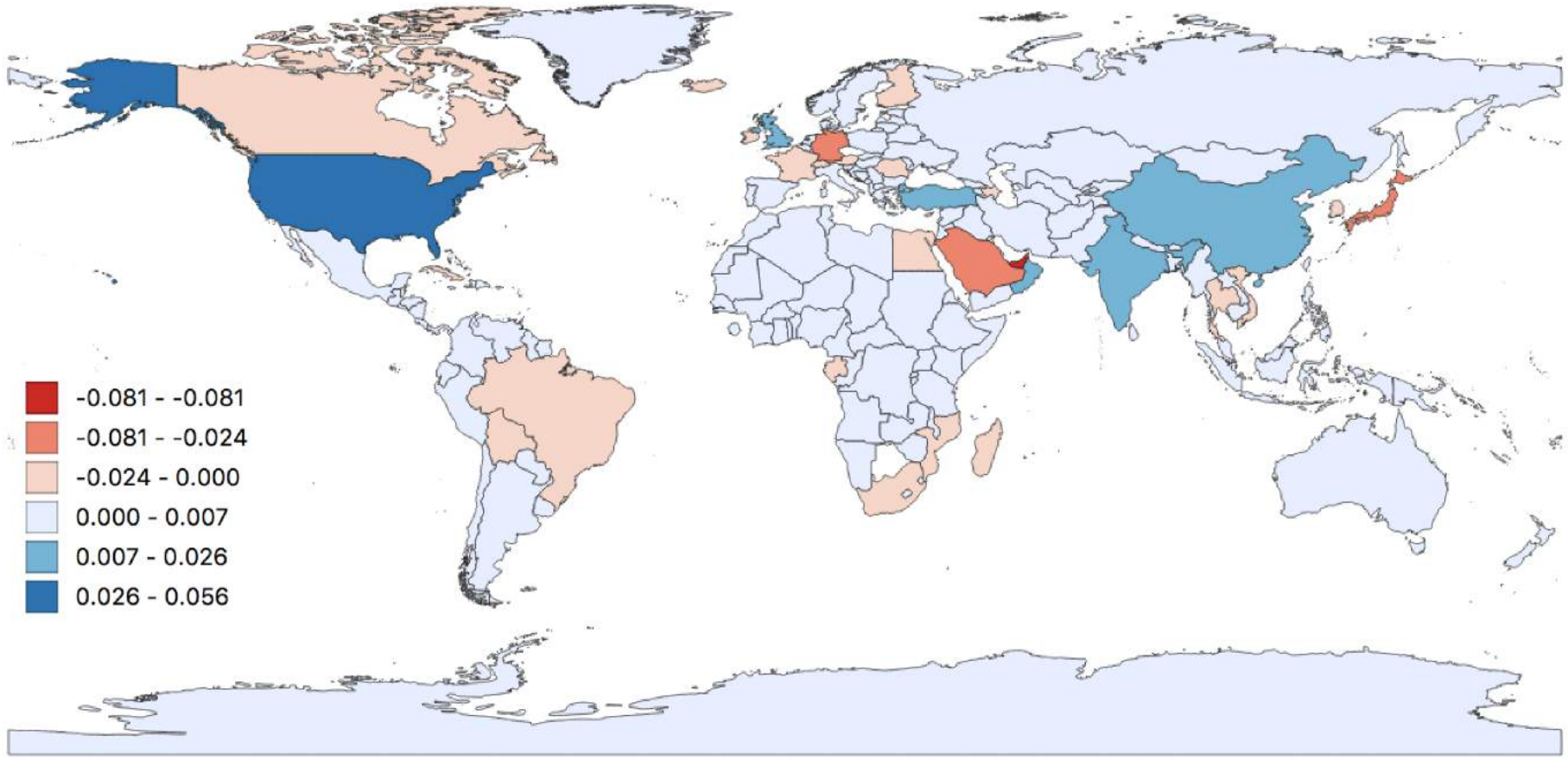
Notes: This scatterplot visualizes the relationship between the post-2016 estimated elasticity of price shocks ($\widehat{\beta}_c$) and the estimated supply shock elasticity ($\widehat{\nu}_c$) across countries.

Figure A.4: Import shares by country of origin in 2016 prior to the blockade



Notes: Figure plots the share of all imports into Qatar in 2016 that is sourced from different countries around the world. The darker red, the higher the import share from this country.

Figure A.5: Changes in import shares between 2016 and 2018 (up to November)

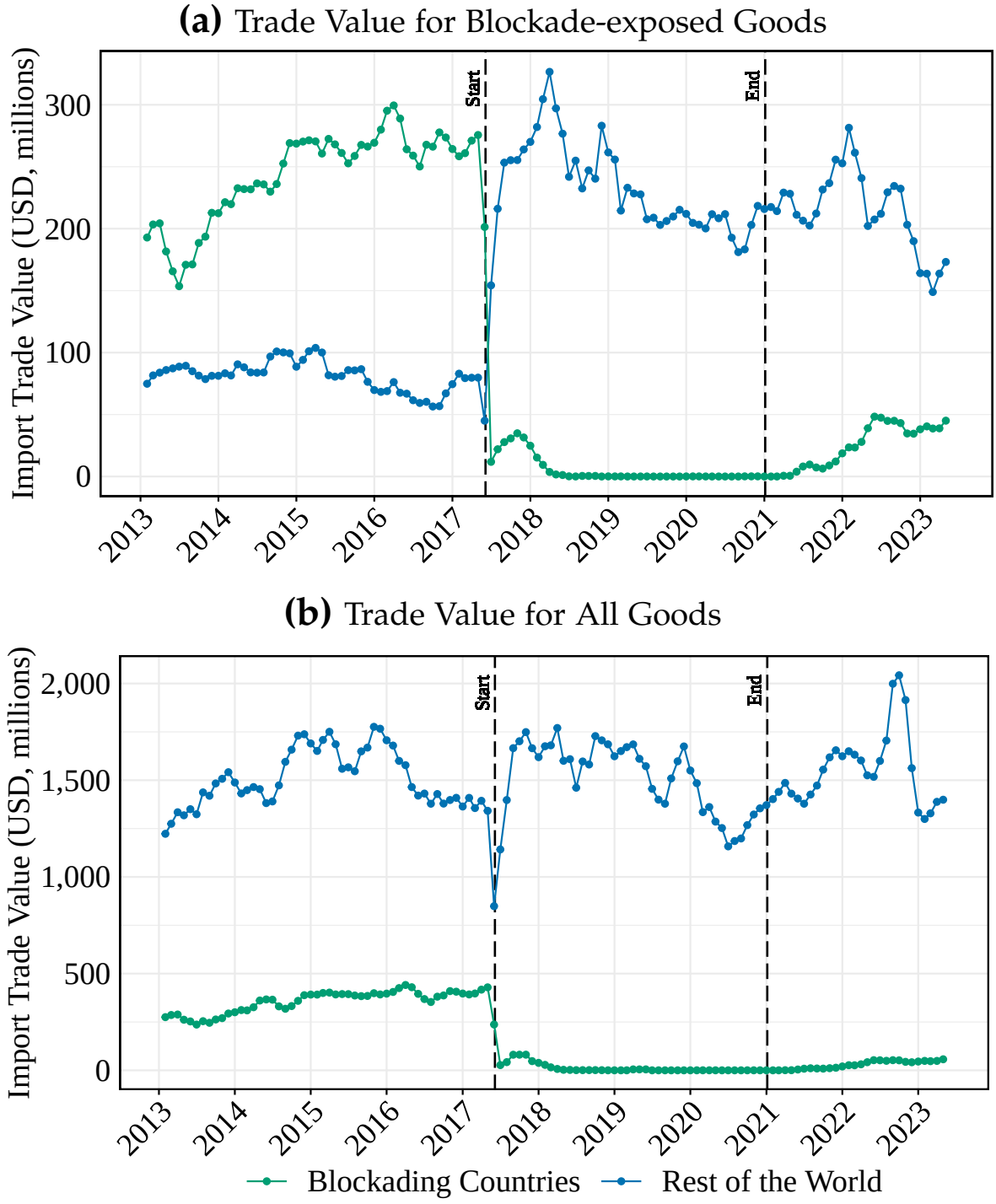


Notes: Figure plots the changes in the share of all imports into Qatar between 2016 and 2018 (up to November). Blue tones indicate an increase in imports from the respective countries while red tones indicate a contraction.

Table A.2: Description of variables

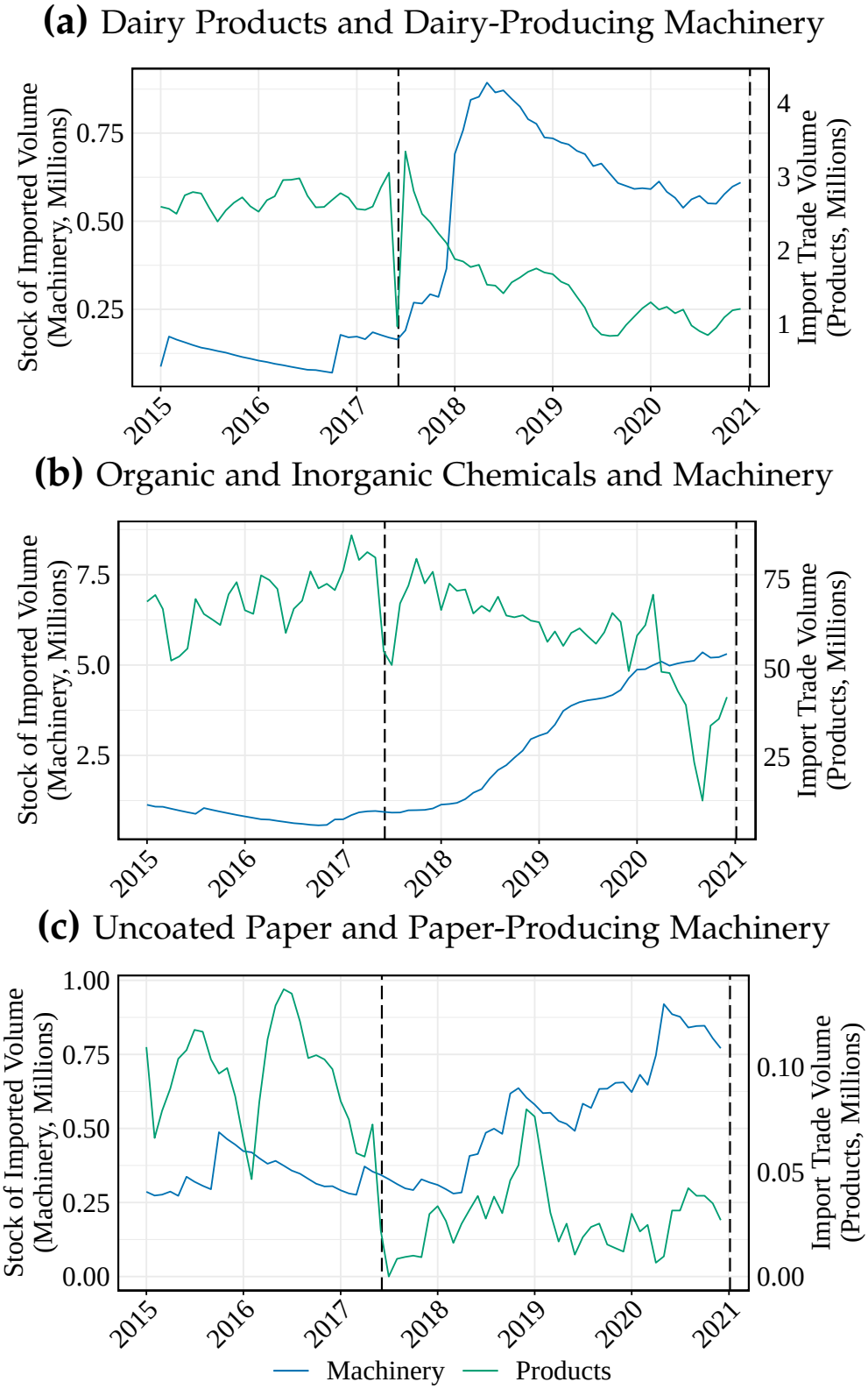
Variable Name	Variable	Variable Type	Variable Description
hs8	Product codes	Categorical variable	Eight-digit Harmonized System code
iso3c	Country codes	Categorical variable	ISO 3 country codes
year	Year	Categorical variable	Year
month	Month	Categorical variable	Month
port	Ports of entry	Categorical variable	Ports of entry: Air cargo, land border, or sea ports
weight	Weight of goods	Continuous variable	Weight (kilograms) of a HS8 import in a month
import_value	Value of imports	Continuous variable	Import value (QAR) of a HS8 import in a month
comlang_off	Common language	Dummy variable	1 for common official language
comcol	Common coloniser	Dummy variable	1 for common colonizer post 1945
distw	Weighted distance	Continuous variable	Weighted distance to Qatar (pop-wt, km)

Figure A.6: The Blockade substantially altered Trading Patterns



Note: This figure shows the monthly value of all goods imports, broken down by country-of-origin into two groups: Blockading Countries' includes Saudi Arabia, UAE, Bahrain, Egypt, Mauritania, Djibouti, and Maldives, and Rest of World', all remaining countries. Series are smoothed using a 3-month moving average, except during May-July 2017. Vertical black dashed lines mark the start and end of the blockade. Panel (a) includes only 'Blockade Exposed' 8-digit HS products, defined as goods where the majority of total import value was sourced from blockading countries in 2016. Panel (b) covers all goods.

Figure A.7: Illustrative Examples demonstrate Qatar's On-shoring Effort



Note: This figure illustrates the impact of the blockade on import volumes along value chains using three stylized examples. We document a gradual or sharp increase in capital machinery and equipment, and declines of import volumes of (likely) finished products. The product series are smoothed using a 3-month moving average, except during May-July 2017.

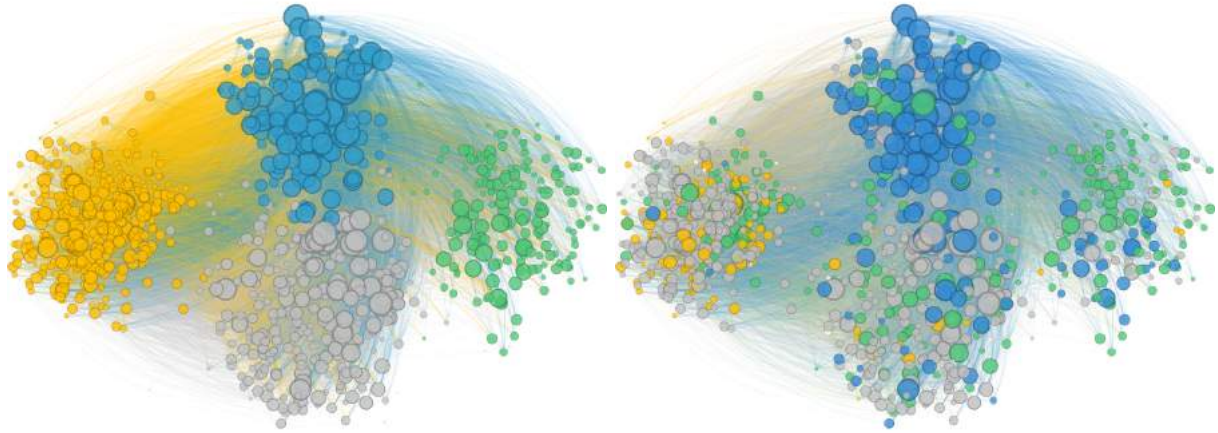
Figure A.8: Map indicating which countries are participating in the Saudi-led economic and political blockade of Qatar



Figure A.9: Network of HS4 Product-level Production Network constructed using AI

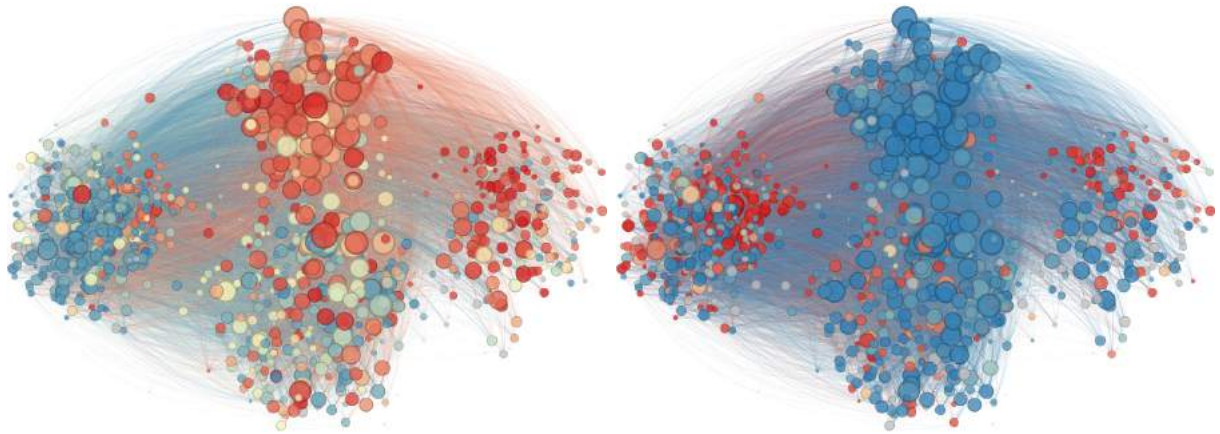
(a) Predominant Link Type (AIP-NET)

(b) Predominant Link Type (BEC classification)



(c) Upstreamness from (Antràs et al., 2012)

(d) Product Complexity Index



Note: This figure presents a multi-panel visualization of the production network, where each node corresponds to a Harmonized System (HS) **4-digit** product code, and edges represent vertical production relationships. The layout, derived using force-based layout algorithms, organizes nodes into clusters by predominant linkage type. **Panel (a)** serves as the baseline plot, showing nodes colored and clustered according to their linkage type: raw materials in yellow, intermediary inputs in grey, capital inputs in blue, and final goods in green. This panel introduces the graph's logical progression in an x-y dimensional framework, where nodes increase in size—indicating higher authority centrality—as we move from left to right and from bottom to top, especially evident in capital and final goods sectors. **Panel (b)** retains this layout but changes node colors according to UN's Broad Economic Categories (BEC) classification (Rev. 5), revealing the missing granularity within each linkage type and highlighting classification mismatches, particularly in non-capital categories. **Panel (c)** transitions to coloring nodes by Upstreamness from red (low) to blue (high), visually emphasizing the negative relationship between authority centrality and upstreamness. Finally, **panel (d)** colors nodes based on the Product Complexity Index (PCI), from red (low) to blue (high), underscoring a trend where larger nodes, indicative of higher centrality, generally display higher PCI, suggesting a discernible correlation between node centrality and complexity within the economic network.

Table A.3: Regression of Authority on PCI and Upstreamness

(a) HS6 Product Level

Dependent Variables:	(1) PCI (Level)	(2) PCI (Z)	(3) PCI (IHS)	(4) Ups. (Level)	(5) Ups. (Z)	(6) Ups. (IHS)
Variables						
Authority	1.2***			-1.6***		
	(0.30)			(0.29)		
Authority (Z)		0.23***			-0.30***	
		(0.06)			(0.06)	
Authority (IHS)			1.1***			-0.66***
			(0.27)			(0.12)
Fit statistics						
Observations	3,074	3,074	3,074	4,435	4,435	4,435
R^2	0.053	0.053	0.054	0.090	0.090	0.086
Adj. R^2	0.053	0.053	0.053	0.090	0.090	0.086
S.E.: Clustered by	HS2	HS2	HS2	HS2	HS2	HS2

(b) HS4 Product Level

Dependent Variables:	(1) PCI (Level)	(2) PCI (Z)	(3) PCI (IHS)	(4) Ups. (Level)	(5) Ups. (Z)	(6) Ups. (IHS)
Variables						
Authority	1.7***			-1.3***		
	(0.31)			(0.22)		
Authority (Z)		0.32***			-0.26***	
		(0.06)			(0.04)	
Authority (IHS)			1.5***			-0.54***
			(0.28)			(0.10)
Fit statistics						
Observations	1,062	1,062	1,062	1,174	1,174	1,174
R^2	0.099	0.099	0.103	0.066	0.066	0.064
Adj. R^2	0.099	0.099	0.103	0.066	0.066	0.064
S.E.: Clustered by	HS2	HS2	HS2	HS2	HS2	HS2

Note: We compare the fit between the Kleinberg Authority Centrality of products in our production network and two other product level measures: (1) Product Complexity Index (PCI), and (2) Upstreamness (Ups.). The unit of analysis is HS6 level products in panel (a) and HS4 level products in panel (b). Columns (1) correlates the product level average PCI from 2008 to 2022 with Authority Centrality of the same product. Column (2) standardizes the two variables and Column (3) applies an inverse hyperbolic sine transformation to the two variables. Columns (4) to (6) conduct the same exercise using Upstreamness instead of PCI. Standard errors are clustered by 2-digit HS level (HS2) and shown in parentheses. Significance Codes: ***: 0.01, **: 0.05, *: 0.1.

Table A.4: Our Network Predicts High Values in Use tables, Total, and Direct Requirements

Dependent Variables:	Use Value			Total Requirements			Direct Requirements		
Model:	(1)	(2)	(3)	(4)	(5)	(6)	(7)	(8)	(9)
Variables									
Network Score	0.0301***	0.0302***	0.0332***	0.1575***	0.1549***	0.1659***	0.1573***	0.1560***	0.1718***
	(0.0075)	(0.0075)	(0.0077)	(0.0394)	(0.0383)	(0.0355)	(0.0358)	(0.0351)	(0.0346)
Fixed-effects									
Upstream Sector		Yes			Yes			Yes	
Downstream Sector		Yes			Yes			Yes	
Upstream Industry			Yes			Yes			Yes
Downstream Industry			Yes			Yes			Yes
Fit statistics									
Observations	41,209	41,209	41,209	41,006	41,006	41,006	41,209	41,209	41,209
R^2	0.03373	0.04498	0.09564	0.03261	0.07453	0.23181	0.03691	0.05154	0.11764
Within R^2		0.03405	0.03677		0.03266	0.03809		0.03649	0.04020

Note: This table reports the regression results according to equation 1. We regress the standardized Input-Output table values on our standardized network scores resulting from aggregating the HS 6-digit level network to the BEA-industry level. Columns (1), (4), and (7) use no fixed effects, columns (2), (5), and (8) employ upstream and downstream sector-fixed effects and columns (3), (6), and (9) employ industry-fixed effects. Both dependent and independent variables are winsorized at the bottom 0.5 percentile and top 99.5 percentile. We cluster standard errors to account for correlation in both the upstream and downstream industries. Significance Codes: ***: 0.01, **: 0.05, *: 0.1.

Table A.5: Robustness of impact of persistent supply shocks affecting downstream goods prices on imports of upstream goods to alternative definitions of the supply shock measures

	(1)	(2)	(3)	(4)	(5)	(6)	(7)	(8)
	different definitions of persistence			*Markov Switch based filter*		*adding contemporaneous controls*		
***Panel A:* log(Import value + 1)**								
AIPNET Link × Supply Shock	0.0046***	0.0048***	0.0074***	0.0026***	0.0046***	0.0058***	0.0050***	0.0051***
	(0.0009)	(0.0008)	(0.0011)	(0.0009)	(0.0009)	(0.0009)	(0.0008)	(0.0009)
No. of estimated FE	178,401,817	177,988,182	178,400,341	169,976,936	165,273,406	178,401,807	178,216,465	177,889,065
R^2	0.94477	0.94477	0.94477	0.94488	0.94480	0.94477	0.94477	0.94477
Observations	1,844,701,890	1,843,351,530	1,844,524,308	1,765,222,553	1,729,658,840	1,844,652,835	1,844,243,749	1,843,057,401
***Panel B:* log(Import volume)**								
AIPNET Link × Supply Shock	0.0084***	0.0070***	0.0117***	0.0077***	0.0090***	0.0087***	0.0091***	0.0094***
	(0.0010)	(0.0009)	(0.0013)	(0.0011)	(0.0012)	(0.0009)	(0.0010)	(0.0011)
No. of estimated FE	178,401,816	177,988,179	178,400,340	169,976,936	165,273,406	178,401,806	178,216,464	177,889,063
R^2	0.93735	0.93735	0.93735	0.93751	0.93742	0.93735	0.93734	0.93735
Observations	1,844,700,721	1,843,350,362	1,844,523,139	1,765,221,456	1,729,657,757	1,844,651,667	1,844,242,580	1,843,056,233
Regression specification:								
Country x HS4	X	X	X	X	X	X	X	X
Country x HS2 Downstream x Year	X	X	X	X	X	X	X	X

Notes: Table presents regression results documenting the impact of persistent price shocks on downstream goods on upstream imports. The exercise explores robustness of the main effects to different definitions of the supply shock. Column (1) to (3) explore different definitions of the main supply shock measure that uses the regression filtering that was described in equation 4. Column (1) presents the main estimation. Column (2) defines the supply shock as a binary shock that persists at least 3 lags excluding the contemporaneous year. Column (3) classifies a shock based on a persistence in supply shock for four consecutive years. Columns (4) and (5) uses a Markov switching model to identify shocks. Column (6) to (8) add the idiosyncratic outlier definition for the contemporaneous, and lagged years interacted with the AIPNET linkage dummy to document that the effects are not confounding idiosyncratic price shocks but rather capture structural or longer price shocks. Standard errors provided in parentheses are clustered at the HS2 by HS2 pair level with stars indicating *** p <0.01, ** p <0.05, and * p <0.1.

Table A.6: Effects of Product-level Blockade Exposure on Exports

Dependent Variable:	Export Volume (Log)		
Model:	(1)	(2)	(3)
Variables			
Blockade Exposure × Post × Non-Blockading	0.179	0.089	0.095
	(0.160)	(0.150)	(0.186)
Blockade Exposure × Post × Blockading	-1.10***	-0.887**	-1.21***
	(0.297)	(0.374)	(0.392)
Fixed-effects			
HS8-Country-Blockading	Yes	Yes	Yes
Year-Month-Country	Yes		
HS2-Year-Month-Country		Yes	
HS4-Year-Month-Country			Yes
Fit statistics			
Observations	880,760	880,760	880,760
R^2	0.567	0.666	0.810

Note: This table reports results from running the regression defined in section 6.2 equation (13). We test for the effect of 'Blockade Exposure', measured for each HS8 product as the proportion of the total value of trade that came from blockading countries in 2016. This is interacted with an indicator variable denoting the start of the blockade and whether the target country is a blockading country. The data used is at the monthly frequency of exports for each HS8 product and target country. We further exclude the period of the blockade. Standard errors (clustered by HS4 product code) in parentheses. We use an IHS approximation for the logarithm. Significance Codes: ***: 0.01, **: 0.05, *: 0.1.

Table A.7: Top 30 Imports by volume across HS2 sections affected by the blockade

HS2	Description	Imports in 2016 from		E_i	Import share
		All countries	blockading countries		
73	Iron or steel articles	1,443.43	412.04	28.5%	4.9%
85	Electrical machinery and equipment and p	3,006.73	327.79	10.9%	10.3%
74	Copper and articles thereof	391.26	289.88	74.1%	1.3%
39	Plastics and articles thereof	718.35	261.21	36.4%	2.5%
72	Iron and steel	509.40	258.95	50.8%	1.7%
4	Dairy produce; birds' eggs; natural hone	393.48	245.25	62.3%	1.3%
84	Nuclear reactors, boilers, machinery and	4,984.55	141.15	2.8%	17.0%
27	Mineral fuels, mineral oils and products	181.39	137.96	76.1%	0.6%
68	Stone, plaster, cement, asbestos, mica o	362.90	124.15	34.2%	1.2%
76	Aluminium and articles thereof	225.93	117.44	52.0%	0.8%
32	Tanning or dyeing extracts; tannins and	172.86	104.11	60.2%	0.6%
7	Vegetables and certain roots and tubers;	268.68	97.61	36.3%	0.9%
71	Natural, cultured pearls; precious, semi	603.02	94.68	15.7%	2.1%
34	Soap, organic surface-active agents; was	165.11	94.06	57.0%	0.6%
94	Furniture; bedding, mattresses, mattress	835.00	93.74	11.2%	2.9%
87	Vehicles; other than railway or tramway	3,690.80	89.24	2.4%	12.6%
22	Beverages, spirits and vinegar	164.63	86.89	52.8%	0.6%
33	Essential oils and resinoids; perfumery,	389.23	85.57	22.0%	1.3%
15	Animal or vegetable fats and oils and th	104.87	76.48	72.9%	0.4%
38	Chemical products n.e.s.	378.74	74.59	19.7%	1.3%
19	Preparations of cereals, flour, starch o	205.14	72.86	35.5%	0.7%
48	Paper and paperboard; articles of paper	178.95	67.70	37.8%	0.6%
25	Salt; sulphur; earths, stone; plastering	107.24	64.42	60.1%	0.4%
2	Meat and edible meat offal	430.22	58.79	13.7%	1.5%
30	Pharmaceutical products	527.57	56.63	10.7%	1.8%
69	Ceramic products	213.33	49.67	23.3%	0.7%
21	Miscellaneous edible preparations	169.32	48.96	28.9%	0.6%
8	Fruit and nuts, edible; peel of citrus f	229.49	44.44	19.4%	0.8%
70	Glass and glassware	166.14	44.38	26.7%	0.6%
1	Animals; live	215.35	43.84	20.4%	0.7%

Notes: Table presents the top 30 imports by volume that have been affected by the blockade of Qatar. Trade volumes ($ million) are measured in 2016, the year before the blockade was announced. HS2 section descriptions are truncated to 40 characters in length.

Table A.8: Summary of AI responses

Description	Min	25%	Median	Mean	75%	Max	N
(a) Number of HS6 codes retrieved Per Section							
Raw	0.00	2.00	3.00	3.52	5.00	14.00	5270
Intermediary	0.00	2.00	3.00	3.21	4.00	13.00	5270
Capital	0.00	2.00	5.00	4.91	7.00	21.00	5270
Overall	0.00	8.00	12.00	11.64	15.00	42.00	5270
(b) Number of Characters Per Section							
Introduction	3	384	445	461.7	516	3932	5270
Raw	4	571	722	742.3	889	3302	5270
Intermediary	73	883	998	1015	1126	3412	5270
Capital	1	1557	1780	1811	2041	3875	5270
Overall	103	3966	4258	4330	4603	8698	5270
(c) Number of Words Per Section							
Introduction	1	55	64	65.96	73	543	5270
Raw	2	80	100	103.6	123	445	5270
Intermediary	10	118	134	136.7	152	485	5270
Capital	1	208	241	244.5	277	514	5270
Overall	16	543	584	593.2	631	1196	5270

Table A.9: Network Properties by Predominant Type of Upstream good

Property	Capital	Intermediary	Raw
(a) HS6 Level			
No. of Nodes	684	1017	1391
No. of Edges	3237	2266	3672
Average Degree	9.4600	4.4600	5.2800
Network Density	0.0069	0.0022	0.0019
Global Clustering Coefficient	0.0660	0.0290	0.0330
Assortativity	-0.0450	-0.0760	-0.0440
No. of Connected Components	122	204	230
Size of Largest Connected Component	562	812	1160
(b) HS4 Level			
No. of Nodes	174	386	506
No. of Edges	3191	3846	5211
Average Degree	36.6782	19.9275	20.5968
Network Density	0.1060	0.0259	0.0204
Global Clustering Coefficient	0.3749	0.1554	0.1790
Assortativity	-0.0388	-0.1350	0.0281
No. of Connected Components	3	22	5
Size of Largest Connected Component	172	365	502

Table A.10: Network Properties by Section

Property	Sec: 6 Chemical	Sec: 16 Machines	Sec: 11 Textile	Sec: 15 Metal	Sec: 2 Animal
(a) HS6 Level					
No. of Nodes	932	887	802	596	345
No. of Edges	2920	5547	2055	1495	82
Average Degree	6.2700	12.5100	5.1200	5.0200	0.4800
Network Density	0.0034	0.0071	0.0032	0.0042	0.0007
Global Clustering Coefficient	0.0250	0.0580	0.0110	0.0230	0.0000
Assortativity	-0.0360	0.0060	-0.1600	-0.0470	-0.2530
No. of Connected Components	96	93	89	59	265
Size of Largest Connected Component	833	795	711	537	14
Share of sample (%)	16.5	15.7	14.2	10.6	6.1
(b) HS4 Level					
No. of Nodes	181	155	152	134	78
No. of Edges	2307	1361	1183	3306	164
Average Degree	25.4917	17.5613	15.5658	49.3433	4.2051
Network Density	0.0708	0.0570	0.0515	0.1855	0.0273
Global Clustering Coefficient	0.3036	0.1419	0.2207	0.4647	0.0860
Assortativity	0.0247	-0.1509	-0.1145	-0.0453	-0.4966
No. of Connected Components	3	7	5	1	11
Size of Largest Connected Component	179	149	148	134	68
Share of sample (%)	14.5	10.7	12.4	12.1	6.2

Table A.11: Network Properties by Upstreamness and Product Complexity Index (PCI) Categories

Property	Upstreamness			PCI		
	Low	Med	High	Low	Med	High
(a) HS6 Level						
No. of Nodes	1499	1546	1390	1025	1024	1025
No. of Edges	7703	3671	5103	2800	2747	6237
Average Degree	10.2800	4.7500	7.3400	5.4600	5.3700	12.1700
Network Density	0.0034	0.0015	0.0026	0.0027	0.0026	0.0059
Global Clustering Coefficient	0.0280	0.0110	0.0290	0.0230	0.0200	0.0540
Assortativity	-0.0580	-0.1260	-0.0170	-0.0460	0.0380	0.0880
No. of Connected Components	66	121	89	79	77	47
Size of Largest Connected Component	1433	1425	1301	945	948	979
(b) HS4 Level						
No. of Nodes	392	391	391	354	354	354
No. of Edges	5746	3252	5326	2485	3344	8729
Average Degree	29.3163	16.6343	27.2430	14.0396	18.8927	49.3164
Network Density	0.0375	0.0213	0.0349	0.0199	0.0268	0.0699
Global Clustering Coefficient	0.2078	0.1188	0.2115	0.1503	0.1414	0.2888
Assortativity	-0.0399	-0.1243	0.0041	-0.1263	-0.1106	-0.0324
No. of Connected Components	2	2	1	8	2	1
Size of Largest Connected Component	391	390	391	347	353	354

B Pete Working Area

Dependent Variable:	ihs(upstream_imp_val)
Model:	(1)
Variables	
upstream_exposure_val_2013_2016_hs6	-1.607***
	(0.3575)
downstream_exposure_val_2013_2016_hs6	0.1795**
	(0.0793)
Fixed-effects	
downstream_hs6-upstream_hs6	Yes
period	Yes
Fit statistics	
Observations	134,537,760
R^2	0.59646
Within R^2	0.00229

Clustered (upstream_hs4 & downstream_hs4) standard-errors in parentheses

*Signif. Codes: ***: 0.01, **: 0.05, *: 0.1*